1976

Continuous Logging Of Borehole Temperature Gradients

John Gary Conaway

CONTINUOUS LOGGING OF BOREHOLE TEMPERATURE GRADIENTS

by

John Gary Conaway

Department of Geophysics

Submitted in partial fulfillment

of the requirements for the degree of

Doctor of Philosophy

Faculty of Graduate Studies

The University of Western Ontario

London, Canada

January, 1976

ABSTRACT

A complete system for continuous logging of borehole temperature gradients has been developed and subjected to field tests with prototype equipment. To meet the requirements of this system, a time-domain operator was derived consisting of a smoothing term, a deconvolution term (to compensate for lag due to the thermistor time constant and probe velocity), and a gradient term. When convolved with raw field data this combined operator will yield directly a high precision, high resolution temperature gradient profile.

The prototype equipment developed for the field tests includes a thermistor probe on a 1 km cable, and a cable winch modified by the addition of a gold slip-ring assembly; the probe is lowered at a constant velocity by a variable speed motor drive assembly. The thermistor impedance is monitored continuously by a low-current digital resistance meter (3 samples per second), the output of which is recorded on magnetic tape for processing by digital computer.

The system was field tested in two partially cased, water filled boreholes. There was good correlation between gradient logs and thermal resistivity profiles from laboratory measurements on core material, indicating that

even in partially cased wells the gradient log is a good approximation of the thermal resistivity profile.

For a lowering rate of 18 m/min, the gradient profile exhibits a repeatibility better than ±0.5 C/km. Comparison of the gradient profile with a fine-scale geologic log indicates a stratigraphic resolution threshold on the order of 2 m for a 10-20% thermal resistivity contrast. For isolated resistivity contrasts of 50-100%, the resolution is better than 0.5 m.

This system will be useful for engineering applications in the petroleum industry, for monitoring the return to equilibrium of a borehole, as an additional aid to core selection in terrestrial heat flow work, and for stratigraphic correlation. In addition, this system may prove useful in other research areas, such as oceanography, arctic permafrost investigations, and studies of groundwater hydrology and pollution.

ACKNOWLEDGEMENTS

I would like to express my appreciation to the following persons and institutions who have assisted during the course of this project:

The National Research Council of Canada for financial support in the form of an operating grant and a Postgraduate Scholarship.

Dr. A.M. Jessop and Messrs. Alan Taylor and Jim Lyons of the Division of Seismology and Geothermal Studies, Earth Physics Branch, Department of Energy Mines and Resources, for expediting the logging of the Ottawa borehole.

Dr. L. Mansinha, for many helpful discussions.

Messrs. Ling, Brunet, and Price for technical assistance with the equipment.

My fellow geophysics graduate students at UWO, for assistance with the well logging, and for constructive criticism and comments.

And especially Dr. A. E. Beck, my chief supervisor, for facilitating the work, and for expert advice and assistance throughout the project.

TABLE OF CONTENTS

LIST OF FIGURES

CHAPTER 1

INTRODUCTION

There exist today several techniques for geothermal well logging which are routinely applied to various problems in the petroleum industry, terrestrial heat flow and geothermal prospecting. Continuous analog temperature logs are commonly used in the petroleum industry for what might be called engineering applications. These include monitoring the extent, quality, and progress of cementing behind well casing, locating zones where drilling circulation may be lost or where liquids or gases might be entering the well, and monitoring the progress of such techniques as artificial fracturing or acid treatment of the country rock (Bryant, 1960; Kappelmeyer and Haenel, 1974).

Analog temperature logs can be rapidly and simply obtained, but lack precision and resolution, for the following reasons. First, it is extremely difficult to measure, store and retrieve analog data with a resolution of one part in 10000. With digital techniques each digit is stored separately, requiring a resolution in this system of one part in ten. Second, a temperature log is essentially an integrated record of the effects of the thermal

resistivities of the various geologic formations present, and as such is effectively lacking in resolution when compared with a log of temperature gradients. The gradient log is essentially a thermal resistivity profile (in the absence of disturbing factors such as groundwater flow and surface temperature effects) and hence is a much more sensitive indicator of subtle changes in the thermal conditions along the borehole. Beck (1976a) refers to this as the T-log, and we will use this terminology for convenience.

The gradient log is generally found directly by differentiation of the temperature log, a process which greatly amplifies high frequency noise. Probably the most important factor contributing to the imprecision of continuous analog temperature logs is the neglect of the probe time constant. As the probe is lowered down the borehole it is not in thermal equilibrium with its surroundings. Hence the probe does not measure the true borehole temperature profile, but rather, the measured temperature profile lags behind the true temperature. Simmons (1965) presented a continuous analog logging system which was designed to minimize this problem through the use of thermistor probes having very small time constants (on the order of one second). Probes having time constants this small are extremely fragile and hence are poorly suited for work in mud filled holes. Furthermore, such probes contain tiny thermistors which are subject to self-heating effects,

resulting in further error. Simmons confined his work to temperature logs, and did not consider gradient logs. Costain (1970) suggested deconvolution of the measured temperature profile by an inverse operator derived from the impulse response of the borehole logging system. This concept will be considered in detail in Chapter 2.

The simplest method of making borehole temperature measurements is the incremental technique (c.f. Beck, 1965). Here the measuring instrument is lowered in steps of, say, 10 m, some time is allowed for it to approach thermal equilibrium with its surroundings, a reading is made, and the process is repeated. Assuming that a total time of three minutes per 10 m step is required, and that each reading is precise to $\pm 0.0025\ ^{o}C$, then a temperature gradient profile with a precision of $\pm 0.5\ ^{o}C/km$ can be obtained with a logging time of 5 hours for a 1 km borehole. If greater resolution is required, however, the logging time (and imprecision) increase greatly. Figure 1.1 illustrates this effect. The ordinate is calibrated in terms of measurement precision ($\pm\ ^{o}C/km$) and logging time (hours). The abscissa is calibrated in terms of desired resolution (m), and reading spacing (m), adhering to the convention of Fourier analysis that a minimum of two data points per cycle are required to define the highest (sinusoidal) frequency component in a given signal. This graph illustrates several important facts. First, the incremental logging technique will yield a precise sketch of the borehole gradient profile

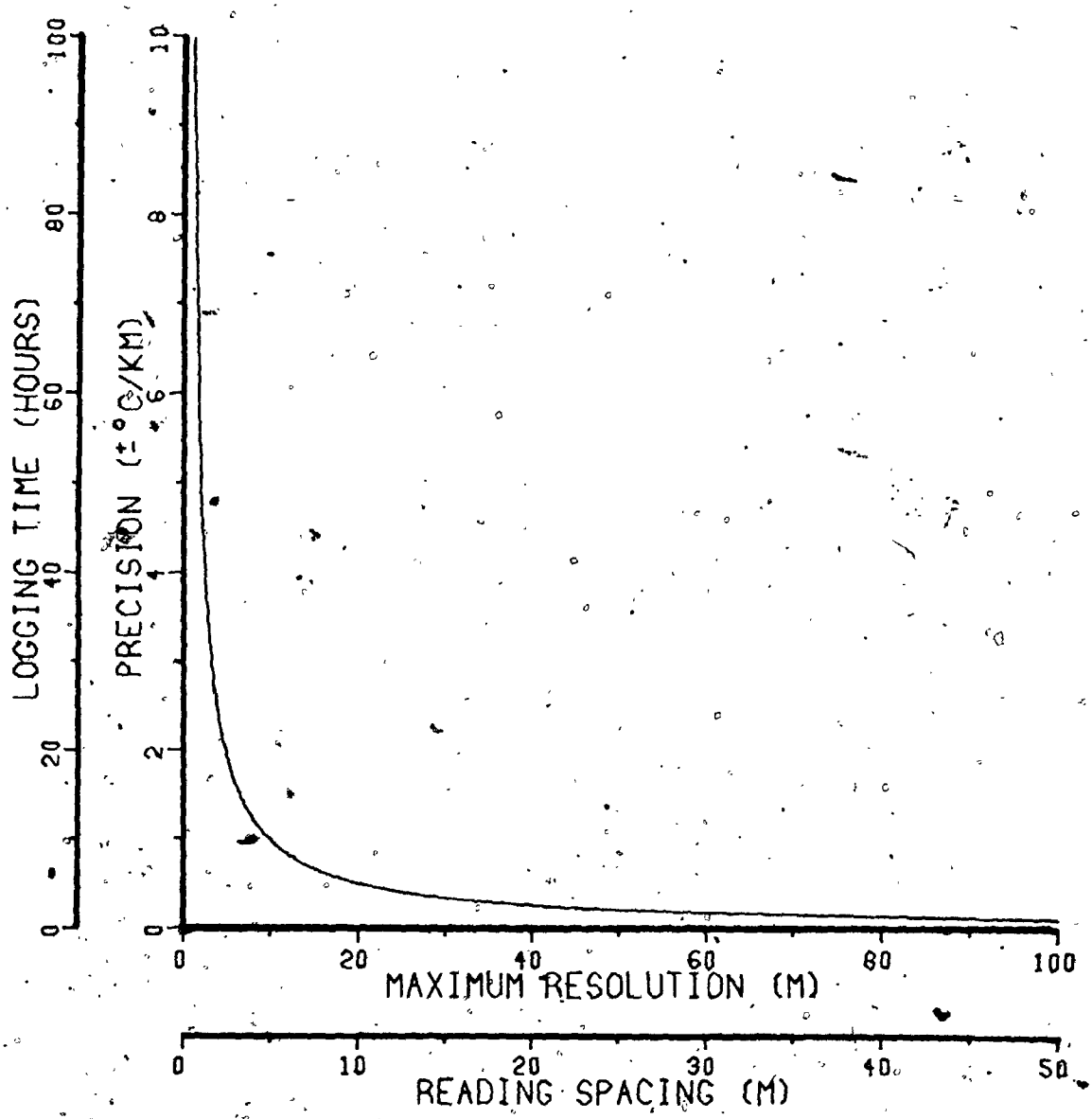

FIGURE 1.1: Precision, resolution and logging time for the incremental gradient logging technique, illustrating the diminishing returns for desired resolution better than about 10m. Figures are based on a 1 km borehole.

if high resolution is not required. Second, if resolution considerably better than 10 m is required, the logging time increases enormously. Third, as the spacing of the readings decreases, precision drops off sharply; other factors which were not included in figure 1.1, such as imprecision in depth interval determination, now become more important and contribute increasingly to the error. If reasonably good precision is to be maintained, some type of smoothing or data averaging technique must be employed, thereby requiring still more measurements in order to maintain resolution. In short, the incremental logging technique, while relatively simple and adequate for most terrestrial heat flow applications, is inadequate for applications where a precise T-log of high resolution is required.

Chapter 5 is devoted entirely to the consideration of possible practical applications of a high precision, high resolution continuous gradient logging technique, and a full discussion will be left until then. At this point it is sufficient to state that the primary stimulus and practical justification for this project originated in the work by Beck (1976a) showing a most remarkable inverse correlation between electrical resistivity logs (E-logs) and thermal gradient logs in two boreholes in Australia (see Chapter 5). Before these logs could be compared the E-logs, which were considerably more detailed than the incremental T-logs, they had to be smoothed over approximately 10 m intervals. It should be far more interesting instead to improve the

the T-log until it is comparable to that of the E-log. Perhaps a fine-scale stratigraphic correlation and structural mapping tool of considerable utility and value might emerge from such investigations. At the least, a high precision continuous gradient logging technique will spare the terrestrial heat flow investigator and others many hours of tedious field work, while producing results of superior quality.

CHAPTER 2

THEORETICAL DEVELOPMENT AND COMPUTER STUDIES

2.1 THEORETICAL BACKGROUND

General statistical deconvolution techniques are well developed in other geophysical areas such as seismology. In seismology it is common practice to assume a basic waveform (e.g. a Ricker wavelet), and use various techniques to identify combinations of these wavelets in the system output. One method for accomplishing this task is based primarily on the work of the American mathematician Norbert Wiener. Essentially, in this technique an input wavelet is assumed and a desired output (such as a spike) is specified. A filter operator is then derived which minimizes the mean square error between the desired output and the actual output. When noise is present in the input, the statistical properties of this noise may be incorporated to design an operator which simultaneously contracts the input wavelet and improves the signal to noise ratio. Due to the overall utility of this technique for many applications, a great deal of literature is available on the subject, especially Rice (1962), and a considerable volume of work by Robinson and Treitel (c.f. Robinson (1967b), Robinson and Treitel

Treitel (1967)).

There are, however, important differences between seismology and continuous temperature logging. In temperature logging, it is easy to determine the system impulse response by exposing the thermistor to a step temperature change and differentiating the response. This will be considered in greater detail later in this chapter. In seismology, the system includes the sections of the earth through which the seismic waves travel, and the output signal from the seismometer includes the modifying effects of these ray paths. Although the seismometer can be calibrated and its impulse response determined, it is not easy to determine the impulse response of these ray paths. Since the complete system impulse response can be determined precisely in the temperature logging case, it should be possible to approach the deconvolution problem analytically. Direct development of a deconvolution operator based on the known system impulse response for this specific case would eliminate the need for a more general statistical approach to the deconvolution problem. Costain (1970) considered the specific problem of deconvolution of temperature logs, but confined his work to theoretical aspects. A brief outline of his procedure follows.

The output from any physical system (y(t)) is equal to the input to the system (x(t)) convolved with w(t), the impulse response of that system (c.f. Kanasewich, 1973):

$$(2.1) \qquad y(t) = \int_{-\infty}^{\infty} w(\tau)\, x(t-\tau)\, d\tau$$

where t is time and τ is a delay term. More simply, this can be written as

$$(2.2) \qquad y(t) = w(t) * x(t)$$

In the case of thermal logging the input is the borehole temperature profile, a function of probe position or, assuming that the probe is lowered at a constant rate, time. The output is the recorded output of the measuring instrument. In order to recover exactly the temperature profile in the borehole, the system output is convolved with an operator which is the inverse of the system impulse response or

$$(2.3) \qquad x(t) = \int_{-\infty}^{\infty} w^{-1}(\tau)\, y(t-\tau)\, d\tau = w^{-1}(t) * y(t)$$

Assume that the equipment to be used consists of a thermistor at the end of a cable, and a digital resistance meter. The step response of this system can be determined by exposing the thermistor to a step change in temperature and recording the output of the meter. The impulse response is then found by taking the time differential of the step response. A step temperature change can be obtained approximately by allowing the thermistor to reach a steady temperature in air, and then plunging it into a water bath.

which is maintained a few degrees above or below room temperature.

The unit step response of the system is approximately a pure exponential of the form

$$\theta(t) = 0 \qquad \text{for } t<0$$

$$\theta(t) = 1-\exp(-t/T) \qquad \text{for } t\geq 0 \tag{2.4}$$

where θ is temperature and T is the time constant of the system (the time required for the system to reach 1-1/e of the final temperature). Differentiating with respect to time gives the impulse response

$$f(t) = \frac{d}{dt}(1-\exp(-t/T)) = \frac{1}{T}\exp(-t/T) \tag{2.5}$$

Let $F(\omega)$ be the Fourier transform of $f(t)$, given by

$$F(\omega) = \int_{-\infty}^{\infty} f(t)\exp(-i\omega t)\,dt = \frac{1}{T}\int_{o}^{\infty}\exp(-\frac{t}{T}-i\omega t)\,dt = \frac{1}{1+i\omega T} \tag{2.6}$$

The inverse operator is then given by

$$F^{-1}(\omega) = 1 + i\omega T \tag{2.7}$$

and in the time domain

$$f^{-1}(t) = \frac{1}{2\pi}\int_{-\infty}^{\infty} F^{-1}(\omega)\exp(i\omega t)\,d\omega = \frac{1}{2\pi}\int_{-\infty}^{\infty}(1+i\omega T)\exp(i\omega T)\,d\omega \tag{2.8}$$

$$= \delta(t) + T\dot{\delta}(t)$$

where $\delta(t)$ is the Dirac delta function. Since we are using discrete rather than continuous data it is necessary to approximate this inverse operator. Costain procedes by assuming the delta function to be represented by a triangle of area A = 1 and base equal to two digitization intervals (figure 2.1a); the height, h, of the triangle is found from:

$$A = \frac{1}{2}(2\Delta t)h = h\Delta t$$

or

$$h = \frac{A}{\Delta t} = \frac{1}{\Delta t} \tag{2.9}$$

where Δt is the digitization interval. $\delta(t)$ is then approximated by two spikes located at $\pm\Delta t$ on the time scale, and with magnitude, H, equal to the slope of the side of the triangle (figure 2.1b), or

$$H = \frac{h}{\Delta t} = \frac{1}{(\Delta t)^2} \tag{2.10}$$

This is an incorrect approximation, as will be shown later. Before convolution of this operator with the measured temperature data it is necessary to normalize the operator so that the sum of the terms in the time domain equals one. In this case it is necessary to multiply each of the three terms by Δt, giving the normalized operator

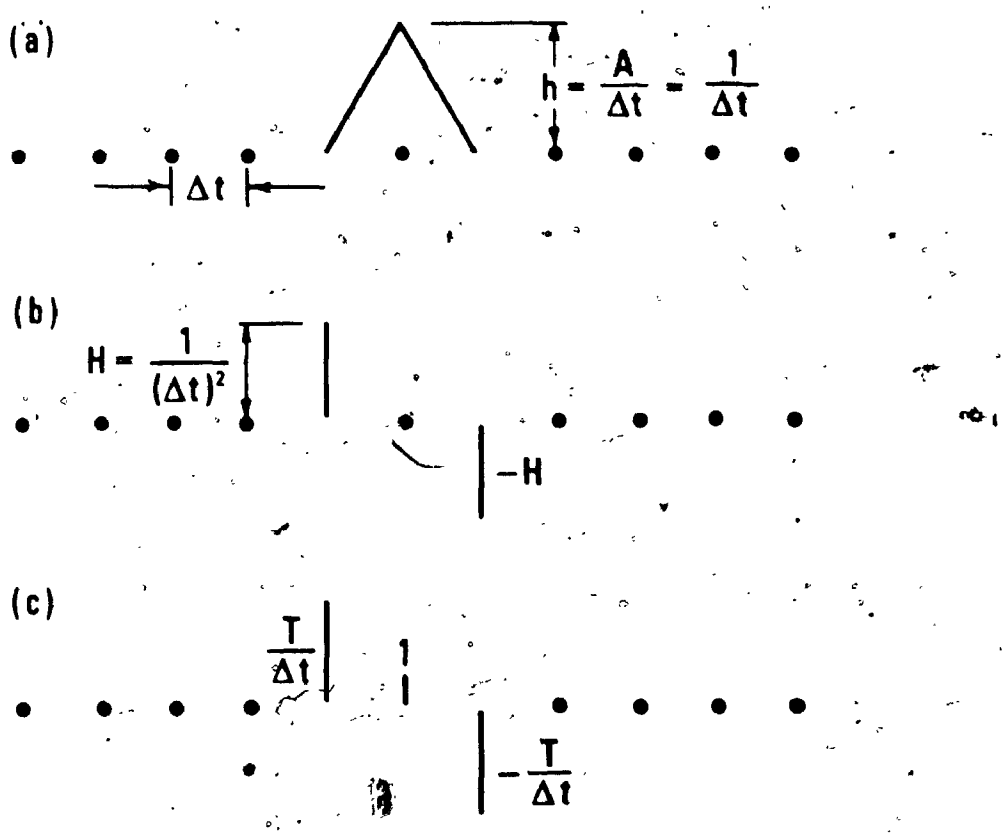

FIGURE 2.1: (a) Approximation of the Dirac delta function
(b) Approximation of the derivative of the delta function (incorrect)
(c) Resulting deconvolution operator (after Costain, 1970)

(2.11) $$f(t) = \left(\frac{T}{\Delta t}, 1, -\frac{T}{\Delta t} \right)$$

The entire deconvolution operator as given by Costain is shown in figure 2.1c.

A more rigorous approach is desirable, and such an approach will be used here for comparison. Applying equation 2.3 to the present case yields the following expression

(2.12) $$\Theta(t) = \int_{-\infty}^{\infty} (\delta(\tau) + T\delta'(\tau))\Theta_m(t-\tau)d\tau$$

or

(2.13) $$\Theta(t) = \int_{-\infty}^{\infty} \delta(\tau)\Theta_m(t-\tau)d\tau + T\int_{-\infty}^{\infty} \delta'(\tau)\Theta_m(t-\tau)d\tau$$

where Θ is actual temperature and Θ_m is measured temperature. Integrating the last term on the right-hand side by parts gives

(2.14) $$\Theta(t) = \int_{-\infty}^{\infty} \delta(\tau)\Theta_m(t-\tau)d\tau + T\delta(\tau)\Theta_m(t-\tau)\Big|_{-\infty}^{\infty} + T\int_{-\infty}^{\infty} \delta(\tau)\Theta_m'(t-\tau)d\tau$$

where the second term must be zero because of the implicit assumption that the energy in the time series is finite.

It is a property of the delta function (c.f. Hsu, 1970), that convolution with any ordinary function yields that function. In other words, $\delta(t)$ is the identity

operator for convolution, or

$$f(t) * \delta(t) = f(t) \tag{2.15}$$

Thus

$$\int_{-\infty}^{\infty} \delta(\tau)\theta_m(t-\tau)d\tau = \theta_m(t)$$

and

$$\int_{-\infty}^{\infty} \delta(\tau)\dot{\theta}_m(t-\tau)d\tau = \dot{\theta}_m(t)$$

or finally

$$\theta(t) = \theta_m(t) + T\dot{\theta}_m(t) \tag{2.16}$$

Consider a measured temperature profile consisting of five points, as shown in figure 2.2. Representing $\dot{\theta}_m$ at t_4 by

$$\frac{\theta_5 - \theta_3}{2\Delta t}$$

and substituting this expression in equation 2.16 gives

$$\theta\Big|_{t=4} = \theta_4 + \frac{T}{2\Delta t}\theta_5 - \frac{T}{2\Delta t}\theta_3 \tag{2.17}$$

On the other hand, the operator in equation 2.11 gives

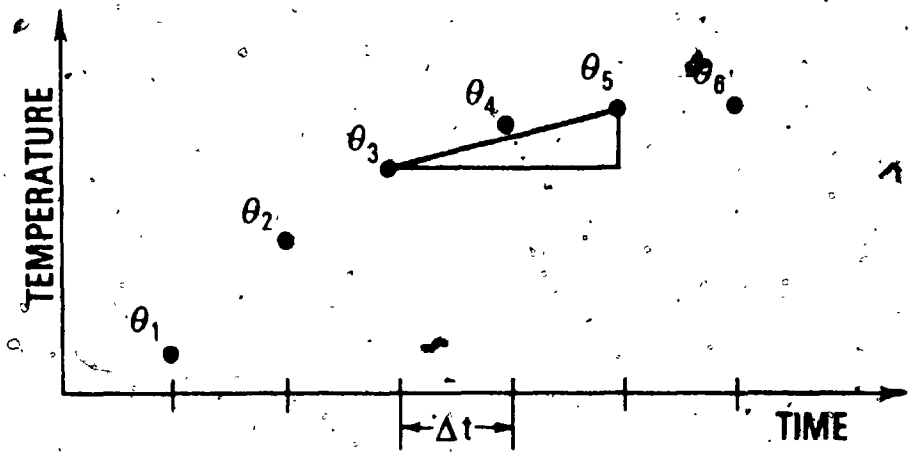

FIGURE 2.2: Technique for numerical differentiation of a time series, which will yield good results if the time series is fairly smooth, as is the case with borehole temperature profiles.

(2.18) $$\theta\Big|_{t=4} = \theta_4 + \frac{T}{\Delta t}\theta_5 - \frac{T}{\Delta t}\theta_3$$

when applied to the same data. It is apparent, then, that Costain's operator is in error, and that the actual operator should be

(2.19) $$f(t) = \left(\frac{T}{2\Delta t}, \; 1, \; \frac{-T}{2\Delta t} \right)$$

The source of this error is to be found in Costain's approximation of the derivative of a delta function. From elementary calculus it can be shown that the derivative of this triangle does not exist at the points $-\Delta t$, 0, or $+\Delta t$ (c.f. Johnson and Kiokemeister, 1964). It is clear however from equation 2.19 that if this (improper) derivative is to be approximated at $-\Delta t$, then its magnitude should in fact be the average of the left and right sided limits at that point, or half the slope of the side of the triangle. This error was presumably made in preparation of the manuscript or in publication, since Costain's several computed examples are correct.

2.2 COMPUTER APPLICATION OF THE THEORY

A temperature profile was generated with the following parameters:

Δt = 0.2 sec

T = 15.0 sec

v = 0.5 m/sec (rate of descent of probe)

This profile is the same as Costain's first example, and has

only 3 temperature gradients of 20.0, 6.7, and 13.3 °C/km respectively. The simulated temperature profile was next convolved with the impulse response of the system to yield a measured temperature profile. These profiles are shown in figure 2.3a. The theoretical actual and measured gradients were obtained at each point as shown in figure 2.2. These gradient profiles are shown in figure 2.3b.

When the derived deconvolution operator (equation 2.19) is convolved with the measured profile using the full precision of the digital computer, the actual gradient profile can be re-obtained with a high degree of accuracy. When the measured temperatures are rounded to the nearest 0.00001 °C, however, the results are as shown in figure 2.3c. This plot exhibits a great deal of noise, and the results are obviously badly degraded by the introduction of this slight amount of error.

A number of further profiles were simulated, deconvolved, and the gradients calculated, and it was found that given the extreme precision maintained at all stages of the calculations by a digital computer, the theoretical deconvolution operator was capable of reproducing any reasonable (or even physically unreasonable) temperature gradient profile to a very high degree of accuracy. This is not satisfactory, however, since the accidental introduction of a very small amount of noise into the calculations has a disasterous effect on the gradient profile, as shown in figure 2.3c. This is due to the fact that the gradient

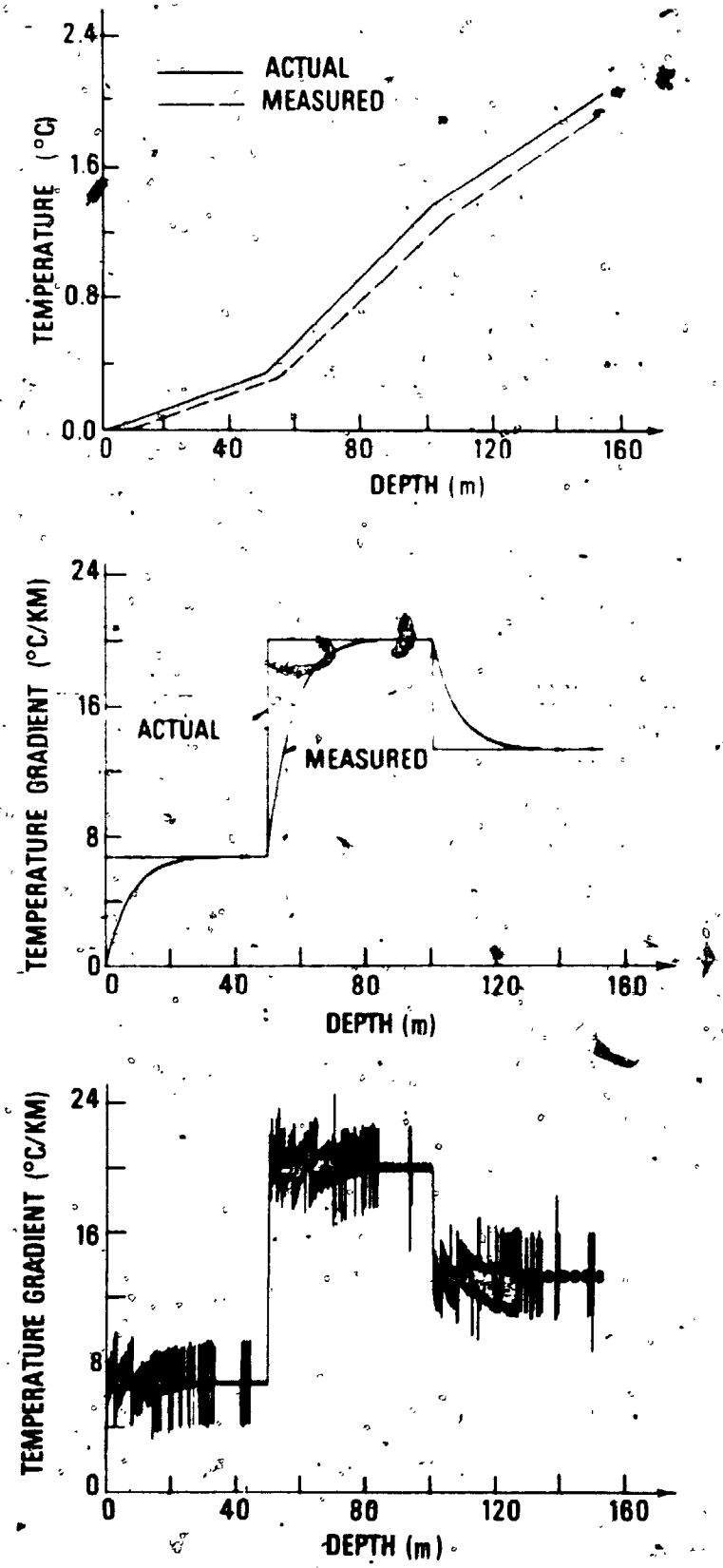

FIGURE 2.3: (a) Simulated actual and measured temp. profiles
(b) Actual (or deconvolved) and measured gradients
(c) Effect of 0.00005°C noise on gradients

$$\theta'(t) = \frac{d}{dt}(\theta_m(t)+T\theta_m'(t)).$$

$$\theta'(t) = \theta_m'(t) + T\theta_m''(t) \tag{2.20}$$

includes both the first and second derivatives of the measured temperature profile, and numerical differentiation accentuates high-frequency noise. Thus the procedure as presented up to this point works quite well under the artificial and nearly noise free conditions of computer simulations, but fails when a small amount of error creeps into the system. Costain mentions the noise problem, but his estimates of the magnitude of noise to be expected in the field have proven to be far too low. It has been our experience that the noise level in the recorded temperature data is so high that a deconvolution scheme which gives primary consideration to noise reduction is to be desired. Costain recommends widening the base of the triangular approximation of the delta function to, say, 11 points and "adding additional positive and negative spikes to δ' ". He does not give details of this procedure, and the ambiguities associated with approximating δ and δ' (c.f. Brigham, 1974) make a more direct approach desirable.

2.3 DIRECT EXTRACTION OF THE DECONVOLUTION OPERATOR

As has been stated previously, the desired deconvolution operator is merely the inverse of the impulse response of the system. This leads to a direct method of

obtaining the desired operator, without making any assumptions as to the form of the step response or impulse response of the system. All that is required is to measure and record the step response of the system, differentiate it numerically, and divide the resulting impulse response into the Dirac delta function 1,0,0,... This may be accomplished analytically using Z-transforms or, more conveniently, by use of a polynomial division routine on the computer. The resulting deconvolution operator can be truncated to any desired length and applied directly to raw survey data to obtain (in theory) the actual temperature profile. The simplicity and directness of this approach give it a certain amount of appeal, and thus it was decided that its practicality be investigated with computer simulations.

Once again, for the purposes of simulation, the system unit step response was first assumed to be a simple exponential function of the form

$$\Theta(t) = 0 \qquad \text{for } t<0$$

$$\Theta(t) = 1-\exp(-t/T) \qquad \text{for } t\geq 0$$

as shown in figure 2.4a. This is differentiated numerically to give the impulse response, figure 2.4b. Dividing this into the delta function 1,0,0,... using polynomial division on the computer, one obtains a deconvolution operator directly. Figure 2.5 shows the NLOGN amplitude spectrum (see Robinson, 1967a) of a 1024 point deconvolution operator, as well as the spectra of 2 point, 4 point, and 8

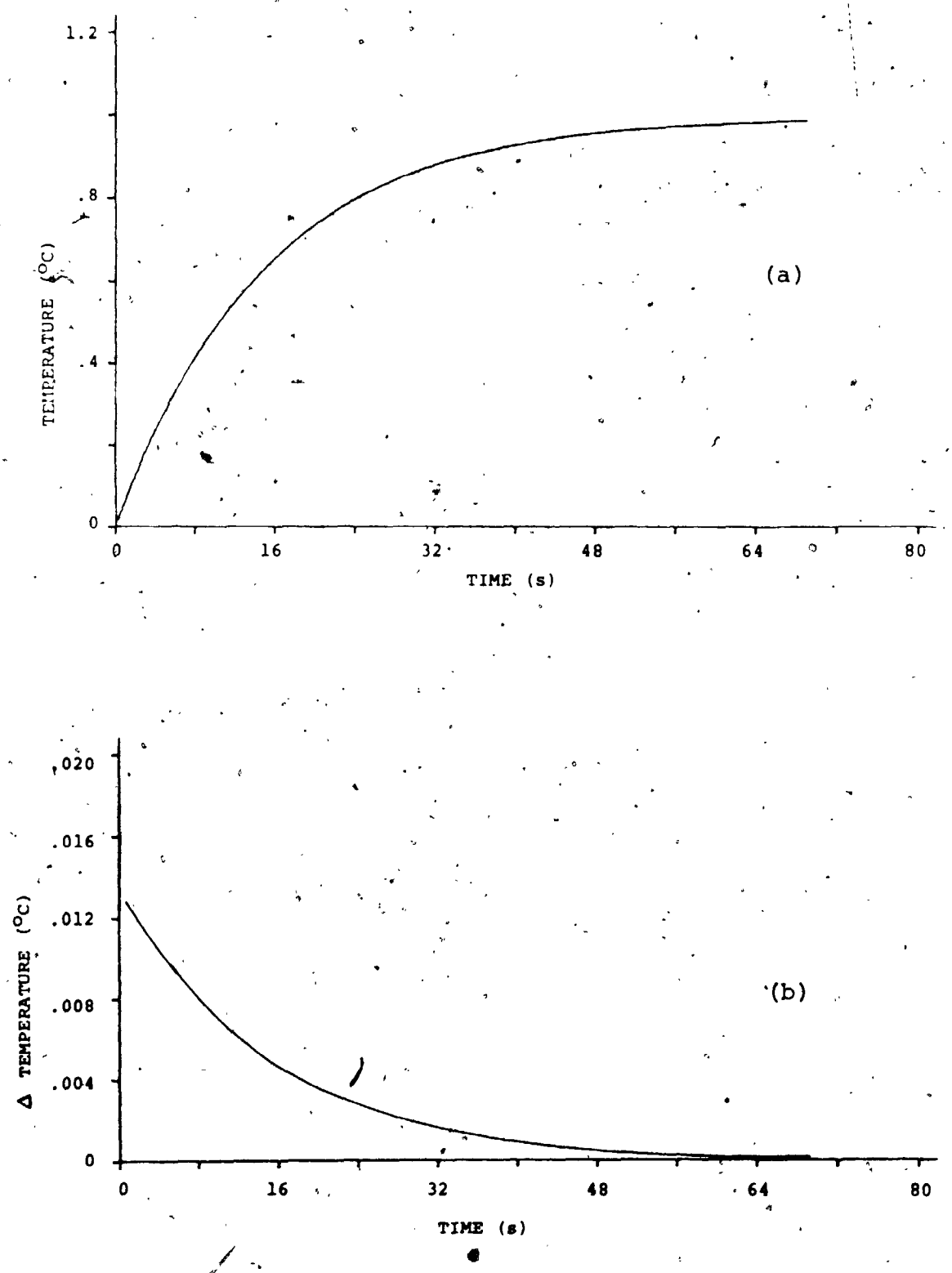

FIGURE 2.4: (a) Exponential step response of an ideal thermistor probe
(b) Corresponding impulse response

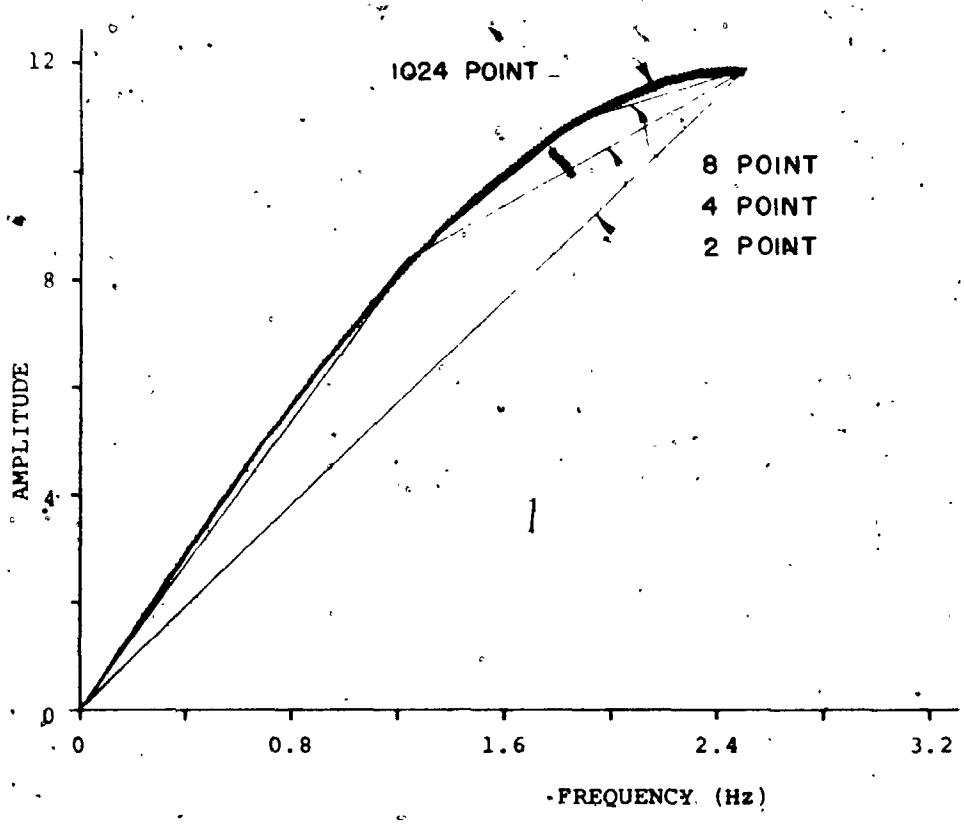

FIGURE 2.5: Amplitude spectrum of the direct deconvolution operator (noise-free).

point truncations of that operator. For the special case of a pure exponential step response, as assumed in this initial simulation, the deconvolution operator is essentially a minimum delay dipole, and could have been determined analytically using Z-transforms. Inclusion of more than two points in the deconvolution operator yields better resolution in the NLOGN amplitude spectrum, but since these extra points are very nearly equal to zero (in theory they are exactly zero), they have little effect in the deconvolution process. This two-point operator was tested on simulated data, and found to work well under noise-free conditions. For noiseless exponentials, this operator is superior to equation 2.19, as it is capable of transforming an exponential exactly into a spike.

Next, a small amount of pseudo-random noise was introduced into the step response (figure 2.6a). This noise was in the range between zero and ±10% of the amplitude difference between two adjacent time series points in magnitude. The step response was differentiated as before to yield the impulse response (figure 2.6b). This was then divided into a delta function to yield a deconvolution operator. The amplitude spectrum of the first 512 points is shown in figure 2.7, which is immediately seen to be radically different from the ideal case. Indeed, this operator is unstable due to its mixed delay nature, and will not converge with time. As the process of polynomial division is carried out further, the operator will approach

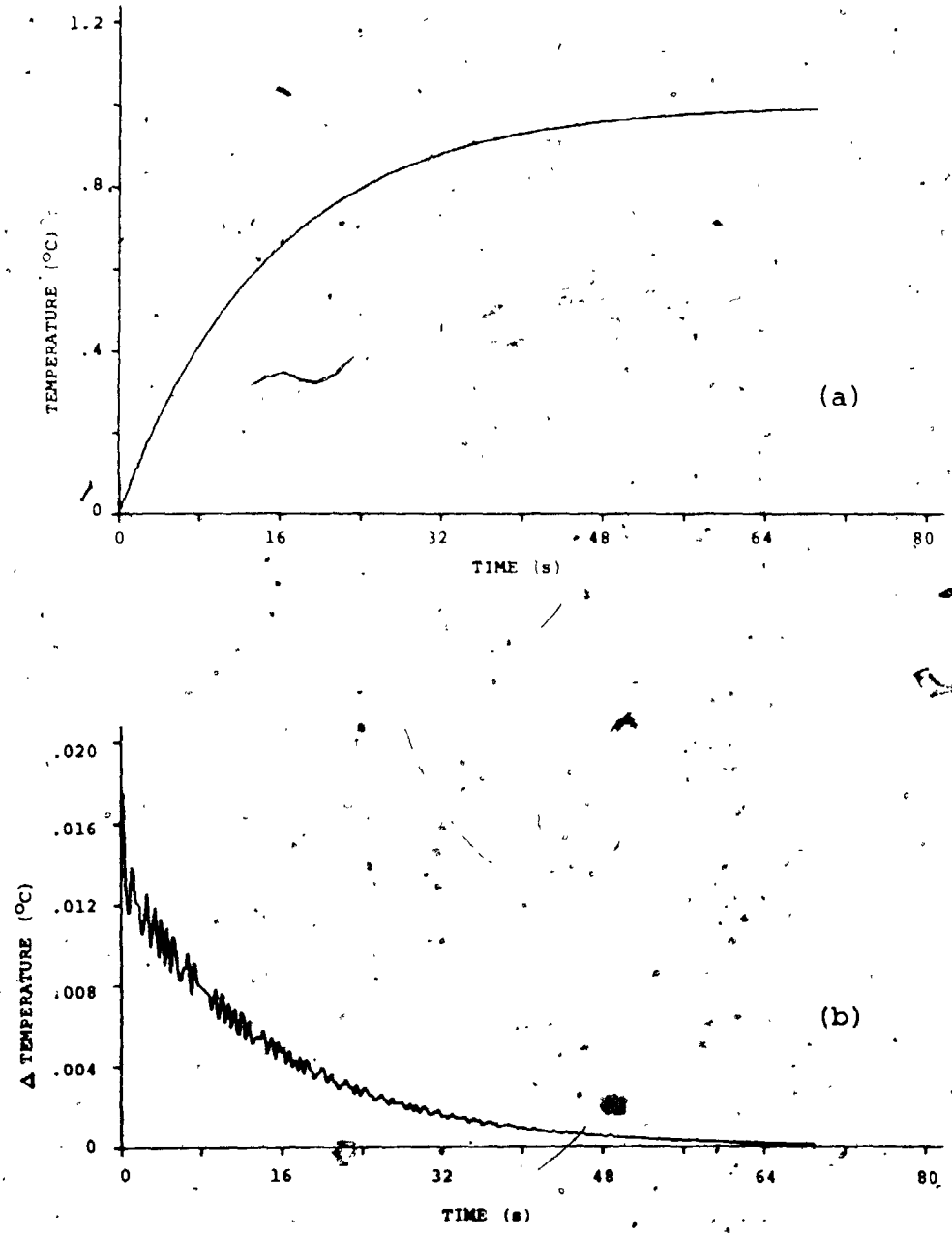

FIGURE 2.6: (a) Step response of ideal probe, with a small amount of noise added
(b) Resulting impulse response

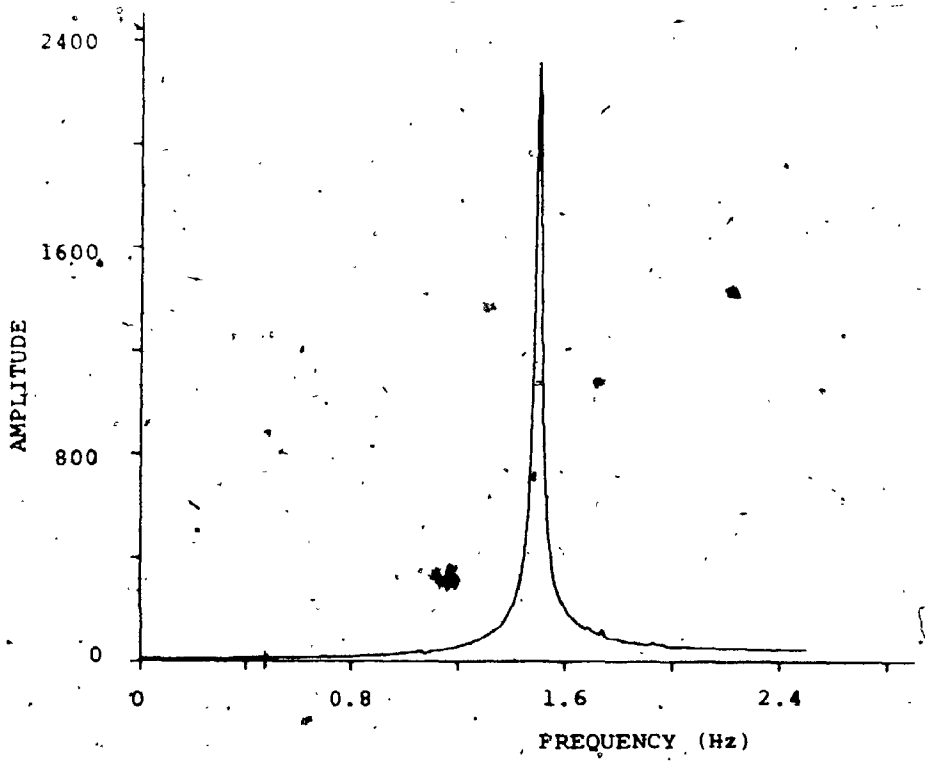

FIGURE 2.7: Amplitude spectrum of the unstable direct deconvolution operator.

infinite amplitude.

A stable inverse operator can be obtained in this case by factoring the Z-transform of the noisy impulse response into dipoles. Those dipoles which are minimum delay are divided into the Delta function to yield stable operators with a memory component only. The maximum delay dipoles are reversed, divided into the Delta function, and the quotients once more reversed to yield stable operators with an anticipation component only. The resulting anticipation and memory components are truncated to convenient lengths and combined by convolution to yield a stable, two-sided inverse filter (see Treitel and Robinson, 1964, for theory and details of this procedure).

The above approach to calculating the deconvolution operator has several major drawbacks.

(a) The noise present in computing the filter is not the same as the noise involved in actual experimental work.

(b) Errors are introduced into the filter by truncation of the anticipation and memory components before combining.

(c) Considerable computing time is involved in calculating the operator.

Because of the above problems, the direct approach to determining the inverse filter was discontinued, and a superior operator was developed, as outlined in the next section.

2.4 DERIVATION OF A USEFUL DECONVOLUTION OPERATOR

The equations for fitting a straight line to a set of

data by least squares techniques are given in most statistics texts (c.f. Miller and Freund, 1965). If the equation for the best fitting line is given as

$$y = a + bx$$

then the two normal equations

$$\sum_{i=1}^{n} y_i = an + b \sum_{i=1}^{n} x_i \tag{2.21}$$

and

$$\sum_{i=1}^{n} x_i y_i = a \sum_{i=1}^{n} x_i + b \sum_{i=1}^{n} x_i^2 \tag{2.22}$$

are solved simultaneously to give a and b. If, however, the x's are equally spaced (i.e., constant sample rate as in the present experiment), then

$$a = \frac{\sum_{i=1}^{n} y_i}{n} \tag{2.23}$$

and

$$b = \frac{\sum_{i=1}^{n} x_i y_i}{\sum_{i=1}^{n} x_i^2} \tag{2.24}$$

where the x's take the values

$$\ldots,-2,-1,0,1,2,\ldots$$

when n is odd, and

$$\ldots,-3,-1,1,3,\ldots$$

when n is even.

If the digitization interval is not unity, then it mus be included in the equations, as shown below:

$$b = \frac{\sum x_i y_i}{\Delta t \sum x_i^2} \tag{2.25}$$

One techniq for approximating the gradient of t temperature profile is to fit a straight line through number of points, calculate the slope, shift by o digitization interval, and repeat the procedure. Th technique results in a good approximation when temperature profile is a fairly gentle curve, as generally the case in actual boreholes. This procedure be accomplished in practice by convolution of a gradie operator, F_G, with the time series, where the j'th term F_G is given by

$$F_G\Big|_j = \frac{1}{\Delta t}\left\{\frac{x_j}{\sum_{i=k}^{-k}(x_i)^2}\right\} \tag{2.26}$$

where $k = \frac{1}{2}(N-1)$; where N is the number of terms in F_G.

Thus for example, if we wished to calculate gradient over 9 points, and if $\Delta t = 0.2$ sec, then

$$F_G = \frac{20}{60}, \frac{15}{60}, \frac{10}{60}, \frac{5}{60}, 0, -\frac{5}{60}, -\frac{10}{60}, -\frac{15}{60}, -\frac{20}{60}$$

Extension of F_G to greater numbers of terms increases smoothing effect. As always there is a trade-off bet reduction of undesirable noise and destruction of us

information.

Recalling equation 2.16:

$$\theta(t) = \theta_m(t) + T\dot{\theta}_m(t)$$

the term $\theta(t)$ can be found approximately by convolving $\theta_m(t)$ with a deconvolution operator, F_D, where

(2.27) $$F_D = TF_G + 1$$

where the term 1 is located at time t = 0 or, for the nine term example of F_G given above,

$$F_D = \frac{20T}{60}, \frac{15T}{60}, \frac{10T}{60}, \frac{5T}{60}, 1, \frac{-5T}{60}, \frac{-10T}{60}, \frac{-15T}{60}, \frac{-20T}{60}$$

A further smoothing effect can be accomplished by replacing θ_m by a term $\bar{\theta}$ (or 'a' in equation 2.23). This is the same as convolving θ_m with the smoothing operator F_S where

$$F_S = \frac{1}{n}, \frac{1}{n}, \frac{1}{n}, \ldots\ldots$$

where n is the number of terms in the operator. If there are 9 terms then each term would be 1/9. An improvement on this is to weight the terms so that those nearest a given point have more effect on the value of $\bar{\theta}$ at that point. One common set of weighting factors corresponds to the familiar 'bell' curve. Whatever form the smoothing operator takes, the sum of the terms in the time domain (A) must be equal to 1. Otherwise, if a DC signal of amplitude Y_1 is

convolved with F_S, the signal will be shifted to a new value $Y_2 = AY_1$.

Considering all of these operators together and noting that convolution is associative, commutative, and distributive (c.f. Kanasewich, 1973), an expression for temperature gradient, $\Theta'(t)$, can be derived:

$$\Theta'(t) = F_G * (\Theta_m(t) + T\bar{\Theta}_m'(t))$$

$$= F_G * (\Theta_m(t) * F_S + (T\bar{\Theta}_m(t)) * F_S * F_G)$$

$$= \Theta_m(t) * F_S * F_G + (T\Theta_m(t)) * F_S * F_G * F_G$$

$$= (1 + TF_G) * (\Theta_m(t) * F_S * F_G)$$

where the term $(1 + TF_G)$ can be recognized as the expression for F_D (equation 2.27). Thus

$$\Theta'(t) = \Theta_m(t) * F_D * F_S * F_G \tag{2.28}$$

The last three terms on the right-hand side may be combined by convolution to produce a single operator which, when convolved with the measured temperature profile, gives the smoothed, deconvolved gradient profile directly.

2.5 TESTING THE COMBINED OPERATOR

As an example of this type of combined operator, figure 2.8a shows a 17 point gradient term, figure 2.8b shows the corresponding 17 point deconvolution term, and figure 2.8c shows a 43 point smoothing term of the stretched cosine

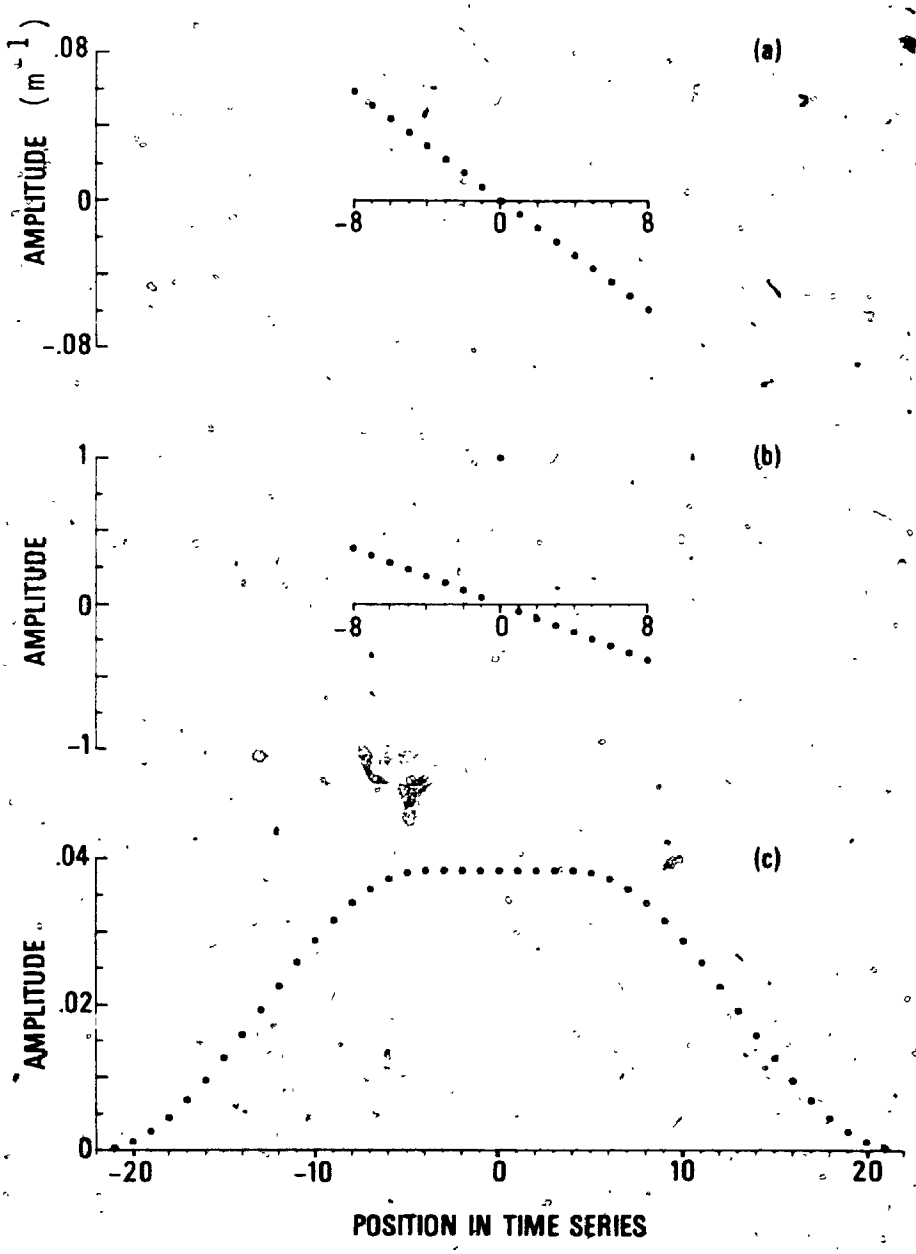

FIGURE 2.8: (a) Example of a 17-pt gradient operator
(b) Corresponding 17-pt deconvolution operator
(c) Example of a 43-pt smoothing operator of the stretched cosine-bell type.

bell type. These are combined by convolution to yield the general operator, figure 2.9. The NLOGN amplitude spectrum (see Robinson, 1967a) for this operator is shown in figure 2.10. The abscissa of this graph is plotted as the inverse of space frequency, wavelength, and shows a high cut-off point at approximately 1-2 meters for this particular case.

A theoretical temperature profile was generated by the superposition of a number of ramps and sine waves of various frequencies (figure 2.11) using the following parameters:

$T = 6.5$ sec

$\Delta t = 0.33$ sec

$V \sim 0.5$ m/sec

This profile was convolved with the theoretical impulse response of the thermistor to give a measured temperature profile, which was then convolved with the general operator to give the deconvolved temperature gradient directly (figure 2.12b). This figure can be compared with figure 2.12a, the actual theoretical gradient. The curve given by the general operator is in good agreement in both shape and amplitude with the theoretical gradient profile, with some smoothing apparent on the sharp corners.

Next, a certain amount of error was introduced into the measured temperature profile. First the data were rounded to the nearest $0.001\,^{\circ}C$ (the approximate precision of our equipment under ideal conditions), then a pseudo-random number algorithm was used to introduce noise of magnitude up to $0.01\,^{\circ}C$, then to $0.1\,^{\circ}C$. The results from the first case

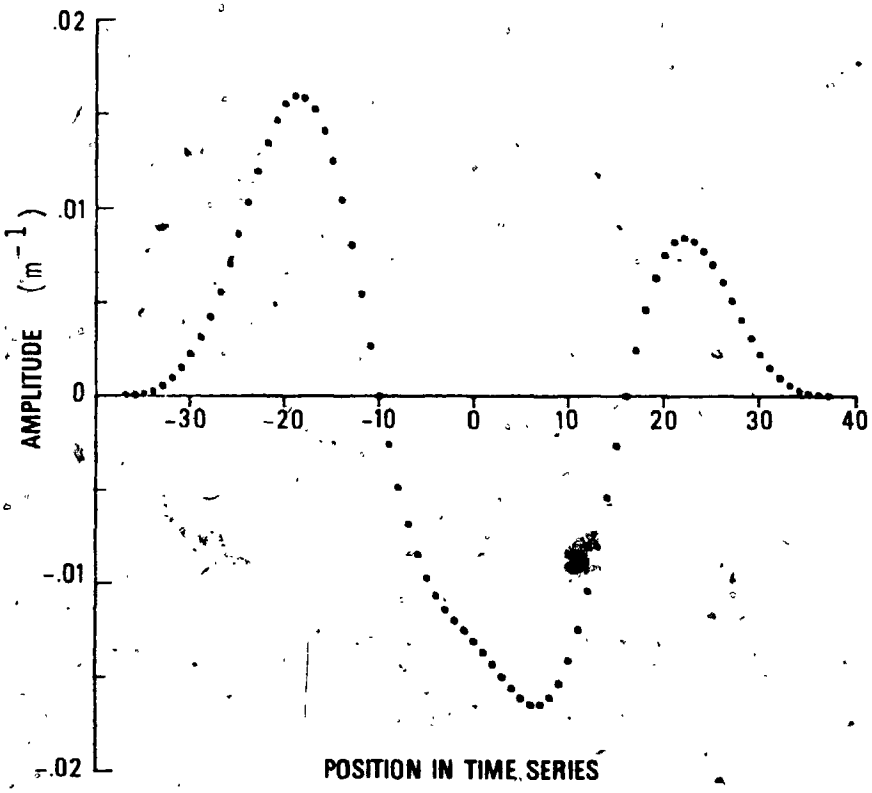

FIGURE 2.9: Example of a 75-point combined operator, made up of the smoothing, deconvolution and gradient terms shown in figure 2.8.

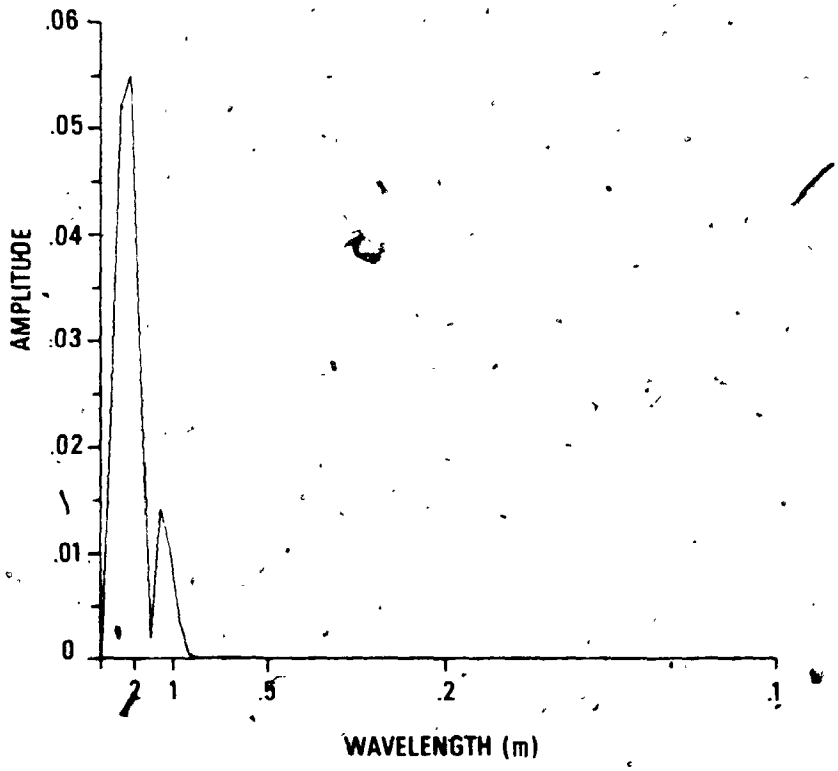

FIGURE 2.10: Amplitude spectrum of the combined operator shown in figure 2.9.

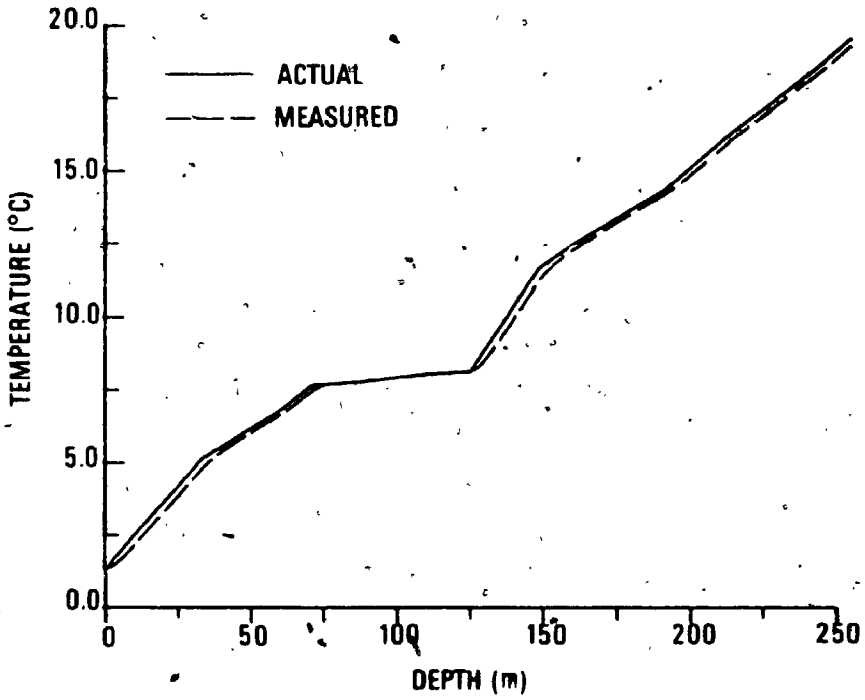

FIGURE 2.11: Simulated actual and measured temperature profiles, for testing the combined operator.

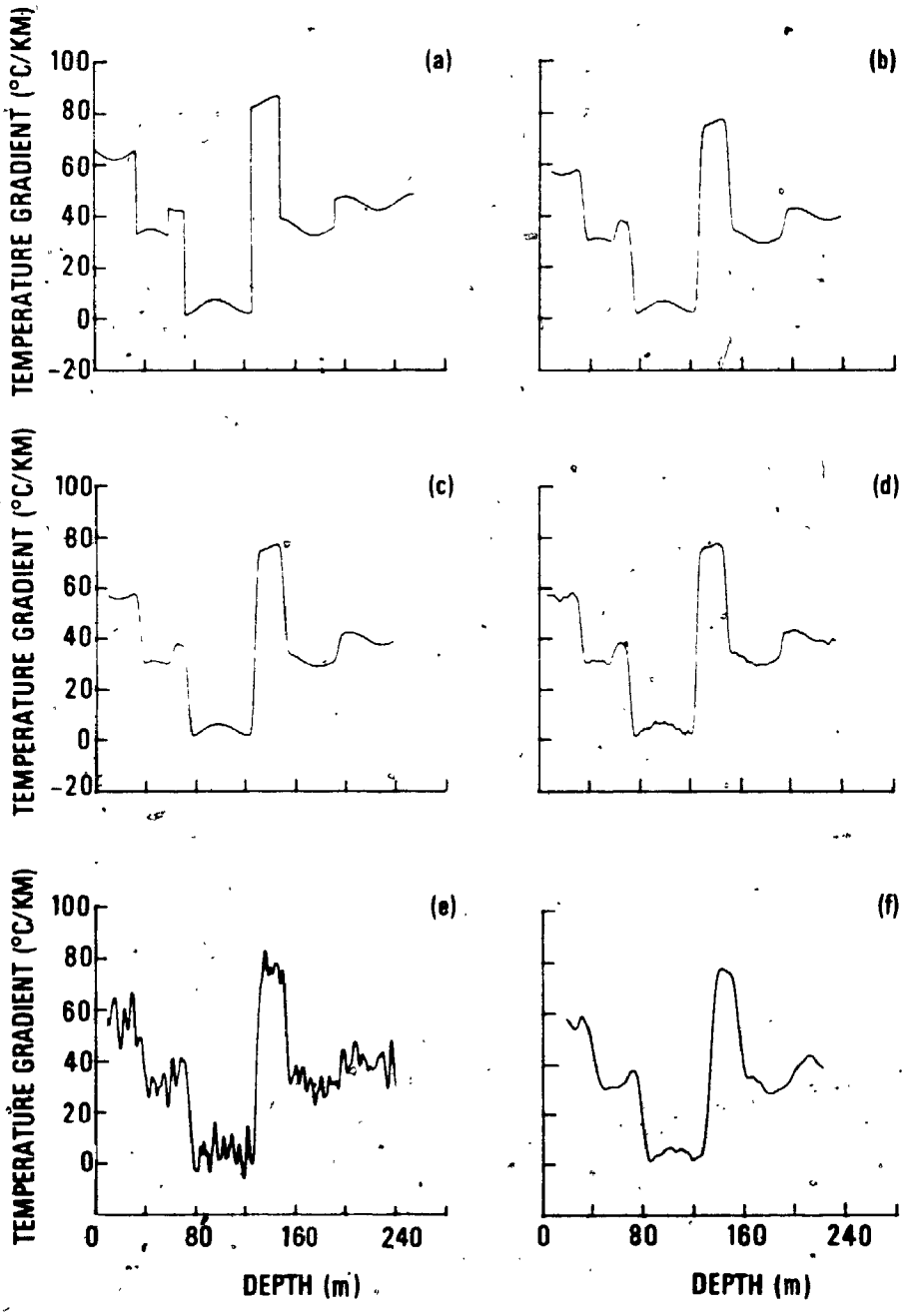

FIGURE 2.12: (a) Theoretical deconvolved gradient profile
(b) Deconvolved by combined operator, no noise
(c) Measured data rounded to nearest 0.001°C
(d) Random error of ±0.01°C added to data
(e) Random error of ±0.1°C added to data
(f) Operator length doubled

were very good (figure 2.12c), from the second case fair (figure 2.12d), and from the third case (figure 2.12e) poor, but, considering the gross noise level represented by this amount of error, the results are surprisingly recognizable. If 3-point gradient and deconvolution operators are used without smoothing on this same data, the error in gradient is approximately 6×10^{4} ^{o}C/km. Figure 2.12f shows the effect of doubling the operator length. Considerable noise reduction is realized, although it is apparent that if the operator is extended excessively, it will eventually smooth away the signal as well as the noise.

2.6 THE EFFECT OF ERRORS IN TIME CONSTANT DETERMINATION.

Figure 2.13a shows the deconvolved temperature gradient profile using the correct assumed time constant T = 6.5 sec. Figure 2.13b shows the gradient when an erroneous time constant T = 13 sec is used in deconvolution. Figures 2.13c and 2.13d show the effects of deconvolving with assumed T = 3.25 and T = 0 sec respectively. The shapes of the curves are distorted and there is some depth displacement. Considering the large magnitude of these assumed time constant errors, however, the deconvolution operator can be considered to be fairly insensitive to small errors in thermistor time constant determination. This is important, since there is some difficulty in achieving precise time constant determinations under actual field conditions. From what has been said above it is apparent that a laboratory determination of time constant should be quite sufficient.

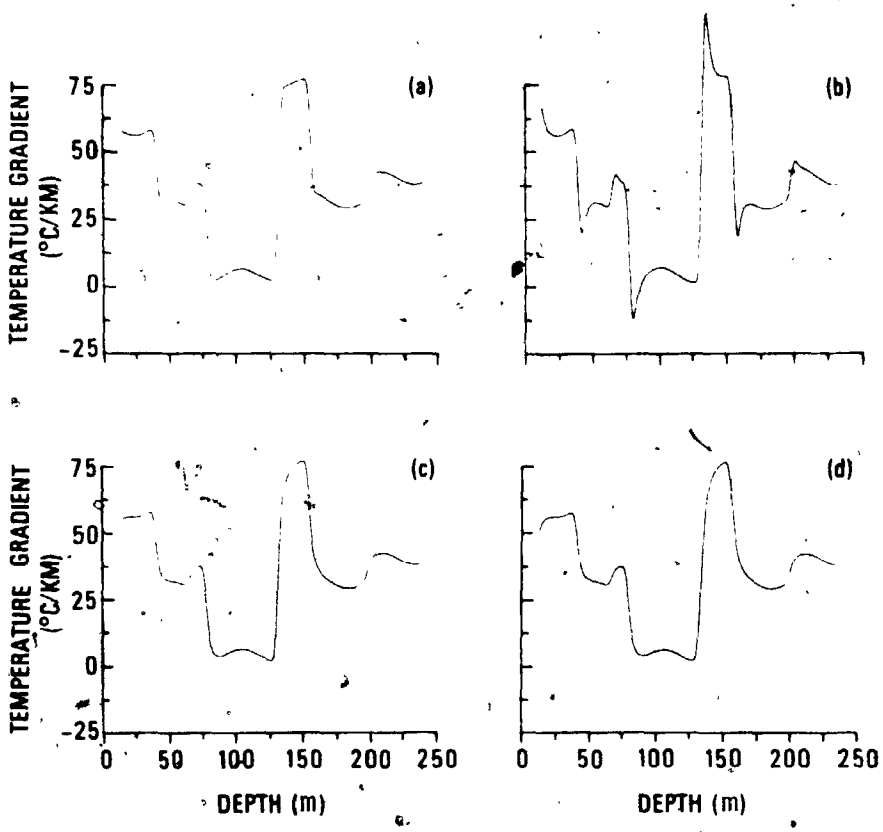

FIGURE 2.13: (a) Deconvolved data using correct time constant (T=6.5 sec)
(b) Deconvolved data using assumed T=13 sec
(c) Deconvolved data using assumed T=3.25 sec
(d) Deconvolved data using assumed T=0 sec

Under some conditions it is acceptable to neglect the thermistor time constant entirely. This is true if a thermistor with a very small time constant is lowered at a small velocity. The inclusion of deconvolution in the combined operator is not difficult, however, and it makes the method completely general. In the majority of cases the probe response should not be neglected, especially in mud-filled holes where heavy-duty logging equipment must be used. Generally, probes having small time constants are fragile and contain tiny thermistors which are susceptible to self-heating effects. They have the advantage in continuous logging of an enhanced resolution threshold. As usual, a trade-off must be made.

In the development of the deconvolution operator (equation 2.27), the system was assumed to have a pure exponential unit step response (equation 2.4). This was then differentiated to give an exponential impulse response. In actual physical systems the step response will never be a true exponential. Figure 2.14a shows an experimentally determined step response for thermistor probe C-20 (see Appendix B), along with the theoretical exponential step response having the same 1-1/e time constant (T=10 sec). The differences between the theoretical and experimental curves appear to be minor, but what is the effect of ignoring this deviation? Figure 2.14b shows the same experimental curve along with a theoretical step response of time constant T=8.5 sec, which has been smoothed by

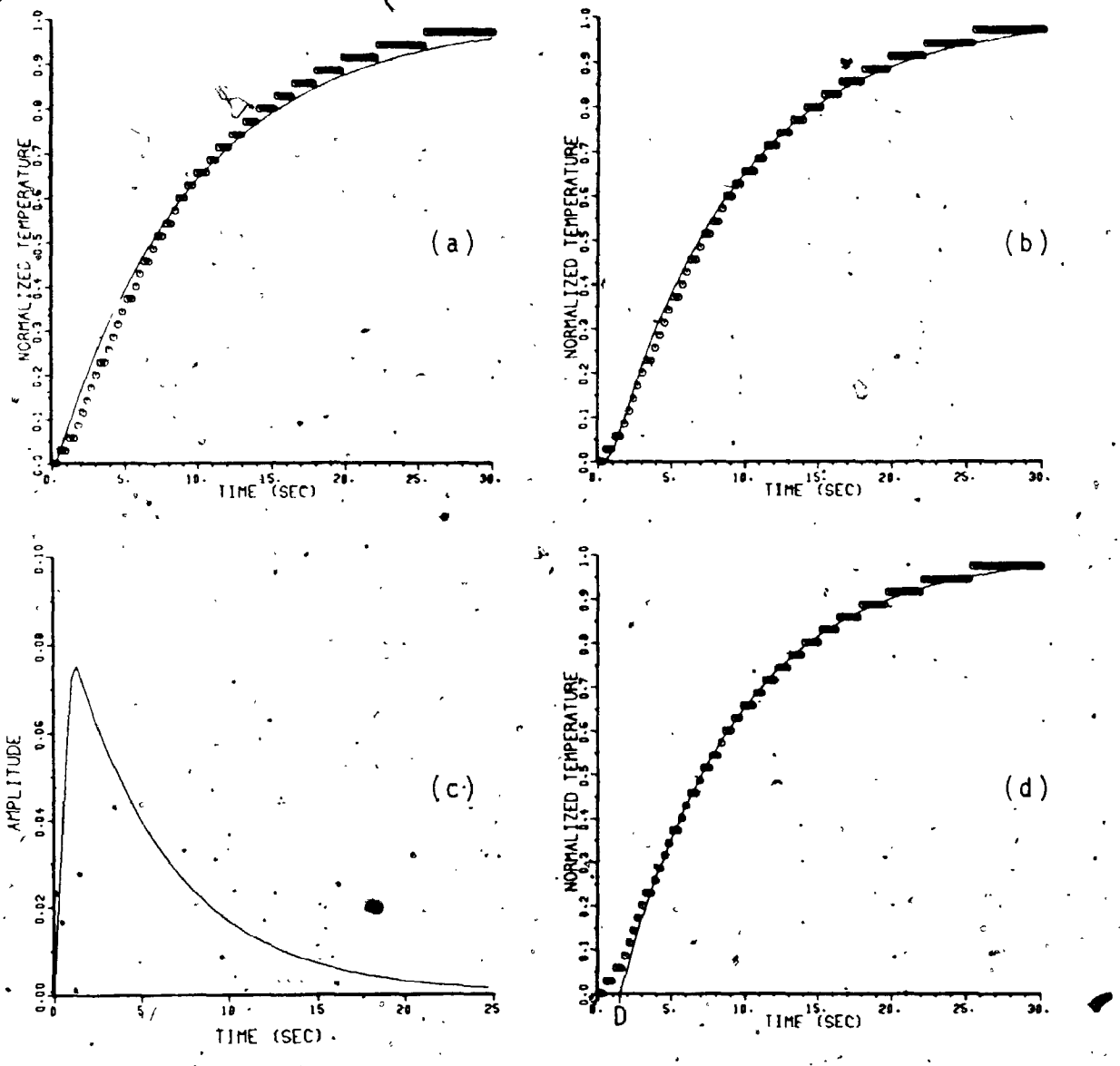

FIGURE 2.14: (a) Experimentally determined probe step response curves (open circles), and the pure exponential having the same 1-1/e time constant. The experimental points are positioned at discrete increments of 0.3 sec in time and 1 ohm in 'temperature'.
(b) Smoothed exponential step response, as described in text
(c) Impulse response corresponding to (b)
(d) Pure exponential response delayed by D sec

convolution with a 5 point cosine bell low pass filter (sample interval $\Delta t=0.3$ sec). Clearly this is a better fit to the data, and this curve will serve to simulate the actual response. The impulse response corresponding to this actual step response was obtained by differentiation, and is shown in figure 2.14c. Another approximation of this actual step response is a pure exponential, offset from zero time by an initial delay of D seconds (figure 2.14d).

In order to investigate the error involved in assuming a pure exponential step response, the theoretical 'actual' temperature profile shown in figure 2.11 was convolved with the actual impulse response (similar to figure 2.14c) using time constant T=5.75 sec to give a measured temperature profile. This was then deconvolved three different ways:

(1) Using a 75 point combined operator assuming T=6.5 sec (the 1-1/e time constant). The results are shown in figure 2.15a.

(2) Using a 75 point combined operator assuming T=5.75 sec (figure 2.15b).

(3) A second measured temperature profile was generated assuming a pure exponential impulse response with time constant T = 5.75 seconds. This was deconvolved using the 75 point combined operator with T = 5.75 seconds used in case (2) above. The gradient profile from this third technique is shown in figure 2.15c.

It is clear that some error results from deconvolving the data assuming an exponential step response (figure

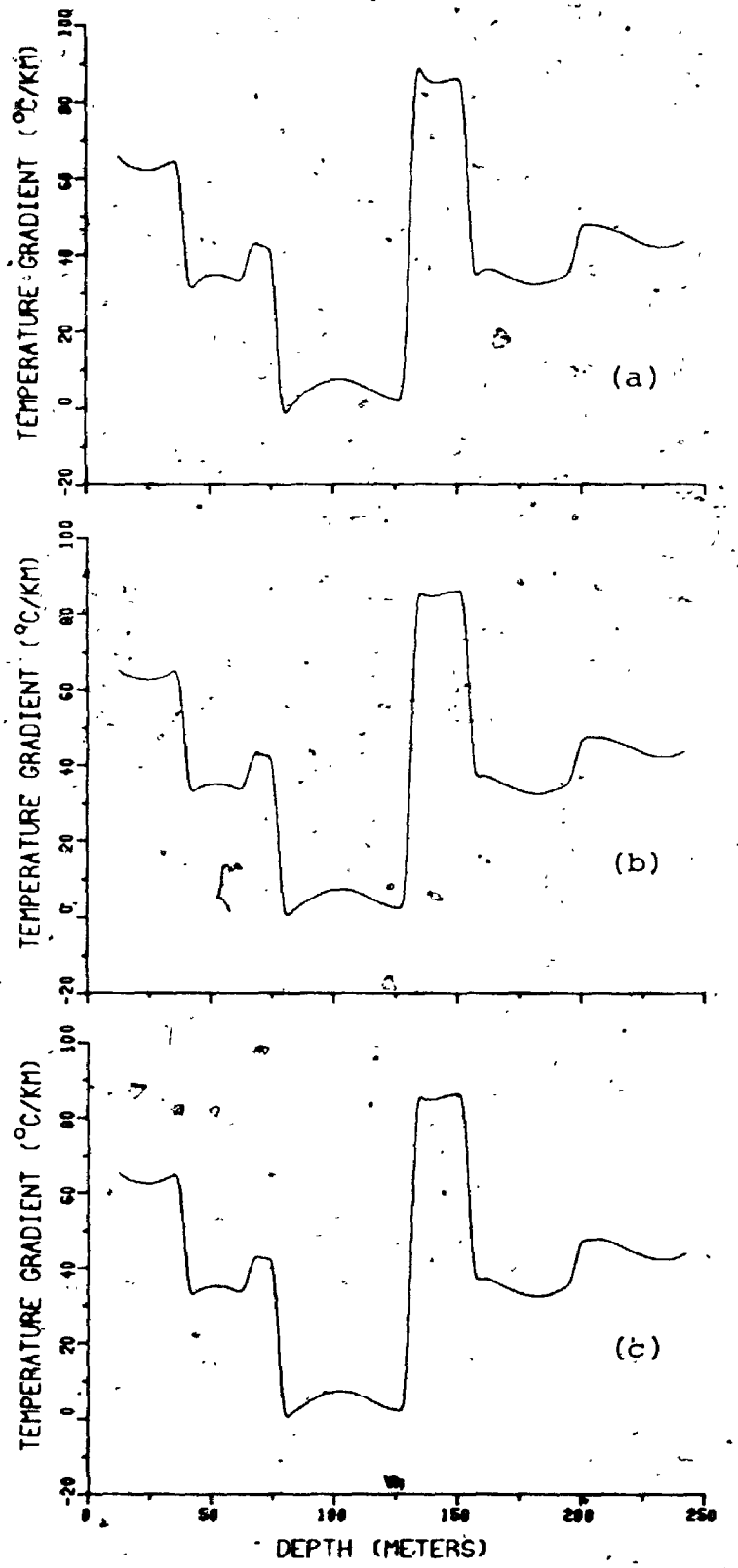

FIGURE 2.15: Effect of shape of the thermistor step response on the deconvolved gradient (see text).

2.15a). The overshoot in this figure is reminiscent of figure 2.15b, where the data were deconvolved using too long an assumed time constant. Figures 2.15b and 2.15c are very nearly identical in form. Although it is not obvious from these plots, ignoring the initial thermistor lag (figure 2.15b) causes a slight shift in depth of the results, in this case of approximately 0.6 meters (2 digitization intervals).

Considering the above results, a general procedure for deconvolving the measured temperature data may be developed:

(1) Determine an experimental step response curve for the thermistor probe.

(2) Fit an exponential curve of time constant T to the data, ignoring the initial lag of D seconds (see figure 2.14d).

(3) Deconvolve the data using the time constant T determined in step 2, and plot the results shifted in space in the sense opposite to the logging direction, and by an amount ΔZ meters where:

$$\Delta Z = (D)(V)$$

where V is logging speed in m/sec. The resulting gradient profile is a better approximation of the actual gradient than if a simple exponential step response is assumed. The error in gradient which results from using a delayed exponential response of the form shown in figure 2.14d,

rather than the true response (figure 2.14b) is quite small. In the preceding simulated example this error in gradient was less than 0.1%, and may be safely ignored.

2.7 OPTIMIZATION OF THE COMBINED OPERATOR

The relative contributions of the various terms in a combined operator of a given length were studied empirically through computer simulations. In each of the simulations the derivative and deconvolution operators were of the same length to simplify computation. The results of some of these studies are presented in figures 2.16a through 2.16f. Figure 2.16a shows the theoretical deconvolved gradient profile (noise free). Pseudo-random noise of ±0.05 °C was added to the measured temperature data, which were then deconvolved to yield figures 2.16b through 2.16f. Figure 2.16b was produced using a very long (71 point) stretched cosine bell smoothing operator (53 point flat plus 9 point half-bell on each end) and 3 point derivative and deconvolution operators, the minimum length which can be used for these latter terms. The results are very noisy, and the major features are poorly reproduced. In figure 2.16c the derivative and deconvolution operators have been lengthened to 17 points, while the smoothing term has been reduced to 43 points (7 point flat plus 18 point sides). The results are considerably improved. Figure 2.16d shows the gradient profile obtained using the same derivative and deconvolution terms as 2.16c, but with the smoothing operator being made up of a longer (25 point) flat and 9

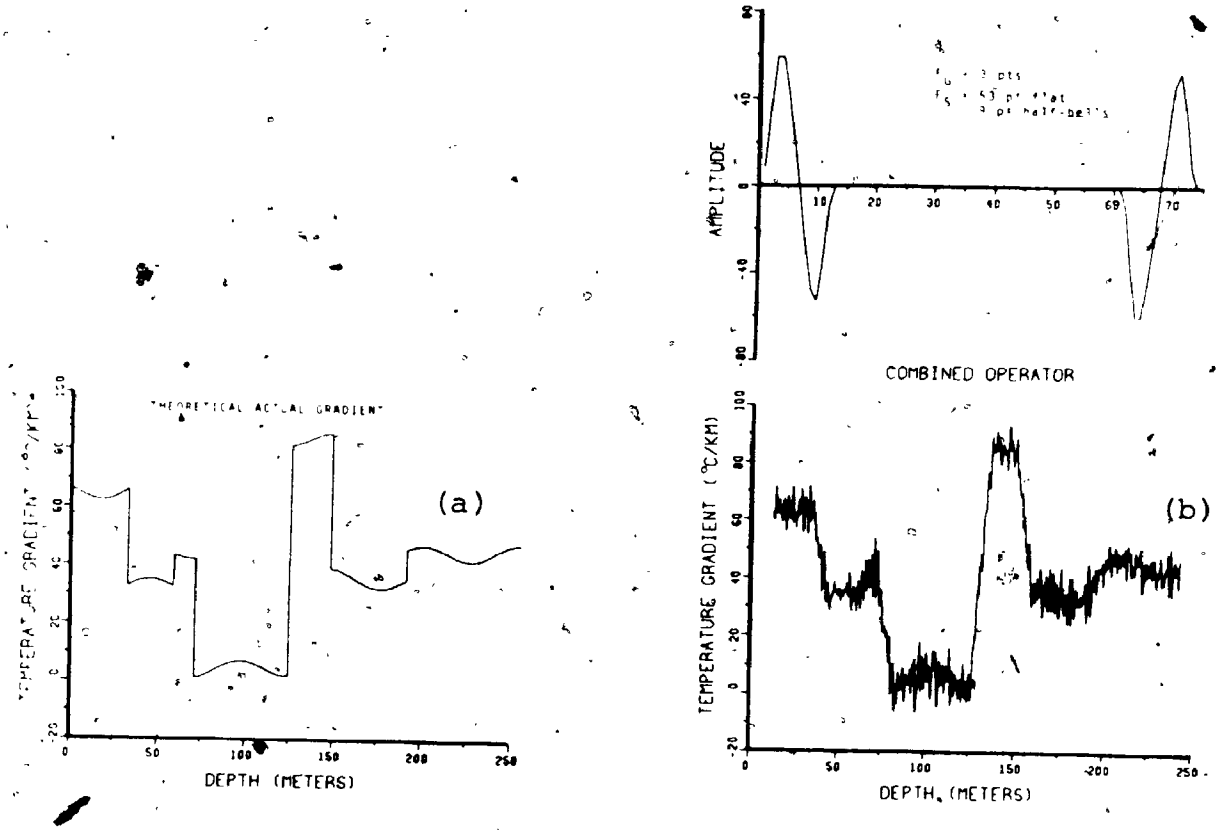

FIGURE 2.16: Effect of the relative lengths of the terms in the combined operator

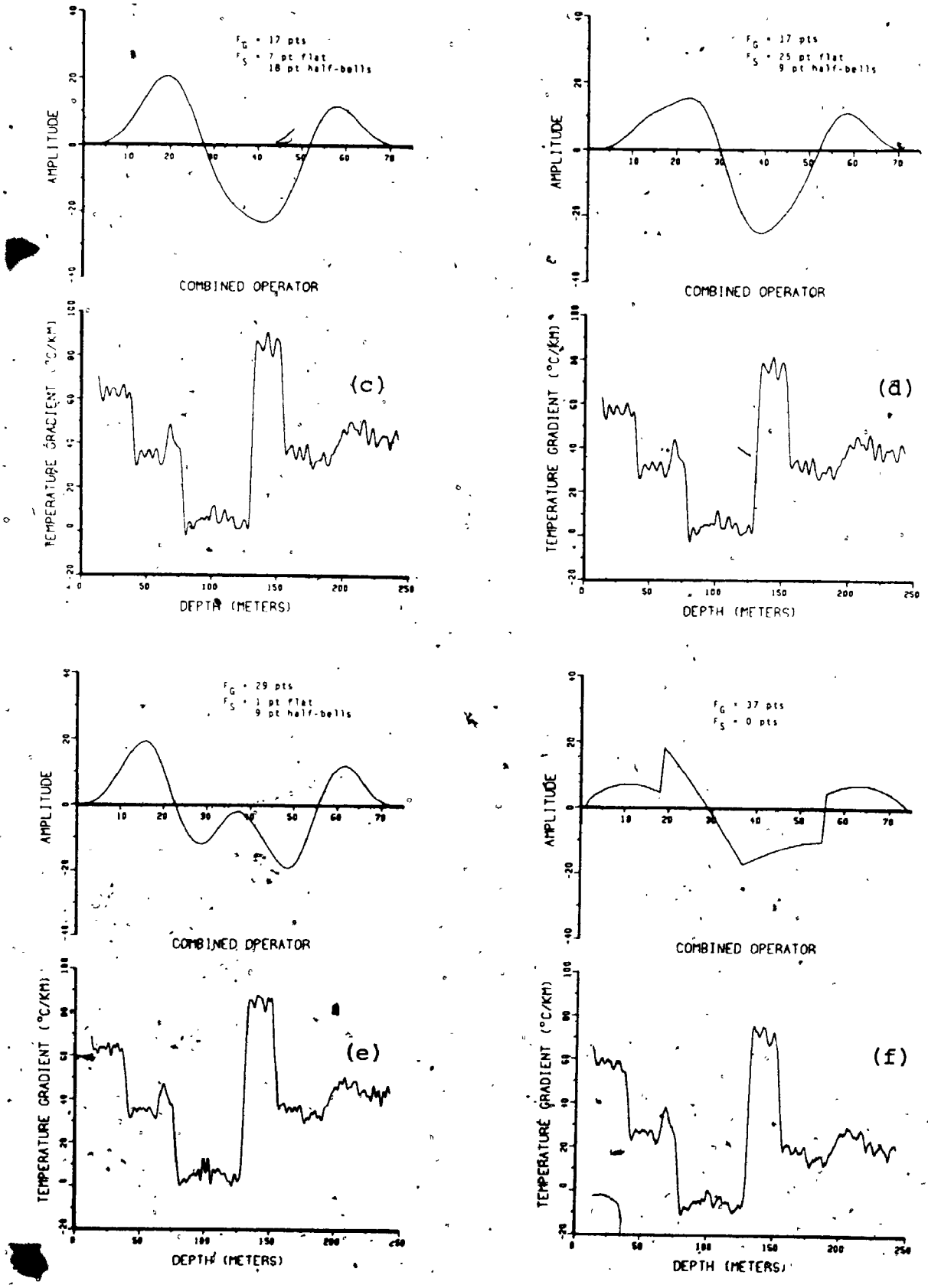

FIGURE 2.16 (continued)

point sides. The results are quite similar to 2.16c, with almost identical noise characteristics. The lengthened flat on the smoothing term causes a slight reduction in amplitude of the main features, especially noticeable in the positive event centered at approximately 150 m depth. Figure 2.16e was obtained using 29 point derivative and deconvolution operators, and a 19 point smoothing term (9 point sides). The results are essentially comparable in quality to figure 2.16c, with the noise of slightly higher frequency and perhaps slightly reduced amplitude. The final simulation presented here, figure 2.16f, shows the effect of leaving out the smoothing term entirely. This profile contains more high frequency noise than 2.16c, and the main features are shifted somewhat in amplitude from the theoretical.

The results of the simulations lead to the following conclusions. Essentially it may be stated that, although the relative lengths of the component terms of the combined operator are not critical, the extremes should be avoided. In general figures 2.16c and 2.16e probably represent the best compromises, and operators within this range should be used. It should be borne in mind that noise characteristics found in experimental data are likely to be different from the pseudo-random noise used in these simulations, and this factor may necessitate slight modifications in filter design.

Thus it is seen that a general operator has been developed which is fairly insensitive to noise and errors in

time constant determination, and which is capable of extracting a reasonably accurate gradient profile from experimentally obtained data. If higher precision is desired, it is possible to lower the probe more slowly, or increase the sampling rate with more sophisticated equipment, thereby increasing the number of points per meter. Thus we are able to preserve to a large extent the true form of the gradient profile, with most of its characteristic details. This is especially important if the continuous logging technique is to be applied to stratigraphic correlation.

This general operator is based directly upon a simple, analytically determined mathematical expression for deconvolution of the measured temperature data (equation 2.16). The derivation of this equation, and the fact that the complete system impulse response can be determined readily by laboratory techniques as described earlier, gives us a distinct advantage over seismologists and others. The seismologists do not know the impulse response of their entire system (including the earth, which acts as a filter), nor can they readily develop analytically a simple and precise deconvolution equation similar to 2.16 for their specific application. The great amount of investigation into statistical deconvolution techniques by seismologists and others represents an alternate approach to the problem which is obviated in the continuous logging technique by the factors discussed above.

Computation and application of the combined operator by the techniques given in Appendix A is a very efficient process, requiring little computer time and core memory. By contrast, the computation of the Wiener optimum operator is a fairly complicated and lengthy process involving considerable matrix manipulation. Tests indicate that the general operator can be computed in less than 1% the CPU time necessary for the Wiener optimum filter computation, using about half as much core memory. An eventual goal of this project is to incorporate a microprocessor unit into the logging equipment chain to allow plotting of the deconvolved gradient profile before leaving the borehole site. In this case these large differences in memory and processing time requirements are especially important.

Equation 2.16 can be applied in ways other than the one presented above to yield a smoothed, deconvolved temperature profile. Higher order curve fitting computer programs, such as a smoothing cubic spline routine, can be made to yield good results. The practicality of this approach was investigated on actual field data, and will be discussed briefly in Chapter 4.

CHAPTER 3

INSTRUMENTATION AND EQUIPMENT

The prototype equipment used in testing the continuous logging technique will be described in some detail in this chapter, and in Chapter 6. This system was assembled at moderate cost in order to investigate the feasibility of the technique. Some improvements in design and construction should be made before the system is put into routine use, and these will be discussed later in this chapter.

3.1 CABLE AND THERMAL PROBE ASSEMBLY

An example of a typical thermistor probe assembly is illustrated in figure 3.1. The sensing unit consists of 10 Fenwal GB 51 L1 glass bead thermistors wired in parallel. The nominal resistance of each thermistor is 100 kΩ at 20 ^{o}C. This arrangement allows optimization of time constant and resolution while minimizing self-heating effects. The thermistors are embedded in epoxy resin, inside a small brass tube. One end of this tube is inserted into a cylindrical teflon shell wherein the electrical connections to the cable are made. This shell is also filled with epoxy. The teflon tube is clamped into the end of a brass split weight, which is streamlined in the form used to

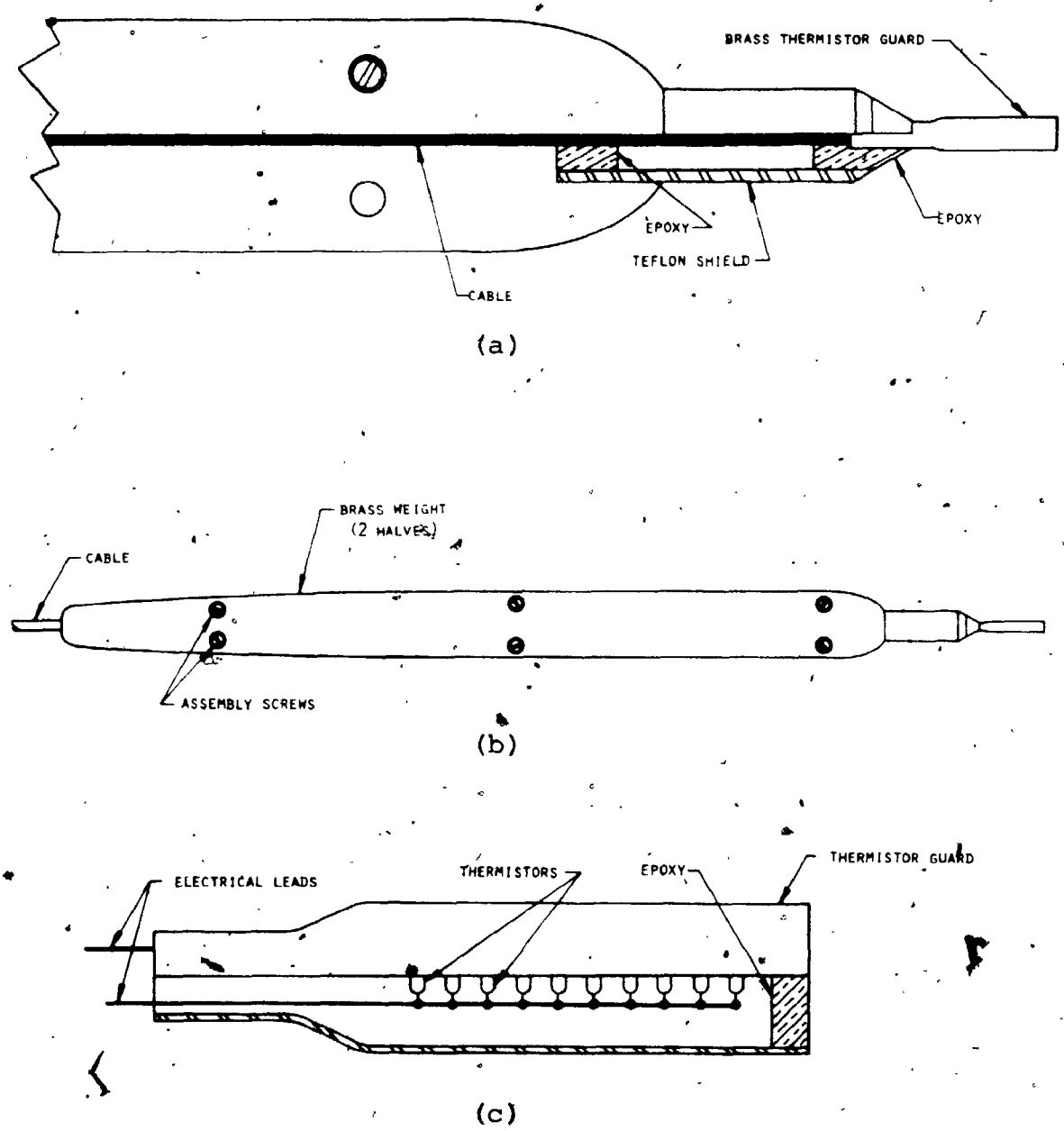

FIGURE 3.1: (a) The front section of a typical thermistor probe assembly, as used in the field tests
(b) The entire assembly
(c) Detail of the thermistor tip

minimize drag at low Mach numbers (c.f. Streeter, 1966). The maximum diameter of the probe is 1.8 cm, and the length is about 60 cm.

The measurement cable was made by Northern Electric, and consists of three individually insulated leads twisted together and encased in a solid insulation, with an overall outside diameter of 4 mm. This cable is quite flexible, an important consideration because of the design of our cable drive assembly (section 3.2). Several other cables tested during the course of this project, including 3 and 4 conductor shielded cables, were found to be inordinately susceptible to electrical noise, and hence were not used (see Chapter 4).

3.2 CABLE DRIVE ASSEMBLY

The constant rate cable drive assembly is shown in figure 3.2, which for the most part should be self-explanatory. Some of the components used in this assembly were salvaged from other equipment (hence the 20:1 speed reduction followed by a 1:3 increase) in order to minimize costs. The Zero-Max model E-3 reversible variable speed reducer was used to add versatility for tests and field applications. This system allows a lowering rate of between 0-17.5 m/min (nominal) in the configuration shown in figure 3.2, along with a maximum raising rate of 25 m/min (nominal). Other speed ranges can easily be obtained by substituting sprockets of ratios other than the 1:3 pair shown.

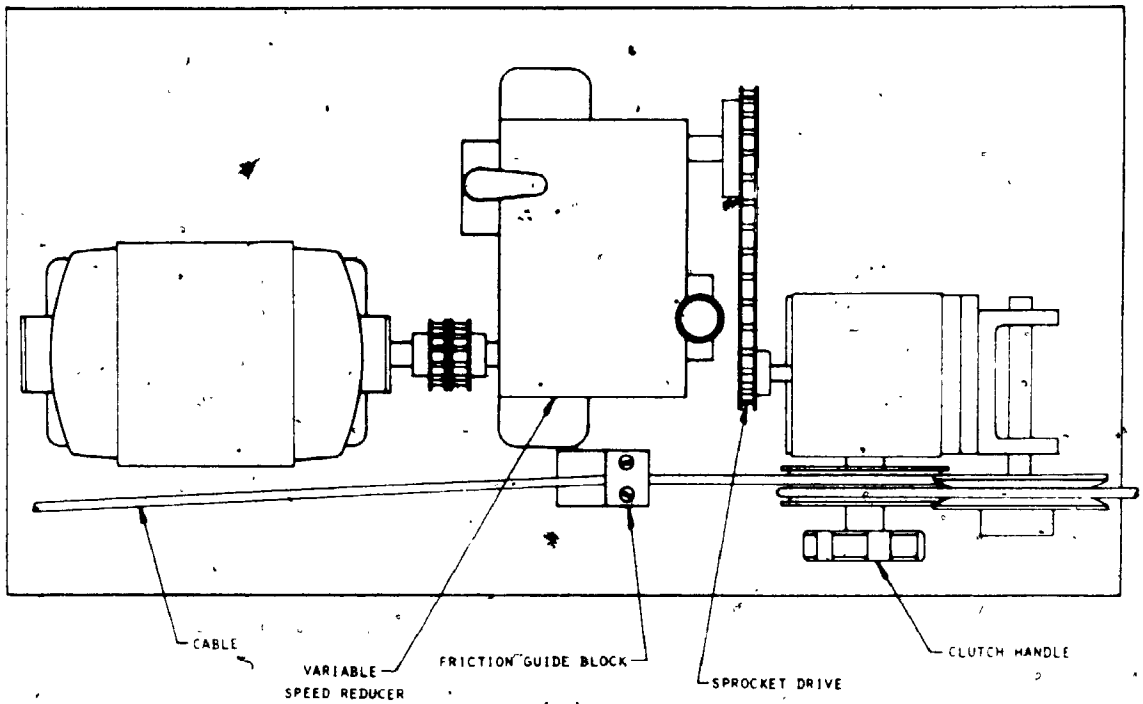

(a)

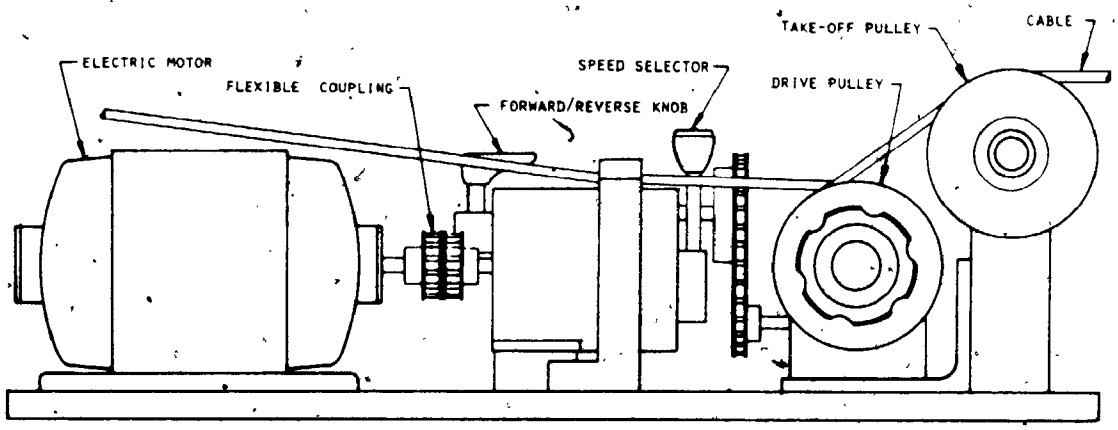

(b)

FIGURE 3.2: (a) Top view of the constant speed cable drive assembly used in the field tests
(b) Side view of the drive assembly

Figure 3.3 shows the pulley assembly which is clamped to the well head. Depth is monitored visually by means of a mechanical counter (not shown). In addition, a microswitch on the pulley assembly sends a pulse to the recording system with every revolution of a calibrated pulley, thereby allowing depth to be correlated with the thermistor readings. It is critical that the pulley bearings be quite free, to minimize the risk of depth errors due to cable slippage.

3.3 WINCH AND SLIP-RING ASSEMBLY

A Sharpe breast-pack winch was modified by the addition of a slip-ring assembly to allow continuous readings to be made, in spite of the rotation of the reel. The slip ring assembly (manufactured by Electro Switch Corp.) consists of six grooved gold rings with gold brushes for low thermal EMFs. Since the cable used had only 3 leads, we were able to use two slip rings per lead in order to reduce the contact resistance and variations in the contact resistance.

3.4 MULTIMETER AND D-A CONVERTER

A 5-1/2 digit (20% overranging) Data-Precision model 3500 digital multimeter with a sample rate of about 3 per sec, and isolated parallel binary coded decimal (BCD) data output was used in the field tests. The digital output from the ones, tens, and hundreds places of each resistance reading (e.g. for a reading of 19,243 ohms, the digits 243) are fed into a three channel digital-to-analog (D-A)

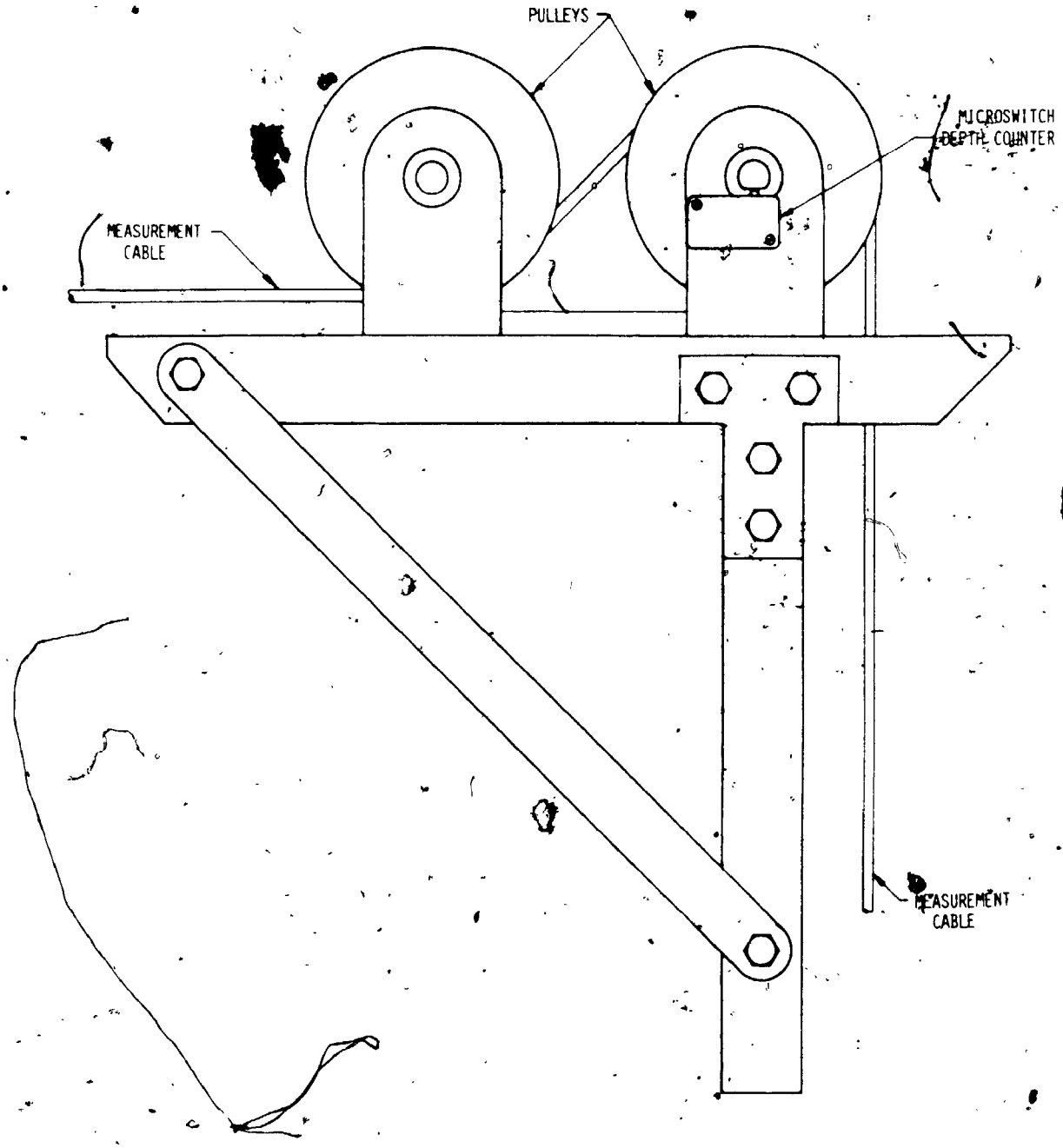

FIGURE 3.3: Well-head pulley assembly with micro-switch depth indicator. Not shown is a mechanical visual depth counter on the opposite side of the assembly.

converter. Only three digits are recorded becau
limitations in the capacity of the digitizer (section
The output for a given channel from the D-A co
consists of a DC voltage between -1.4V for the di
(zero), and +1.4V for the digit 9. The analog
levels from these three channels are recorded on m
tape, along with a fourth channel which includes
signals from the well-head pulley microswitch, summed
data display signals from the digital meter indicati
each new resistance value is being displayed. Figu
shows diagramatically the four channels of informatio
are recorded on magnetic tape, for a series of 8 res
readings and 3 revolutions of the well head pulley
signals). The repeating square pulses in channe
indicate when each new resistance reading is
displayed, information which is required by the
program which assembles the series of resistance a
values from the digitized tape (see Appendix A).

3.5 FIELD RECORDER AND DIGITIZER

The four channels of information described abo
recorded on four channels of a 7-channel FM tape
(Geotech model 17373). This recording is later play
into a PDP-11 analog-to-digital (A-D) converter, whe
record is sampled at any desired rate up to 2000 sam
second for up to 4 channels of information. At th
the data is in a form which can be handled by
programming (Appendix A), and is no longer pron

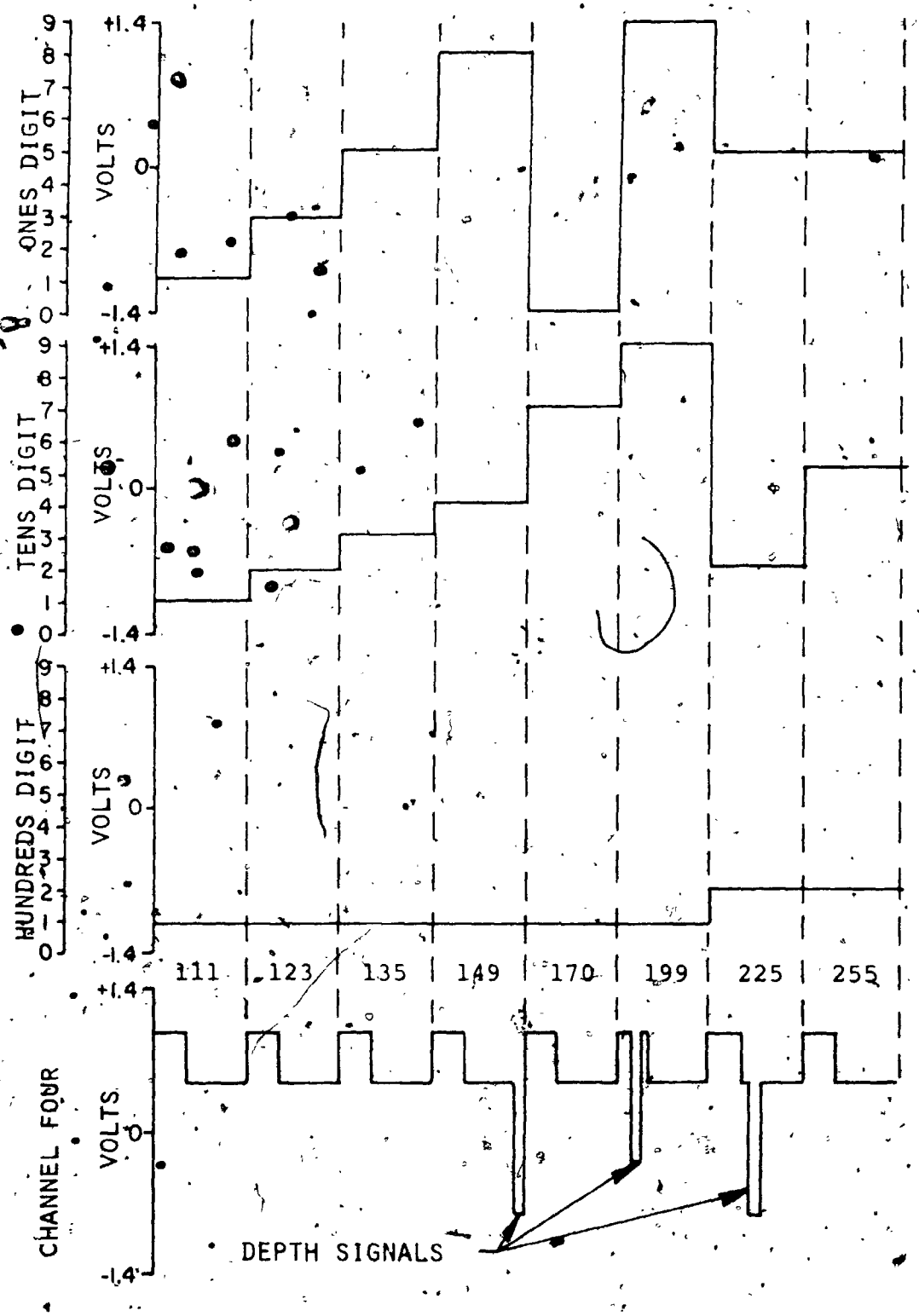

FIGURE 3.4: Diagramatic illustration of the four channels of information from the D-A converter, recorded on magnetic tape.

introduction of noise (except through an error in that programming).

Figure 3.5 shows a block diagram of the prototype data acquisition system used in the field tests. Figure 3.6 shows a plan-view layout of all of the continuous logging equipment, as it might appear during a field experiment.

3.6 REFINING THE EQUIPMENT

During the course of this study, certain improvements were made in the logging equipment which should be noted. Of primary importance was the great noise reduction achieved by doubling the number of thermistors from 10 to 20. This will be explained in detail in Chapter 4.

The production of a probe assembly which accepts interchangeable plug-in thermistor tips greatly facilitated the experimental work. This device uses two O-rings as a seal, an arrangement which proved to be quite satisfactory for the 600 meter boreholes logged in the field tests. Boreholes of greater depths may require a more elaborate system of seals.

The tension block (see figure 3.2) is spring loaded and exerts a constant clamping pressure on the cable in order to provide the back-tension necessary for this type of drive assembly. It was noted, however, that as the weight of the cable in the borehole increased, the clamping pressure had to be increased to compensate, at the risk of damage to the cable, or binding and seizing of the cable. A self compensating back-tension is now provided by means of a

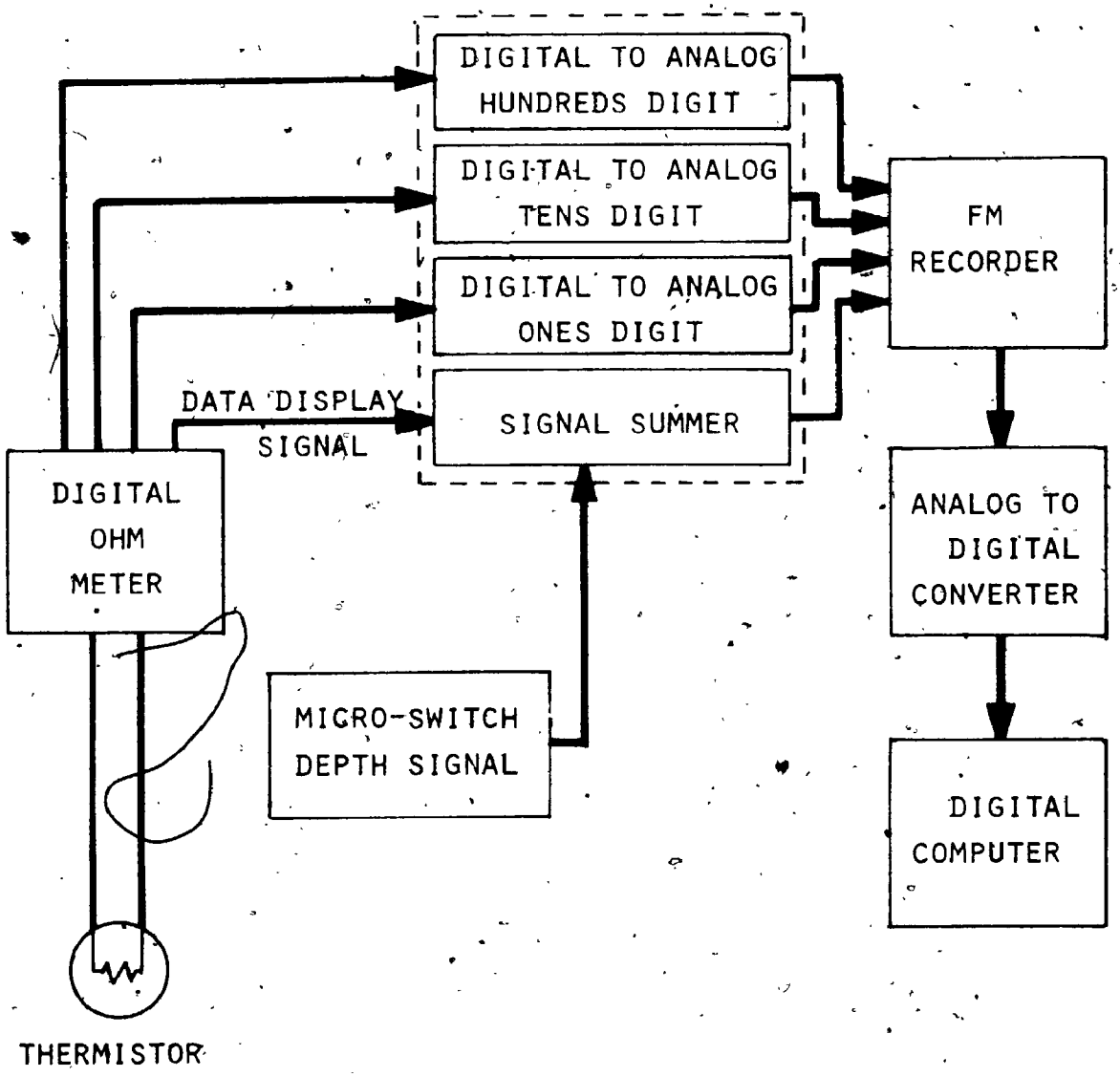

FIGURE 3.5: Block diagram of the data acquisition system

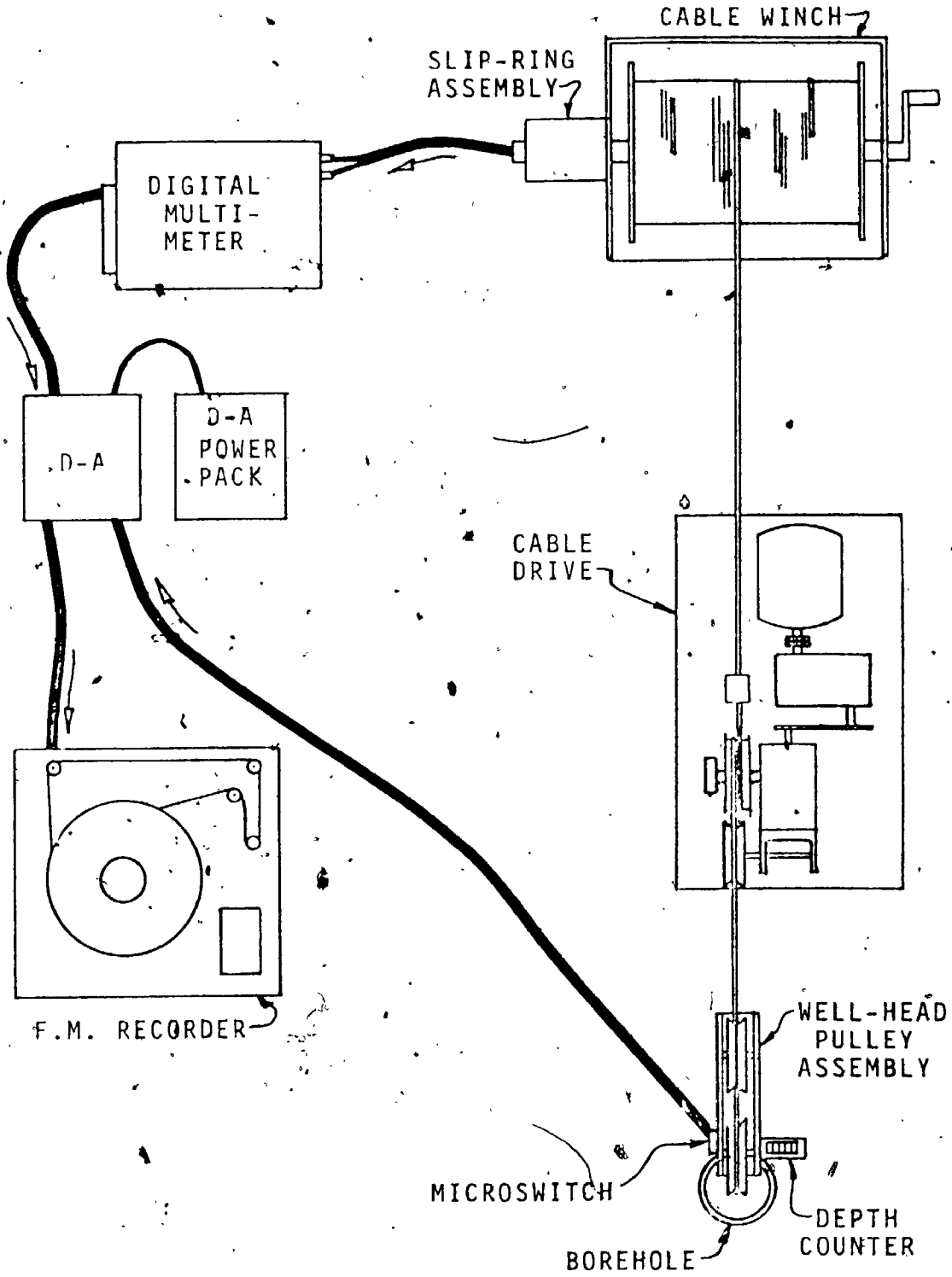

FIGURE 3.6: Plan view layout of the prototype continuous logging equipment

friction brake on the cable reel. As the amount of cable in the borehole increases, the diameter of the remaining layers of cable on the reel decreases, thus decreasing the effective lever arm, and increasing the effective back-tension.

The introduction of a buffered synchronous or incremental digital tape recorder should simplify the logging system somewhat. Specifically, this device would record depth information and resistance readings in a form which is immediately computer compatible. This would eliminate the D-A converter and power-pack, and the analog tape recorder, as well as the digitizing process and the computer program which interprets the digitized tape (see Appendix A). Elimination of these last two steps would reduce data processing costs by approximately 90%, and would greatly facilitate the data reduction process.

With our present equipment it is difficult to produce a log while raising the probe, due to the difficulty in keeping constant tension on the cable (as required by the constant speed drive) by operating the winch reel manually. A simple system for relieving this problem to some extent is shown in figure 3.7. The weight, W, would allow for variations in cranking the winch, and would maintain a constant back-tension, subject to the limitations imposed by inertia and pulley friction. The addition of a motor driven winch would of course greatly facilitate this up-hole logging process.

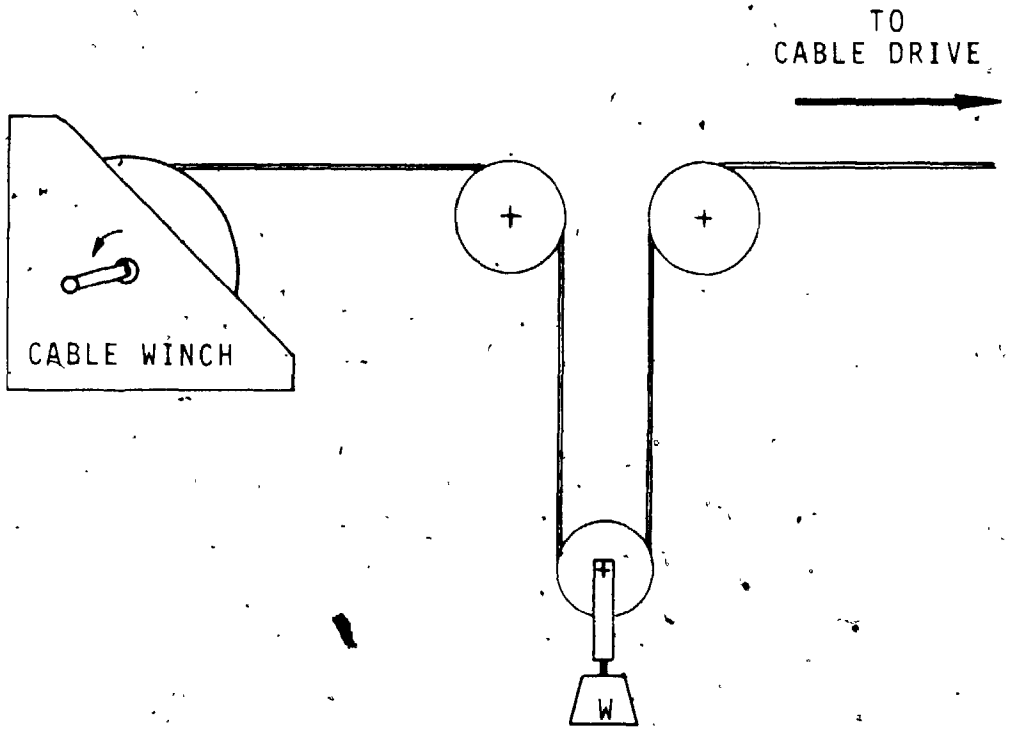

FIGURE 3.7: A simple system for maintaining cable tension in up-hole logging.

CHAPTER 4

FIELD TESTS AND RESULTS

4.1 THE U.W.O. BOREHOLE

Initial field tests of the prototype logging equipment described in the previous chapter were carried out in the borehole on the campus of the University of Western Ontario. This borehole is 592 meters deep, water filled, and cased to a depth of 441 meters. A nearly complete core of the hole was saved in drilling, and this core material has been studied extensively. Features of the borehole and the core material have been described by Beck and Judge (1969), and Judge (1972). Included in these works are incremental profiles of temperature, temperature gradient, and thermal resistivity, which were used as standards of comparison for the continuous logging results. Detailed geologic logs of the core material have been made by Sanford and Koepke (1963), and Upitis (1963). The latter work is the more detailed, and has been used for the geologic correlations in this chapter.

Two features of the U.W.O. borehole detract from its suitability as a test site. The University campus is a noisy environment electrically, and thus is a bad place to

make delicate electronic measurements. In addition, the water in the borehole is highly saline, due to the fact that the hole passes through the salt-bearing Salina Formation. This salt solution is not only corrosive, but is also an excellent electrical conductor. Obviously the integrity of all electrical insulation in the cable and probe is essential, especially deep in the borehole where increased hydrostatic pressures are encountered.

Numerous difficulties were encountered in the initial field tests, including equipment problems and leaks in the probe assembly. Especially troublesome was the omnipresent electrical noise. This was manifested primarily as a cyclical variation in the resistance reading of perhaps 20-200 ohms with about 2 seconds period (see figure 4.1), along with occasional noise bursts of hundreds of ohms. Extensive tests were performed in order to determine at what point in the equipment chain this disturbance originated. Possible ground loops were eliminated by common-point grounding directly to the well-head. The electrical slip rings were tested for contact problems. A possible leakage of salt water into the cable was investigated. A Faraday cage of aluminum foil was constructed around the cable supply reel, to guard against electrical pick-up in that region. Laboratories in the adjacent building were checked for heavy-duty electrical equipment.

Several characteristic features of the noise led to the conclusion that it was electrical pick-up from the cable,

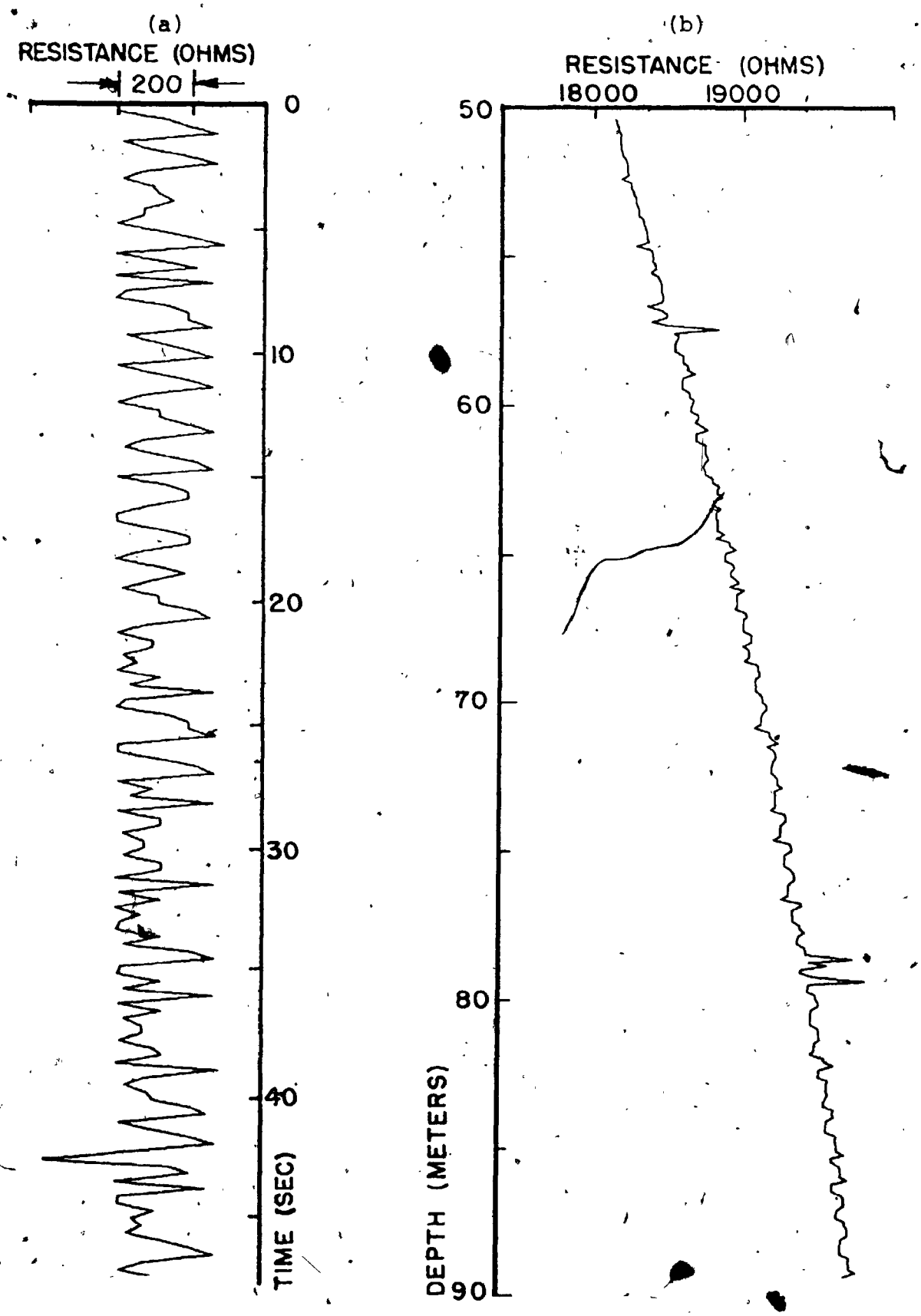

FIGURE 4.1:- Characteristic form of the electrical noise
(a) probe fixed at 200 m (b) probe moving

probably originating primarily in the length of cable between the winch and the well-head. First, this same cyclical variation of the resistance reading (of, say, ±5 ohms) was encountered in laboratory measurements with test leads as short as 1m. Second, it was noted that the noise could be reduced to some extent by shortening the length of cable exposed between the supply reel and the well head. Third, less noise was observed on Sundays and holidays than on weekdays, undoubtedly due to the fact that less electrical equipment was in operation in the vicinity of the borehole.

Three T-logs of the U.W.O. borehole were obtained successfully during a two month period from May through June, 1975. All of these experiments were performed on holidays, because of the noise problem. In each of these three cases it was necessary to remove noise spikes greater than about 20 ohms from the raw data (see figure 4.2) before processing, due to the inordinately large influence these spikes exert on the least squares smoothing operation. It should be noted that it is extremely unlikely that a naturally occurring temperature profile could cause a spike of 20 ohms or more of the type shown in figure 4.2, given a thermistor time constant greater than a very small fraction of a second. This noise removal was first accomplished manually with the aid of a computer print-out of the differences between each successive pair of resistance readings. Later the noise removal process was performed

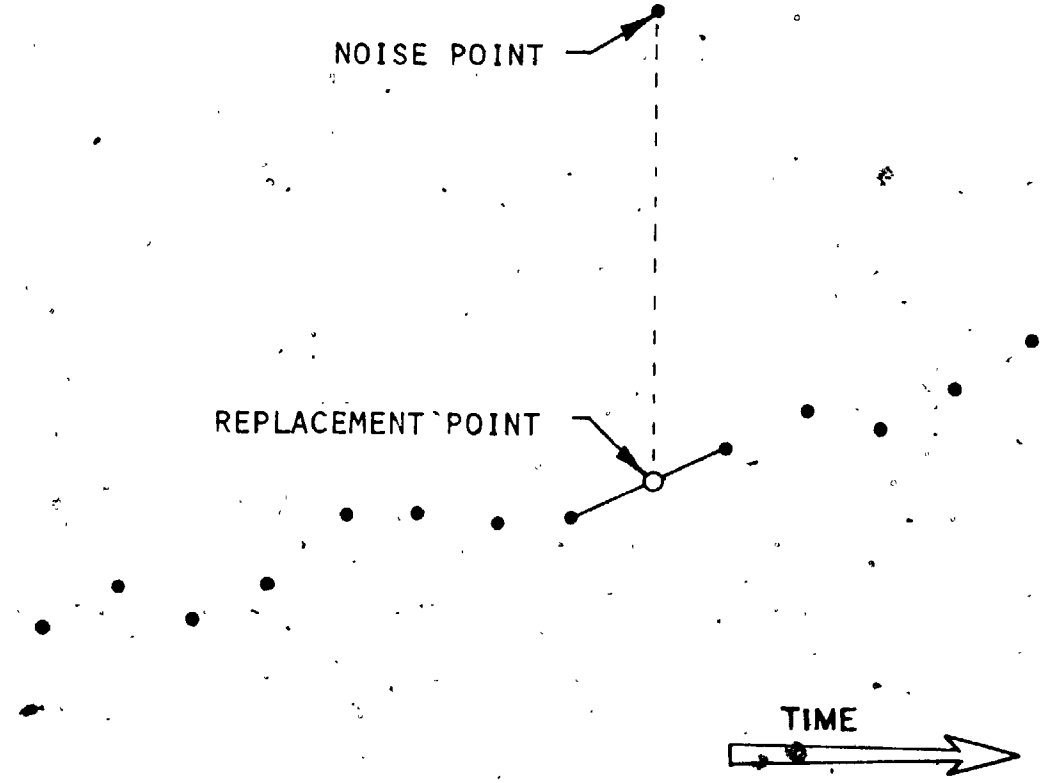

FIGURE 4.2; Illustration of the scheme used for manual removal of large noise spikes in the early field tests

more easily with the aid of a graphic display CRT computer terminal, using an interactive, on-line technique. On the order of 1-2% of the instrument readings were removed in this manner before the data could be processed successfully by the techniques given in Appendix A.

The results of these first three field tests were presented by Conaway and Beck (1976). The three continuous T-logs obtained at nominal logging speeds of 8 - 10 m/min are shown in figure 4.3, along with the incremental profile at 3 meter intervals from Beck and Judge (1969). This figure shows the excellent agreement in amplitude and overall form between the continuous and incremental techniques. It is also obvious that considerably more meaningful detail is present in the continuous logs, although it is difficult to assess the repeatibility and precision of the technique from this figure.

Next, a data stacking signal enhancement technique was tried, taking the running mean of the three curves. This yields a profile which in theory has been reduced in noise; in practice, however, it is still impossible to rely on a given peak as being 'real'. Data stacking would be more useful as a noise reduction technique if, say, a dozen runs of the same borehole were available; obviously this is an impractical proposition.

In figure 4.4 the three continuous profiles are plotted together, with the spaces between the curves filled in. This is essentially a continuous error-bar representation of

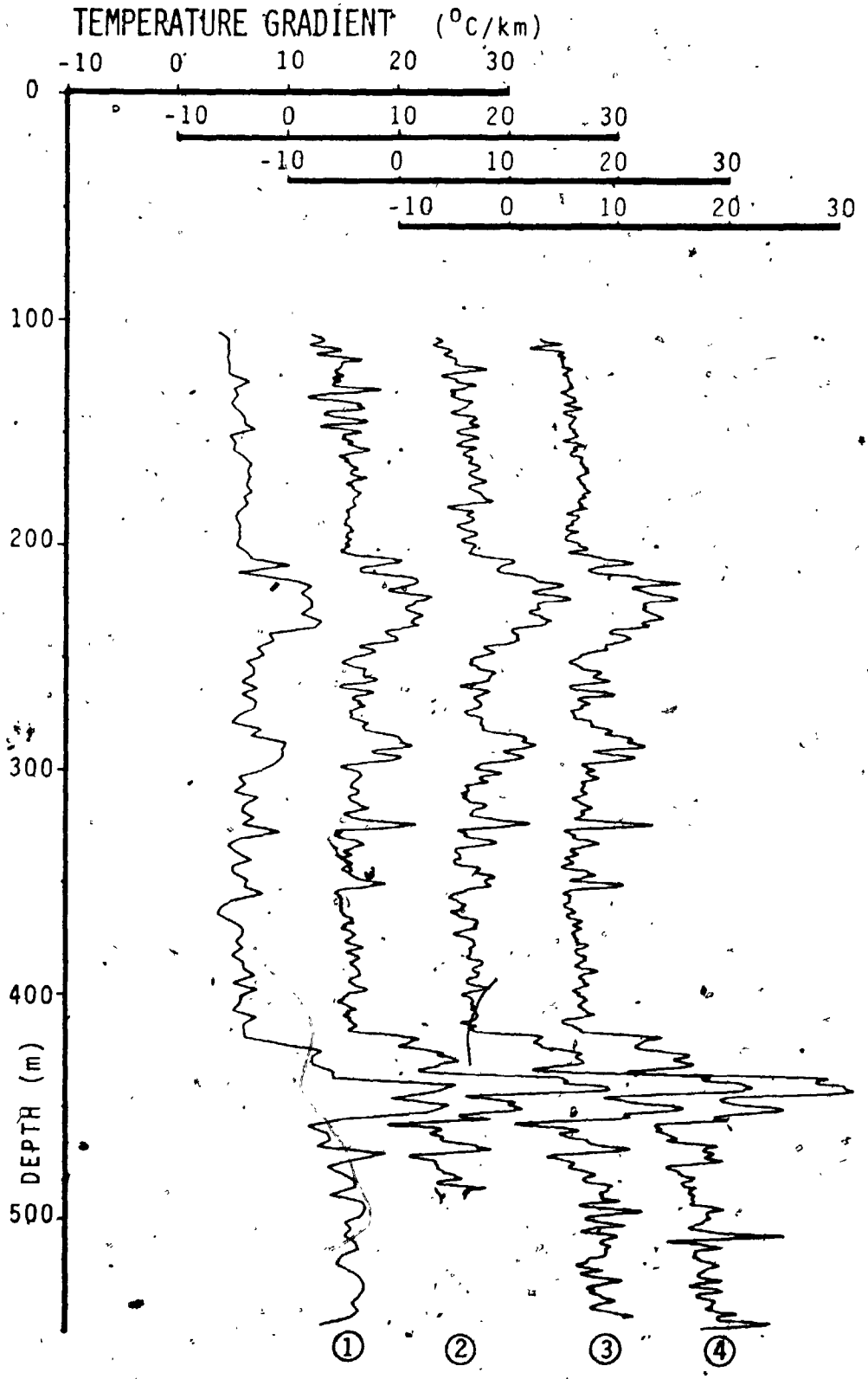

FIGURE 4.3; Incremental gradient log of the UWO borehole (curve 1) and three continuous logs (2-4)

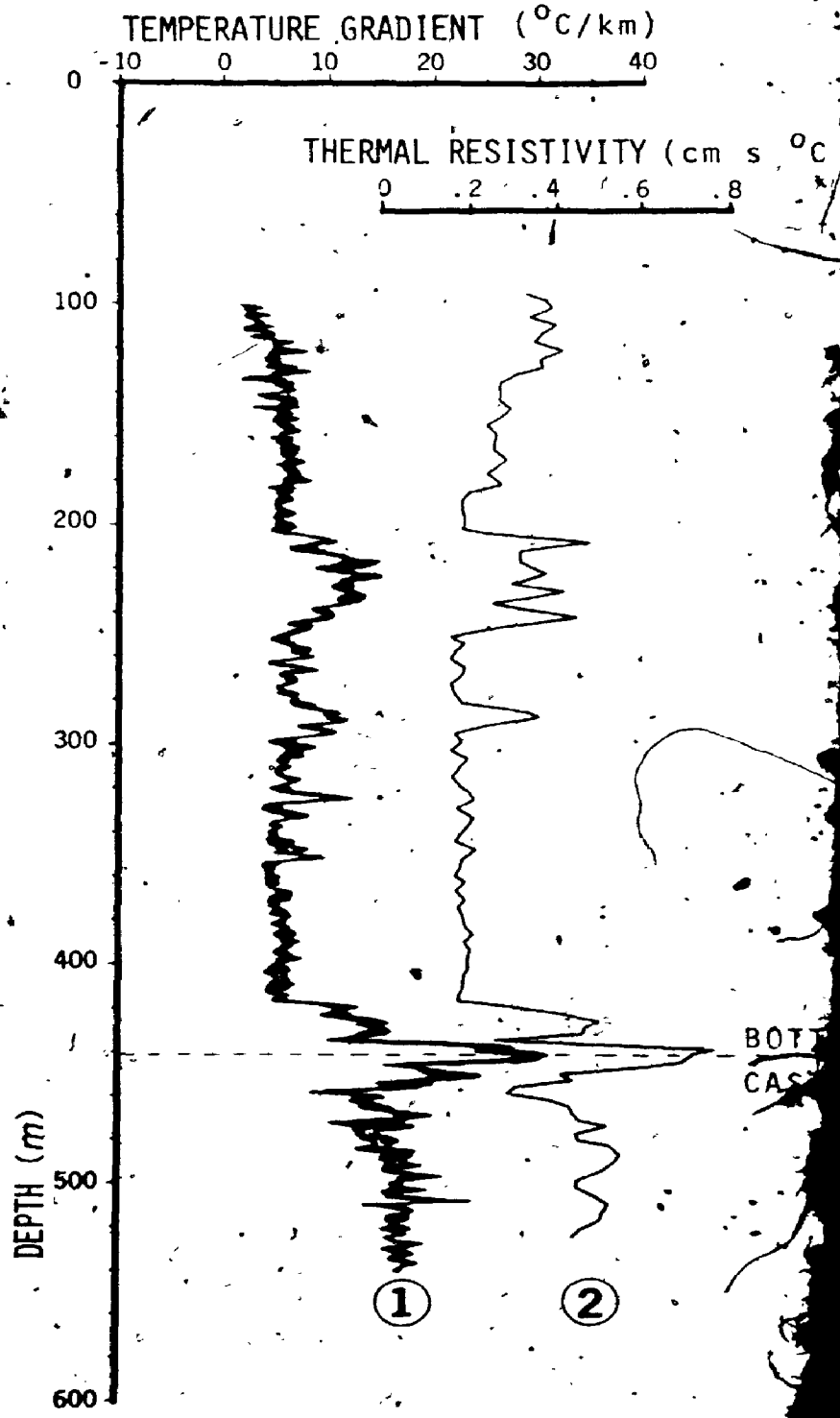

FIGURE 4.4: Continuous error-bar form of the T
explained in text (curve 1), along
thermal resistivity profile (curve

the data, and is an excellent way to evaluate the system. This profile (or rather, the original plot which was reduced to produce this figure) shows a mean precision or repeatibility of approximately $\pm 1^{\circ}C/km$, and a resolution threshold of about 2 meters. Also plotted in figure 4.4 is the incremental thermal resistivity profile obtained from laboratory measurements on core material at 4 meter intervals (Beck and Judge, 1969). The overall agreement between the two curves is quite good except near the top of the borehole, which is not in thermal equilibrium due to recent climatic effects. A comparison of these curves shows that the T-log is a good approximation of a thermal resistivity profile in the absence of disturbing factors such as ground water flow or surface effects. In addition, it can be seen that the well casing, which ends at 441 meters, has little apparent effect on the T-log. Thus, this technique has the distinction of being applicable to both uncased and cased boreholes.

4.2 THE NOISE PROBLEM

Good results were obtained in the first three field tests by the expedients of working during electrically quiet periods and removing the remaining large noise bursts from the records manually. This, however, imposes unreasonable restrictions on the continuous logging system if it is to be put into routine use. Even though most boreholes and wells are located in fairly isolated surroundings, reduction of the noise problem was judged to be an important step in the

development of the continuous logging system.

A detailed description of the various paths followed in trying to isolate and eliminate the electrical pick-up is of little interest, but the information obtained during several months of investigations has led to a simple technique which greatly reduces the effects of electrical interference without actually identifying the source. It was noted that the noise level varied approximately linearly with the thermistor impedence. Thus by doubling the number of parallel thermistors in the probe from 10 to 20, the nominal resistance of the assembly was reduced by half, as was the noise. On the other hand, the halving of the resistance range of the probe also reduced the resolution by half, thereby leaving us where we started, with the following very important exception. Lowering the resistance range of the thermistor package allows us to use a more sensitive scale on the digital multi-meter (10 kΩ instead of 100 kΩ) having a higher test current (100 μA instead of 10 μA). Induced noise currents therefore exert only about 10% as much effect under these conditions, thereby yielding approximately a 90% reduction in interference, everything else (e.g. probe time constant) being equal. The increase in self-heating from the increased current passing through the thermistors had no visible effect on the resistance values (i.e. the effect was less than 1 ohm, the limit of resolution of the multimeter).

4.3 TESTING THE IMPROVED LOGGING SYSTEM

The continuous logging system was once again tested in

the UWO borehole in order to evaluate the effectiveness of the noise reducing alterations. The improvement in results was dramatic indeed. Examination of the raw data shows virtually no apparent noise beyond the unavoidable round-off error of 1 ohm. Out of a raw time series of 14000 resistance readings, only five noise spikes were recorded, each less than .10 ohms. This can be compared with nearly continual noise of tens and sometimes hundreds of ohms with the old system (see figure 4.1).

Figure 4.5 presents the deconvolved gradient profile from the down-hole log (i.e. the log made while the probe was being lowered down the hole) at a nominal descending rate of 18 m/min. A comparison with figure 4.3 shows a reduced noise level with the new system, especially evident in the upper part of the log. This is in spite of the fact that a shorter operator was used in deconvolution, in order to maintain resolution at the higher (nearly doubled) probe velocity.

Figure 4.5 also presents the results of an up-hole log (i.e. made while the probe was being raised) made with the improved system at a logging rate of 25 m/min. Even though resolution has been somewhat reduced compared to the down-hole log, due in part to the greater logging speed, the curves are nonetheless in good agreement in overall magnitude and form. An up-hole log can serve at least as a rough check on the down-hole log, and in general one might as well be made since the probe must be removed from the

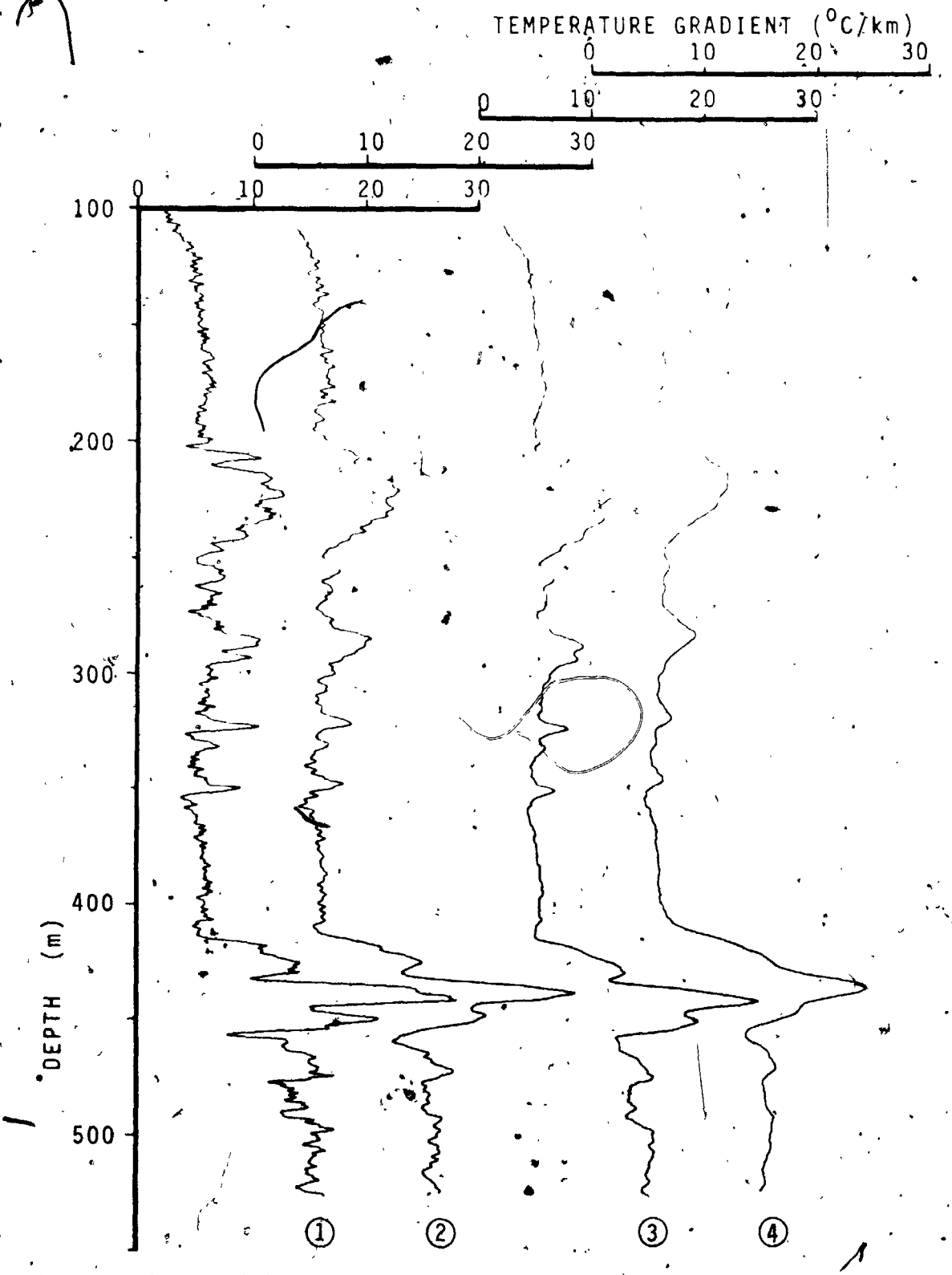

FIGURE 4.5: (1) Down-hole log, 18 m/min, improved system
(2) Up-hole log, 25 m/min, improved system
(3) Down-hole log, not deconvolved
(4) Up-hole log, not deconvolved

borehole anyway. The up-hole logging process includes several sources of error not found in down-hole logging. The thermistor tip is at the bottom of the cable and probe, and hence measures temperatures which have been influenced by the temperatures of the apparatus. Furthermore, the probe tends to stir the water as it is raised, thus blurring the details of the log. Finally, the water level in the borehole is altered by the volumetric displacement of the probe and cable. This causes the water above the probe to be raised into higher sections of the borehole (sometimes many meters higher) at different temperatures, thereby introducing errors into the measurements.

Figure 4.5 also shows the effect of ignoring the thermistor time constant (i.e. leaving the deconvolution term out of the combined operator). In both the down-hole and up-hole cases, the un-deconvolved curve lacks most of the fine detail of the deconvolved one, and is displaced in the direction of probe motion. This figure presents a convincing statement of the necessity for deconvolution if maximum precision and resolution are desired.

Deconvolution of the data may also be accomplished through the use of higher-order curve fitting techniques, as mentioned in Chapter 2. Two different smoothing cubic spline routines were used to apply equation 2.20 to the measured data, with no improvement in results over those obtained using the combined operator. These higher order techniques have the disadvantage of being 10 to 100 times

more costly in computer time than deconvolution using the combined operator (see Appendix A).

Figure 4.6 presents two temperature profiles of the UWO borehole: the incremental log, run in 1966, from Beck and Judge (1969), and the deconvolved continuous log run in August, 1975. Since the two curves differ somewhat in form, especially near the top of the borehole, the temperature profile was spot-checked in December, 1975, with a number of steady-state temperature measurements (plotted in figure 4.6 as solid circles). Clearly, the increase in temperature near the top of the borehole is real. It seems reasonable to attribute the bulk of this increase to a new building which was constructed near the borehole in 1965. This building is roughly 15 meters by 40 meters, extends about 3 meters below the ground surface, and is situated 2 meters from the borehole. Representing the building by a sphere of radius 10 meters located in an infinite medium as shown in figure 4.7, the following equation from Carslaw and Jaeger (1959) can be used to give an order of magnitude estimate of the temperature disturbance:

$$\Delta\theta = \frac{R\theta_s}{r} \operatorname{erfc}\left(\frac{r - R}{2(\kappa t)^{\frac{1}{2}}}\right) \tag{4.1}$$

where r is distance from the center of the sphere

κ is thermal diffusivity

t is time (duration of the disturbance)

θ_s is surface temperature of the sphere (relative to

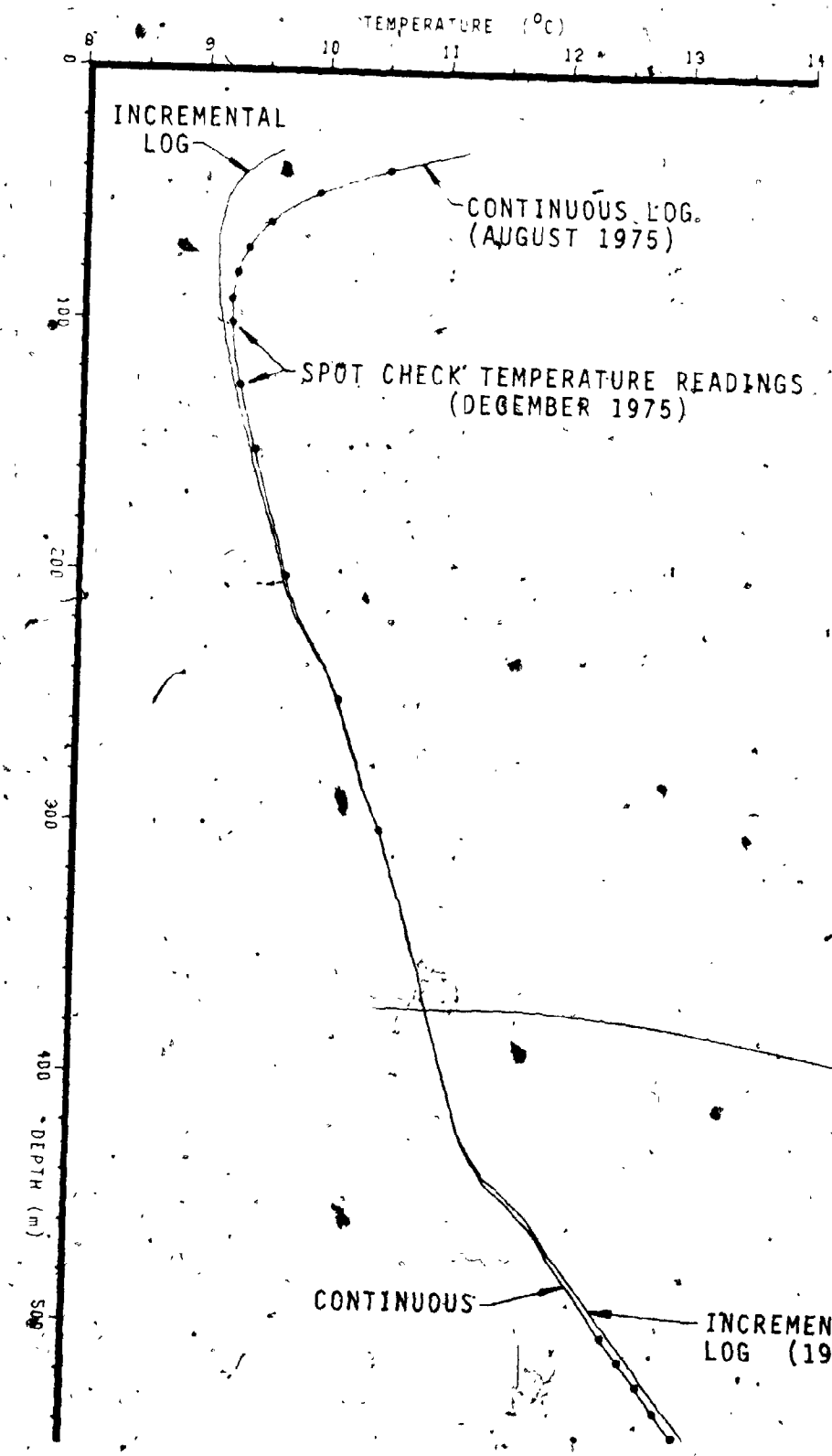

FIGURE 4.6: Two temperature logs of the UWO borehole.

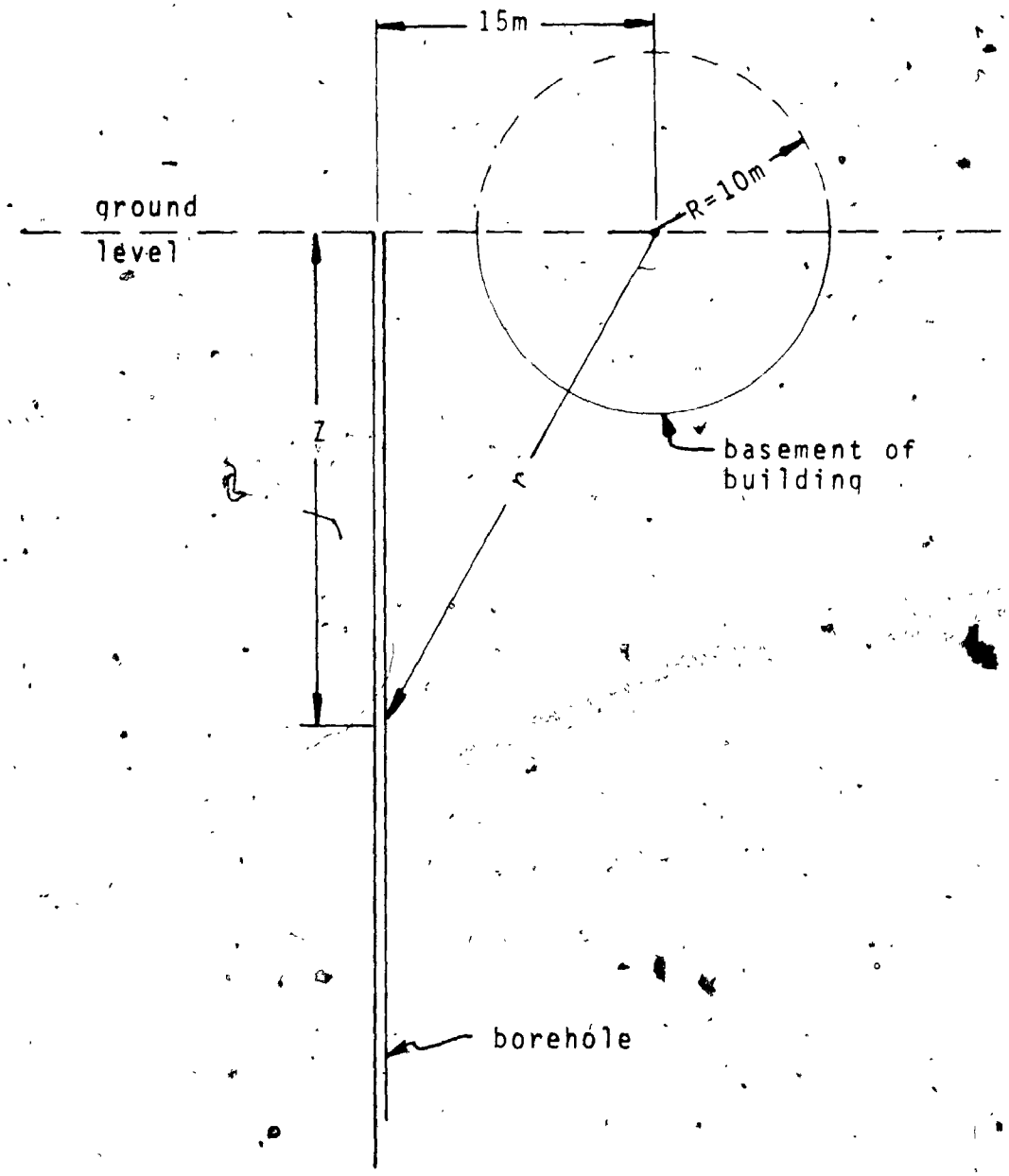

FIGURE 4.7: Configuration used for estimate of the thermal effect of building adjacent to the UWO borehole.

the surrounding medium.

$\Delta\theta$ is temperature change at depth Z and time t.

Assuming $\kappa = 0.012\ cm^2\ sec^{-1}$

$t = 10$ years

$\theta_s = 13\ ^{\circ}C$

gives $\Delta\theta = 0.72^{\circ}C$ at depth Z=40m, and $\Delta\theta = 0.13^{\circ}C$ at 60 m. At depth Z=100 m the effect has diminished to $\Delta\theta = 0.001^{\circ}C$.

It is clear, then, that the building could account for a change near the top of the hole such as seen in figure 4.6. Undoubtedly the observed variation of the temperature profile with time throughout the borehole is the resultant of many different effects. The decreased temperature in the lower section of the borehole cannot at present be explained satisfactorily. Beck (1976b) relates thermal disturbances at depth to a number of inferred climate changes ranging from 100 to 120000 years ago, in a computer simulation. Calculations along these lines indicate that these climate variations could account for no more than about $0.001^{\circ}C$ of the observed temperature difference (approximately $0.06^{\circ}C$) at 550 m depth. Many other factors, such as groundwater flow, the effect of the well casing, complicated return of the borehole to equilibrium, and depth errors due to pulley slippage or variations in pulley calibrations and cable stretch must be considered. Maximum accuracy in the temperature profile requires that a four lead measuring technique be used, in order that the lead resistance be self-compensated. Since we had only a three lead cable the

four lead technique could not be used.

Further study will be required before a reasonable explanation for these variations in the temperature profile with time can be proposed. Of primary importance here is the excellent agreement between the continuous log and the incremental spot-check readings.

4.4 THE OTTAWA BOREHOLE

At this point in the project it was decided that valuable information might be gained if the continuous logging system were to be tested in one or more boreholes which have been logged electrically. Efforts were made over a period of several months to locate and gain access to boreholes of this type in southern Ontario. Due to a combination of strictly enforced plugging regulations and considerable buck-passing by both industry and the provincial government, these efforts proved fruitless. Access was gained, however, to the 600 m water-filled borehole on the grounds of the Dominion Observatory in Ottawa. Although this hole has not been logged for electrical resistivity, incremental temperature gradient and thermal resistivity profiles have been compiled (Jessop and Judge, 1971), albeit not in such detail as the ones for the UWO hole. The Ottawa borehole is cased to a depth of 334 m; the upper half of the hole passes through Paleozoic sediments while the lower half penetrates into the Precambrian.

Figure 4.8 shows three continuous T-logs of the Ottawa

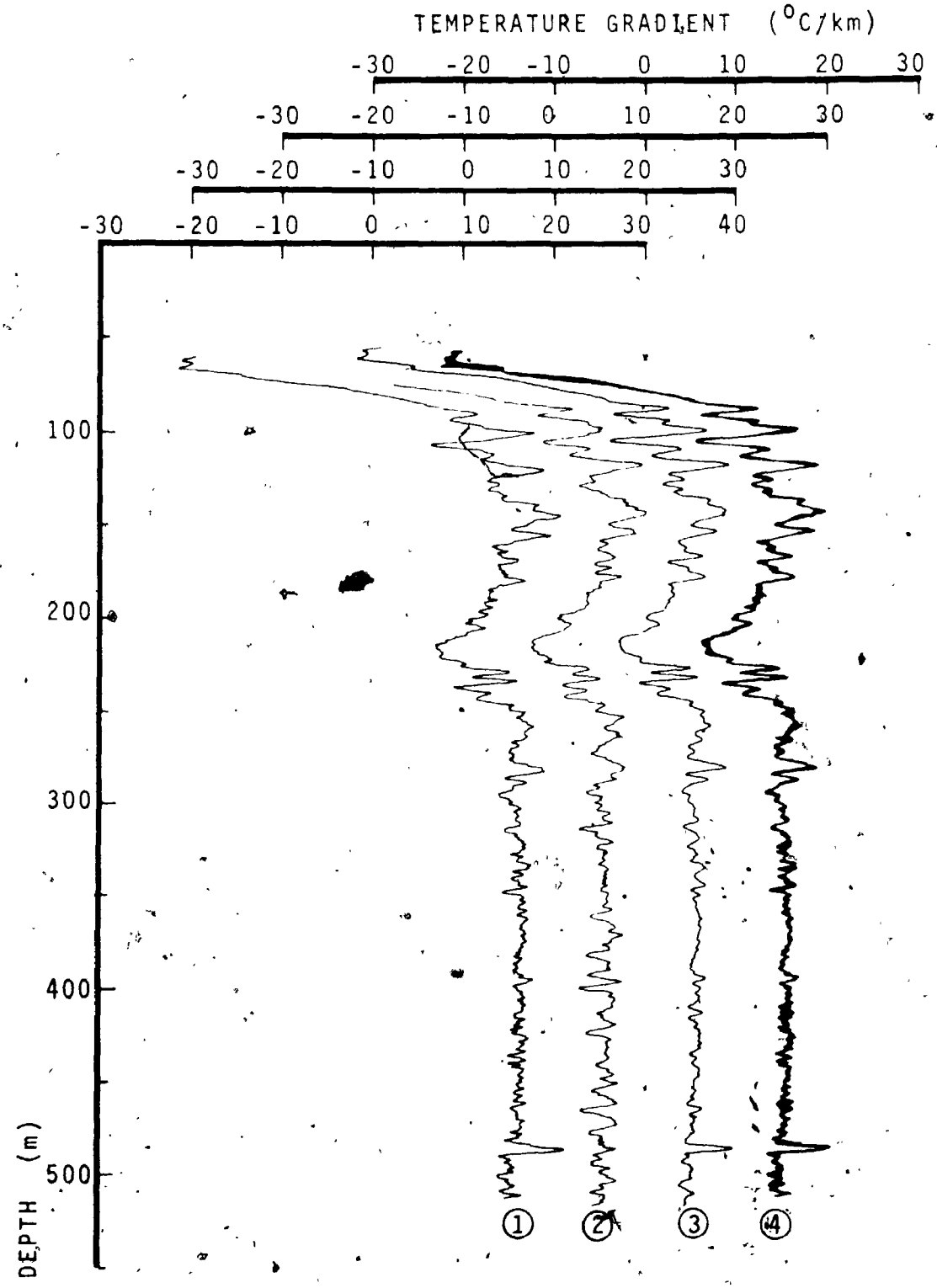

FIGURE 4.8: (1) Down-hole log of the Ottawa borehole, 18 m/min
(2) Up-hole log, 18 m/min
(3) Down-hole log, 9 m/min, heavily smoothed
(4) Curves 1 and 3 superimposed; filled-in

borehole, made with the improved logging system in October, 1975. Curve 1 is a down-hole log run at 18 m/min (nominal). Curve 2 is an up-hole log run at approximately the same speed showing considerable disagreement in detail with (1), especially in the lower part of the hole. Curve 3 is a down-hole log run at half the above speed, or 9 m/min (nominal). This curve has been produced by a combined operator roughly twice the length of the one used to produce (1), thus yielding comparable amplitudes in the sharper major features, such as the double spike at 225 m. This was done so that (1) and (3) could be superimposed to give (4), which gives a good measure of the repeatibility of the improved system. In this case the apparent mean repeatibility (evaluated over two runs) is better than $\pm 0.5^{\circ}C/km$. A good indication of resolution can be obtained from a study of the sharper features of curves 1 and 3 (especially in the pre-reduction form of this figure). The apparent resolution threshold at a lowering rate of 18 m/min is on the order of 2 m (from curve 1). From this it may be reasoned that the resolution threshold at a logging speed of 9 m/min should be on the order of 1 m, all else being equal. Curve 3 was obtained at 9 m/min, but has been heavily smoothed so that it might serve as a check on the log made at faster speeds.

The performance of the up-hole log (curve 2) can be evaluated by comparison with curve 4. The up-hole log is in good agreement with (4) in the upper part of the borehole,

down to about 200 m. Below this level the quality of the up-hole log deteriorates somewhat in detail, although the overall form and magnitude is in reasonable agreement. The sources of error in up-hole logging are discussed in section 4.3.

In figure 4.9, curve 1 is the incremental thermal resistivity log based on laboratory measurements on core material (Jessop and Judge, 1971). Curve 2 is the 9 m/min continuous gradient log (the same as (3) in figure 4.6). Curve 3 is the incremental temperature gradient log, also from Jessop and Judge. Again the fundamental agreement in the shape of the gradient log and the resistivity profile is apparent. The upper part of the T-log (above, say 150 m) shows distortion due to surface temperature effects. The incremental gradient log is in good agreement in magnitude and overall form with the continuous log, with the obvious exception of the peak at about 160 m. This peak is attributed to groundwater flow, and is known to vary with time (Jessop, 1975). Clearly, the continuous log contains enormously greater meaningful detail than the incremental profile. For a 600 m borehole, the continuous profile requires on the order of one hour logging time, while the incremental profile, even for the crude resolution seen in curve 3, requires several times this figure (see figure 1.1).

Figure 4.10 presents two temperature profiles for the Ottawa borehole. The incremental log was run in January,

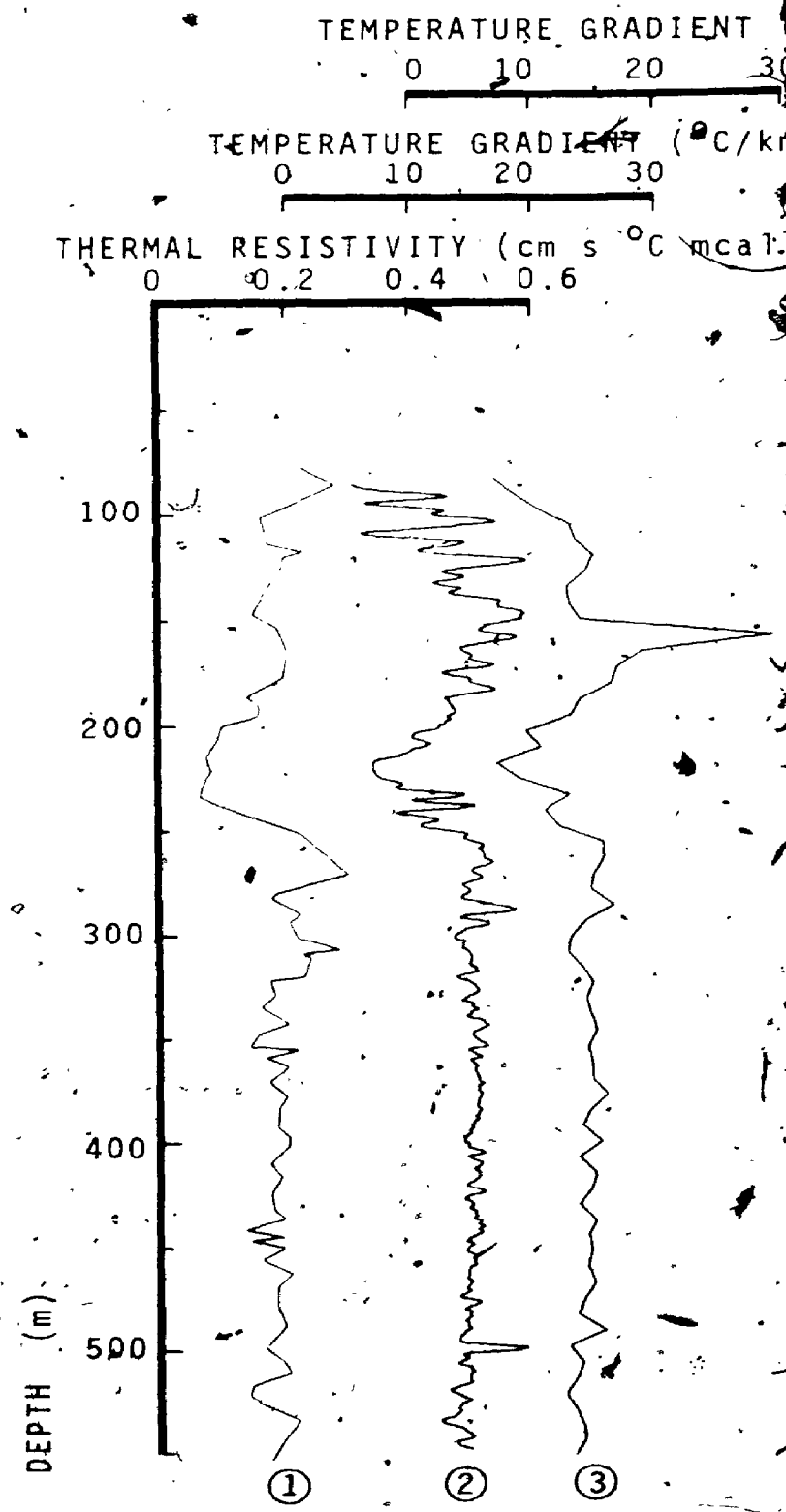

FIGURE 4.9: (1) Thermal resistivity profile of O
(2) Continuous T-log (curve 3 from
(3) Incremental gradient profile

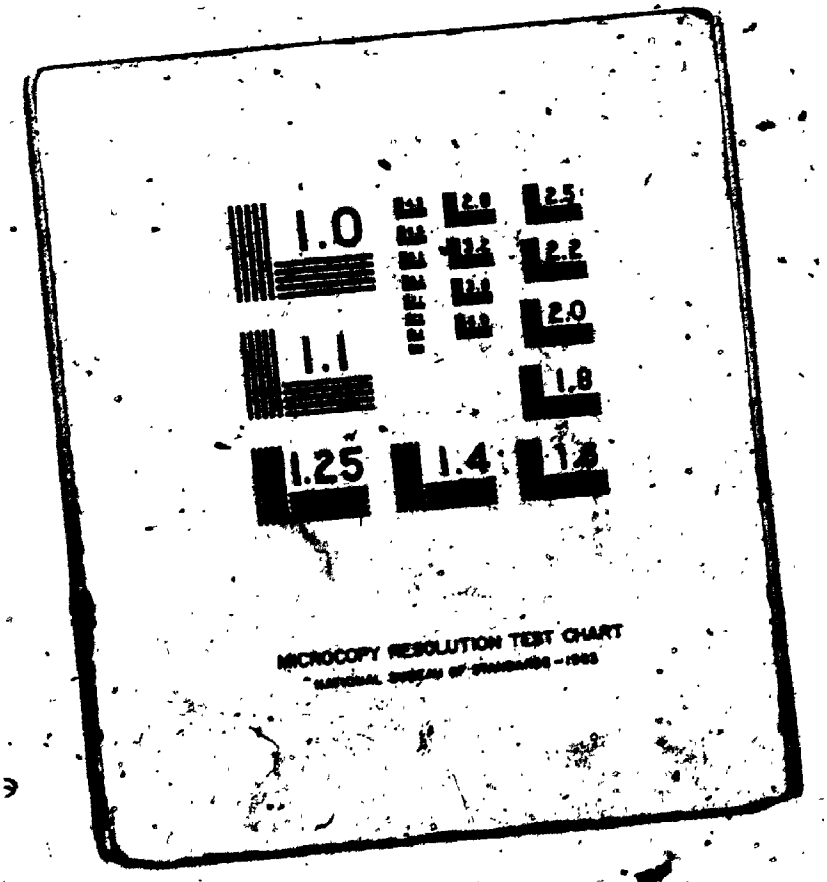

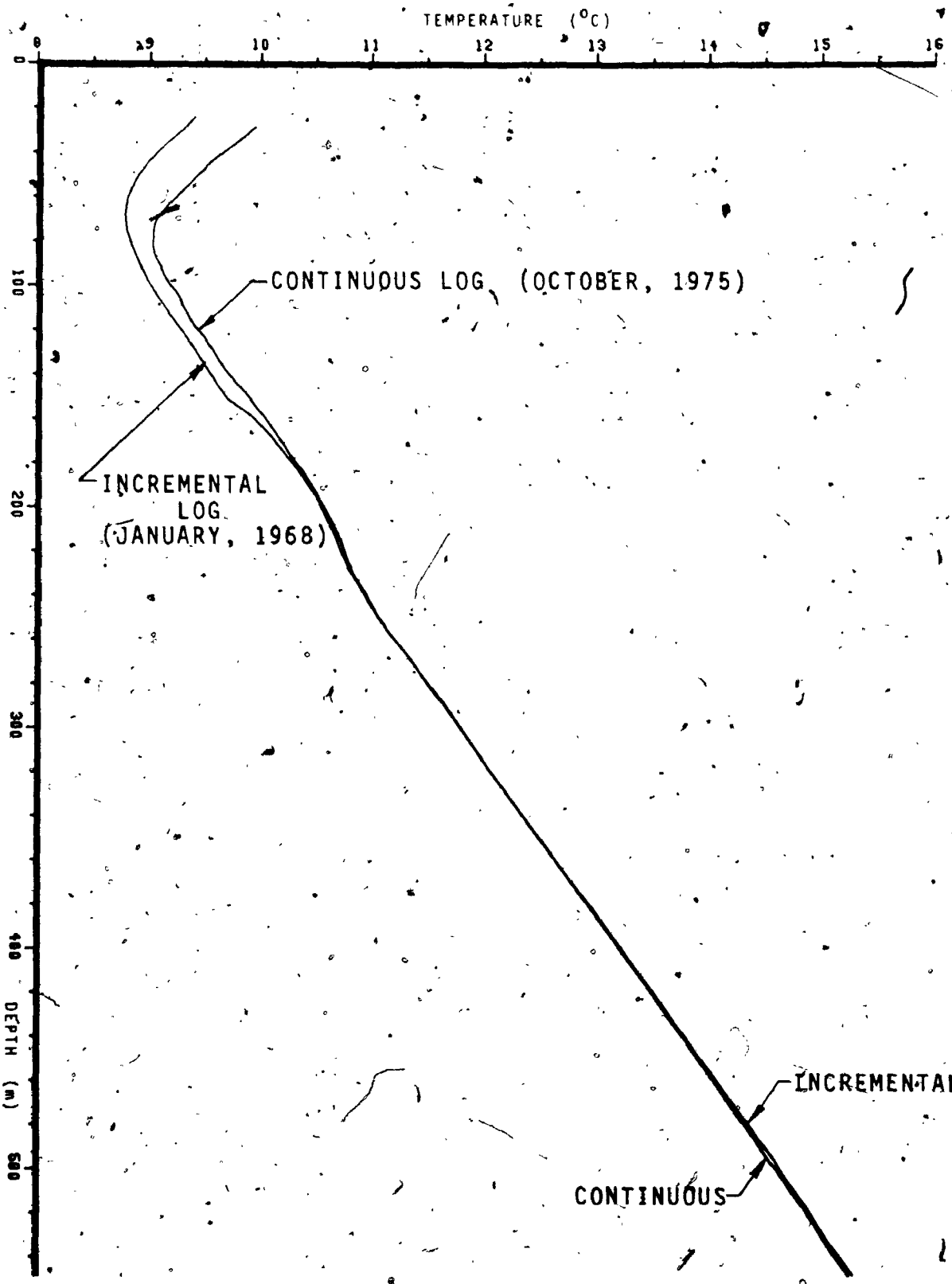

FIGURE 4.10: Two temperature logs of the Ottawa borehole

1968 (from Jessop and Judge, 1971), while the deconvolved continuous log was run in October, 1975. The same warming of the upper section of the borehole seen in figure 4.6, is found in figure 4.10 for the Ottawa borehole, as is the slight decrease in temperature in the lower part of the borehole. The presence of nearby buildings (considerably older than in the UWO case) and topographic effects, as well as known water flows in the upper part of the borehole complicate matters considerably. As in the case of the UWO borehole, greater study will be required before a reasonable explanation for these variations can be proposed.

4.5 CONTINUOUS GRADIENT LOGS AND THE GEOLOGY

Geologic logs are available for both the UWO and Ottawa boreholes, and these will be presented in this section, along with the T-logs of these holes. The geologic log for the Ottawa borehole was obtained from Jessop (1975), and is shown in figure 4.11. Also shown in figure 4.11 is the 9 m/min gradient log, which has been smoothed with a shorter operator than that used for curve 3 in figure 4.8. The lower section of this borehole (below about 240 m) is in the Precambrian, characterised by a fairly uniform thermal gradient of about 15°C/km. The upper portion of the borehole passes through several sedimentary formations, including the Rockcliffe, Oxford, March and Nepean. The most striking correlations between the T-log and the geology are found in the Rockcliffe Formation, where three thin (2 to 4 m) shaly layers are interbedded into the sandstone.

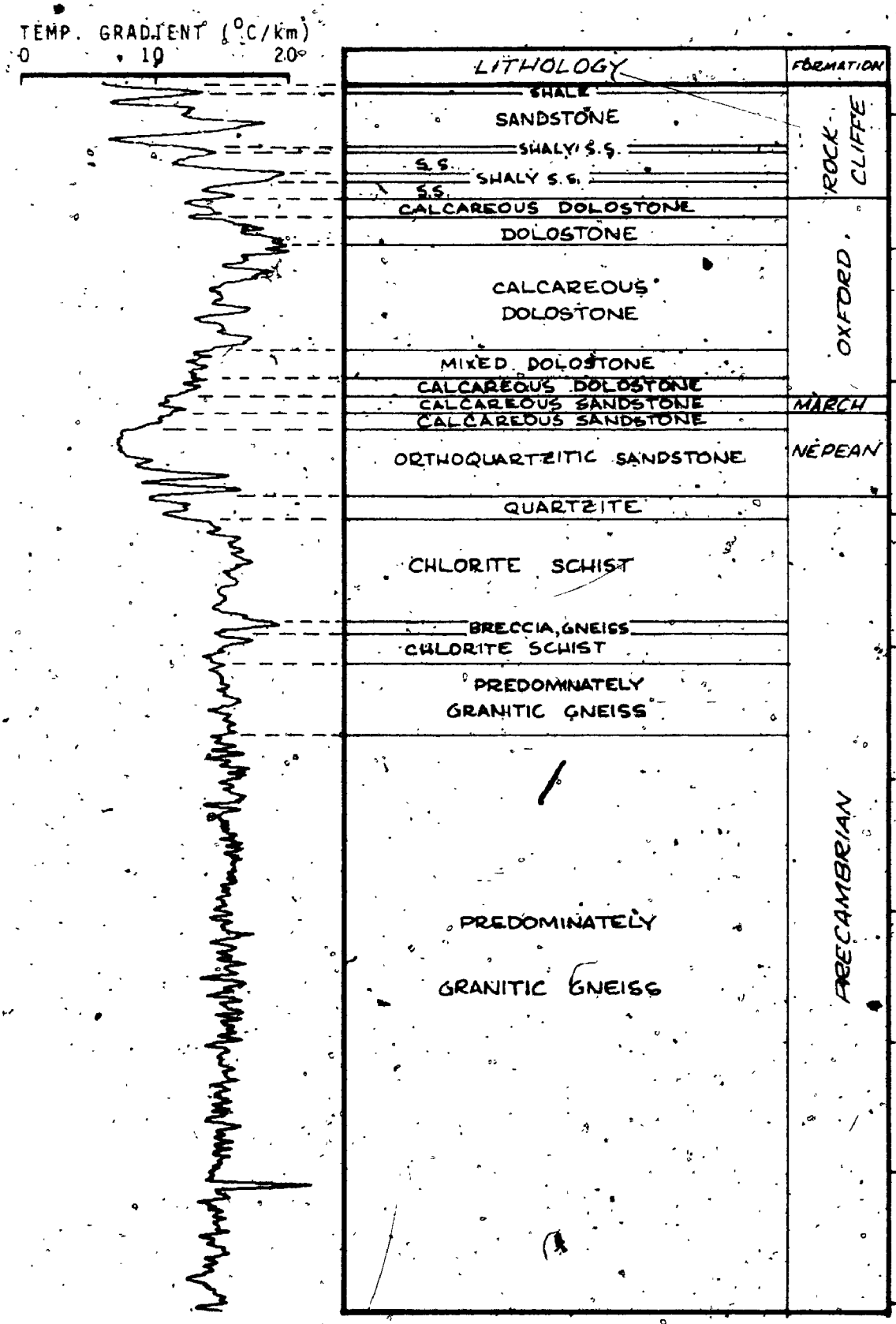

FIGURE 4.11: Comparison of the continuous T-log and the geology for the Ottawa borehole

These are marked in the T-log by sharp positive peaks on the order of 5 ^{o}C/km greater than the ambient gradient in that region. Although several other apparent correlations with the geology can be seen in figure 4.11, in general the geologic log is insufficiently complete to allow detailed evaluation of the correlation throughout the Ottawa borehole.

An extremely detailed geologic log is available for the UWO borehole. This work, by Upitis (1963), is a meter-by-meter description of the core material, including estimates of percentages of secondary materials included in the main rock type in each section, as well as descriptions of interbeds and laminations down to a few centimeters thickness. Of course, a T-log obtained at a logging speed of 18 m/min is unlikely to reveal details of geologic features a few centimeters thick, but the fine detail of this geologic log is nonetheless useful. It allows evaluation of the response of the T-log not only to sharp and gross geologic changes, but also to subtle trends in the lithology (as, say, a dolostone with shale interbeds grades into shale with dolostone interbeds). Figure 4.12 shows a geologic column for the UWO borehole, illustrating the main features. Certain correlations with the T-log (curve 1 from figure 4.5) are immediately apparent at this scale. Working from the top of the borehole down, some of these will be described briefly.

The carbonates from 100 to 200 meters are characterised

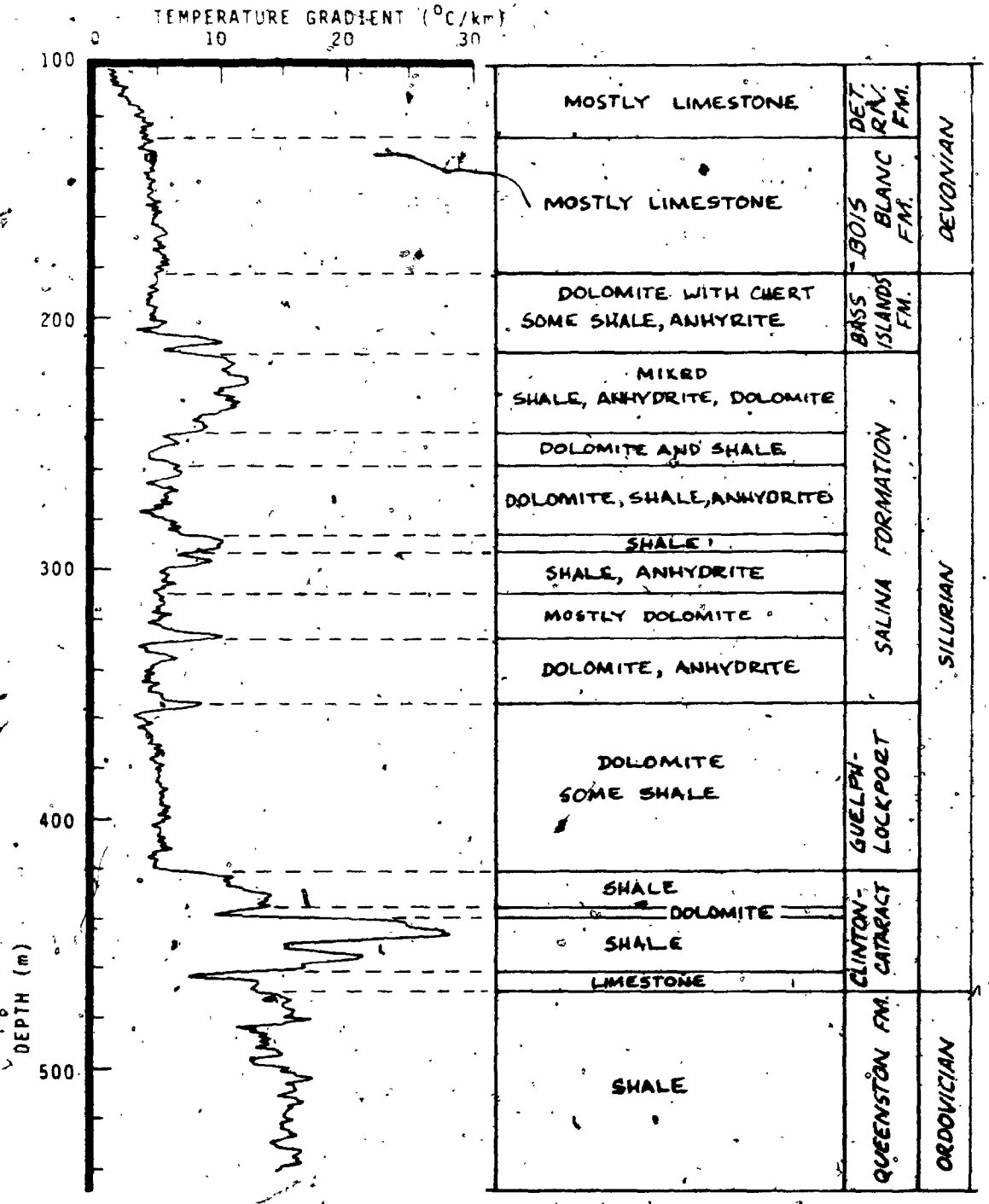

FIGURE 4.12: Comparison of the continoous T-log and the geology for the UWO borehole. For detailed sections, see figures 4.13 - 4.15.

by a fairly quiet and uniform gradient profile of about 5°C/km. The gradual increase in gradient from 1 to 5°C/km at the top of this section can be attributed to surface temperature effects. At a depth of approximately 180 m the transition from Devonian limestone (Bois Blanc Formation) to Silurian dolostone (Bass Islands Formation) is marked by a small but distinct drop in the gradient of approximately 1°C/km. Examination of figures 4.3 and 4.4 confirms this drop.

The Salina Formation is composed predominately of dolostone, characterised by gradients on the order of 5°C/km. Throughout the Salina, interbeds of anhydrite and shale occur, characterised by positive peaks of 2 to 5°C/km above the ambient gradient. The degree to which peaks of this type represent the actual gradients of these interbeds depends on the thickness of the interbed relative to the combined operator length. Assuming a lowering rate of 9 m/min, a sample interval of 0.3 seconds, and a combined operator length of 49 points, then the combined operator will be effectively 2 meters long in space. Any stratum which is at least 2 meters thick will be represented accurately in the gradient profile near the center of the bed, with the edges of the anomaly being somewhat rounded (recall figure 2.12). A stratum significantly thinner than 2 meters in this case will be represented in the gradient profile by a cosine bell shaped anomaly, which will be broader at the base than the actual interbed, and reduced

somewhat in magnitude from the true gradient.

The Guelph-Lockport Group consists primarily of dolostone with a small amount of very thin shale interbeds. The gradient throughout this section is quite uniform, at about 5°C/km).

In the Clinton-Cataract Group, the alternating shales and carbonates cause distinct corresponding changes in gradient. The greatest gradients occur in this section of the borehole; between 440 and 450 meters. It is unfortunate that the well casing ends at 441 meters, in a region having very large, sharp changes in gradient. If the casing ended in a quiet section of the borehole, it would be possible to evaluate the effect of the casing on the gradient profile. Preliminary consideration might suggest that the sudden increase in gradient at about 440 meters is due in large part to the ending of the casing, but examination of the thermal resistivity profile (figure 4.4) shows clearly that this is not the case.

The Queenston Formation consists entirely of shales, mostly reddish brown, with some greenish grey types near the top. This formation is characterised by gradients of 10 to 15°C/km.

The gross correlation between the thermal gradient log and the geology is quite good, and therefore a more detailed comparision is in order. The borehole between about 190 and 550 meters has been divided into three sections; the geology and the thermal gradient profiles for these sections

are presented in figures 4.13 - 4.15. All of the major trends and changes in the lithology along the borehole are described in the geologic columns. Study of these three figures reveals some very interesting fine-scale relationships between the geology and the T-log, and overall the correlation is excellent. A detailed description of these relationships would be tedious, and would offer little that cannot be ascertained from examination of figures 4.13 - 4.15. It is interesting, however, to note several of the finer-scale geologic features which correlate well with the T-log. Among these are:

(1) The anhydrite bed at 250 m (0.7 m thick)

(2) The shale-dolostone-shale sequence at 260 m (the dolostone being 0.3 m thick)

(3) The shale bed at 268 m (1.4 m thick)

(4) The anhydrite bed at 335 m (1.6 m thick)

(5) The shale stratum at 355 m (0.4 m thick)

It should be emphasized that each of these events can be found, not only in the gradient profile presented in figures 4.12 - 4.15, but in each of the continuous profiles shown in figure 4.3 as well. Obviously these are not spurious correlations.

Another interesting observation is that, although a detailed description of the Queenston shales is given by Upitis, the facies changes in this formation (e.g. from reddish-brown to greyish-green shale) do not appear to line up with the larger variations in gradient. This would

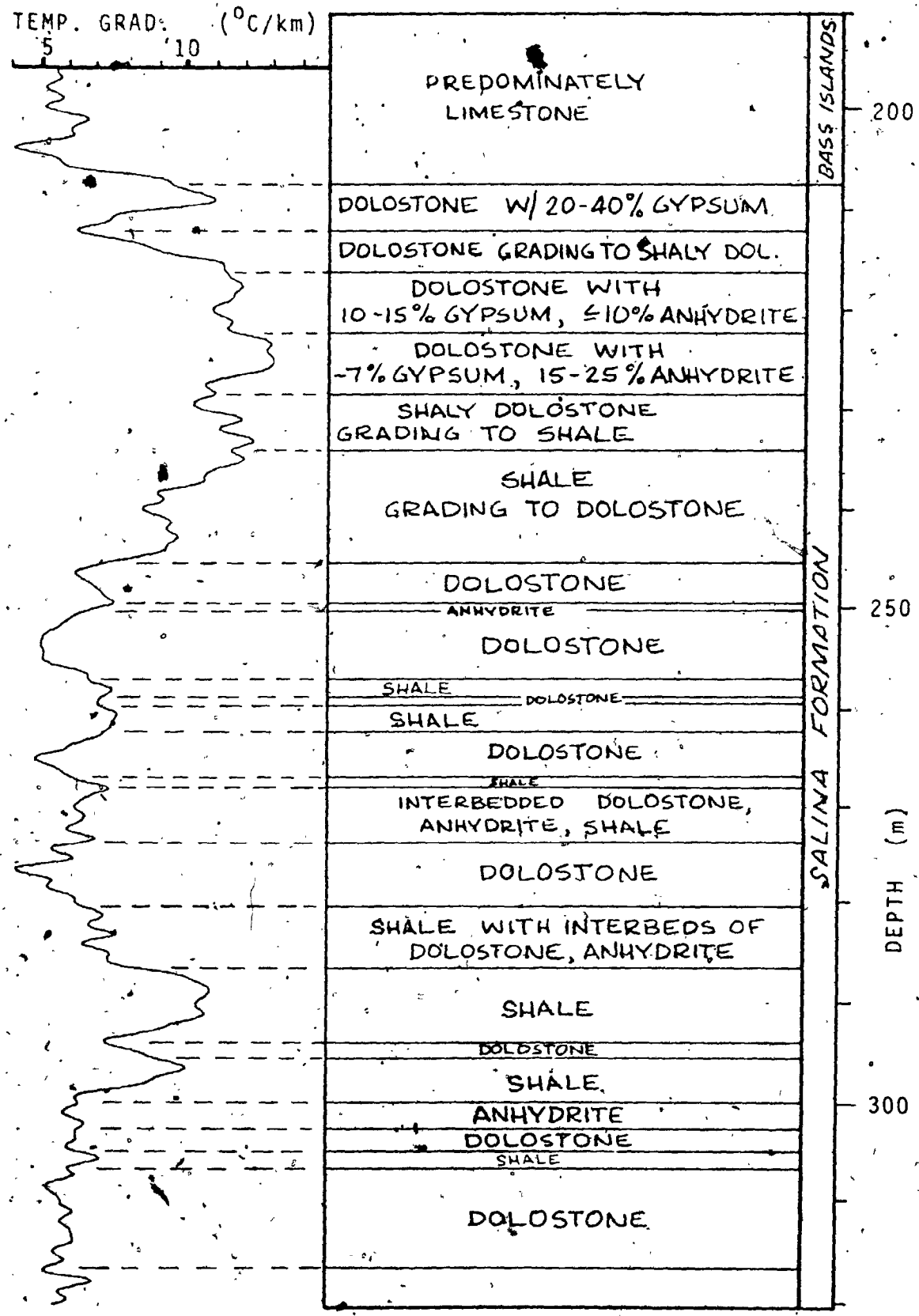

FIGURE 4.13: Detailed comparison of the geology and the continuous T-log in the UWO borehole, part 1.

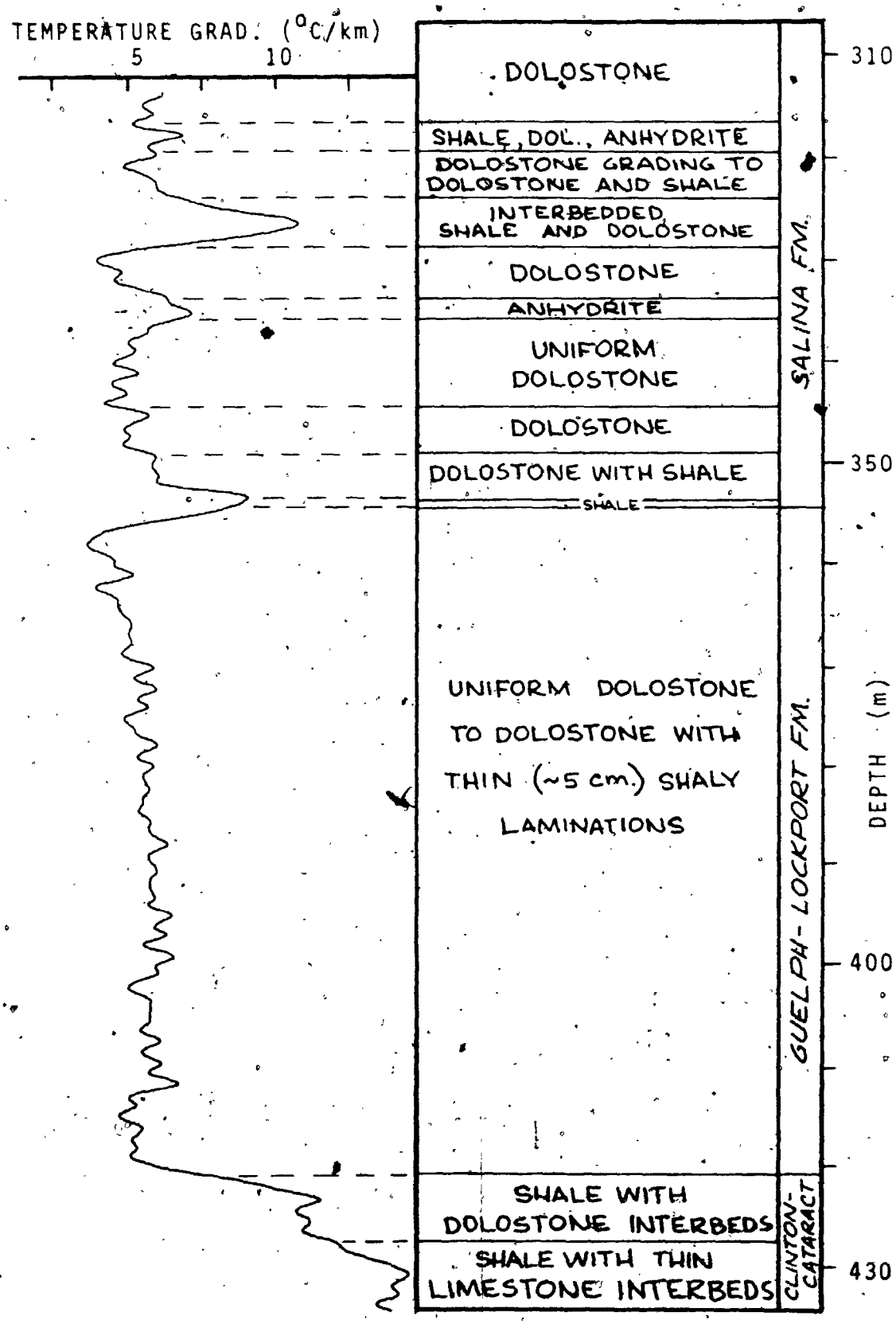

FIGURE 4.14: Detailed comparison of the geology and the continuous T-log in the UWO borehole (part 2)

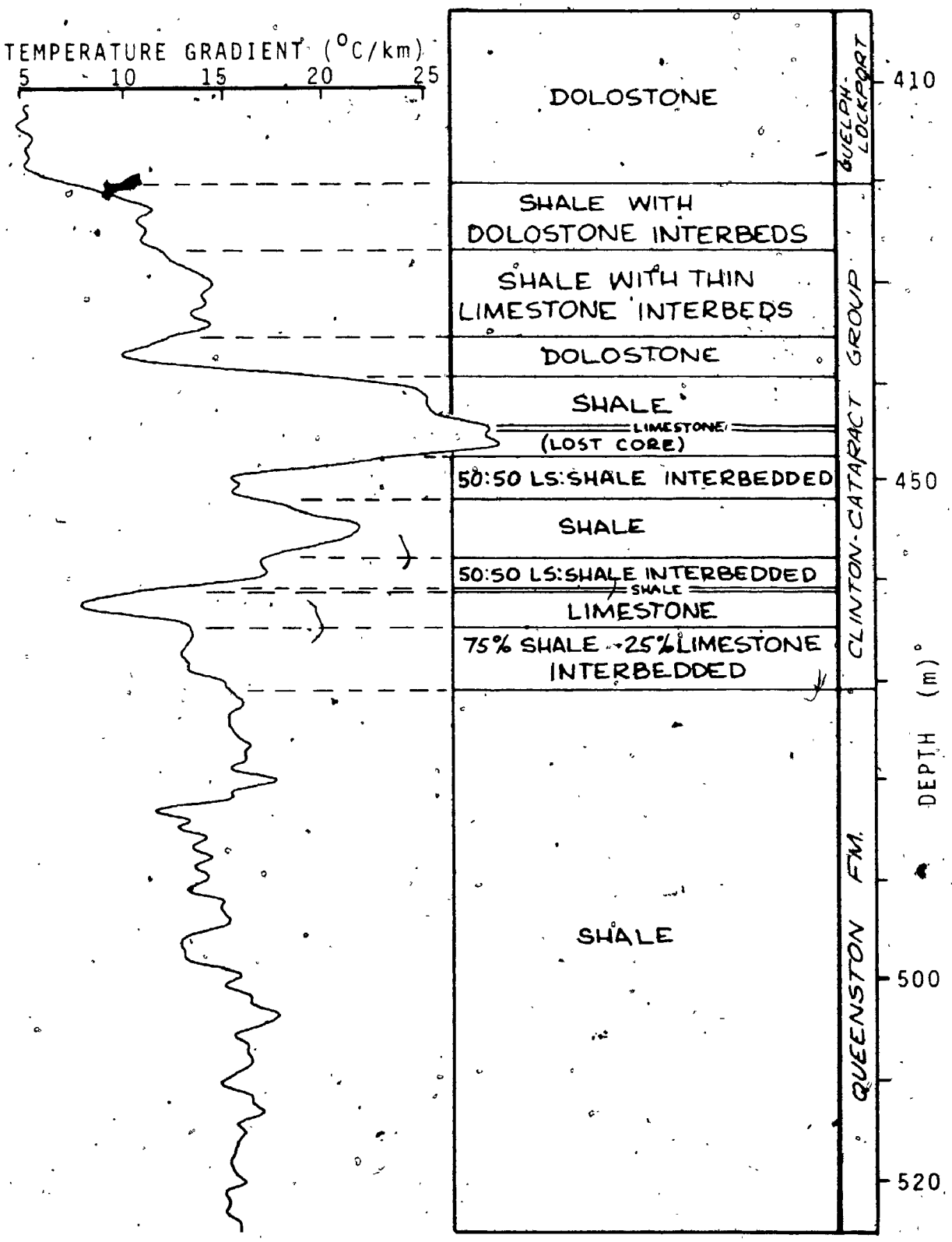

FIGURE 4.15: Detailed comparison of the geology and the continuous T-log in the UWO borehole, part 3

indicate that the thermal resistivity through this formation varies with some physical parameter not considered by Upitis, possibly porosity. Section 5.2 presents a general discussion of the relationship between porosity and thermal resistivity.

It would be difficult to cite a precise figure for the resolution of the continuous gradient logging system under all conditions. The correlations seen in figures 4.12 - 4.15, however, allow an empirical estimate of resolution to be made. Assuming that electrical noise is not a considerable problem (as it was for us before the logging system was improved) then it can be stated that an isolated stratum of significantly contrasting thermal resistivity (as, say, a dolostone to a shale) of thickness approximately 0.5 meter, separated from other significant changes in lithology by at least one combined operator length, should be clearly detectable at a logging rate of 18 m/min. An alternating sequence of thin strata (say, 10 half-meter layers of rock type A interbedded with 10 half-meter layers of rock type B) will be characterised by a fairly uniform gradient profile of magnitude intermediate between the gradients characteristic of A and B alone. The individual strata would not be well resolved. More subtle changes in lithology would of course have to extend over longer depth intervals in order to be detectable, as exemplified by the Silurian-Devonian interface in figure 4.12. In this case the gradient contrast is on the order of

15%, yet the interface is quite clearly indicated. Thus, under the conditions given above, it is reasonable to cite a resolution of 0.5 meters or better for a thermal resistivity contrast of 50-100%, decreasing to a resolution of several meters for a thermal resistivity contrast of 10-15%.

CHAPTER 5

APPLICATIONS

In general it may be argued that, all other factors being equal, any scientific measurement should be made as precisely and accurately as possible. In the case of thermal logging, the expense and difficulties involved in reaching and logging a given borehole are generally great enough to justify maintaining maximum precision in the logging process, especially when such precision requires no more, and often considerably less logging time. The poor resolution of conventional thermal logs might hide some interesting or important features of the borehole. Furthermore, should later studies require greater resolution than available with conventional temperature or gradient profiles, it would not be necessary to return to the borehole (if, indeed, it had not been sealed) and log it once again.

Naturally, the above argument must be tempered by the realization that the more complicated equipment used in the continuous logging process is more expensive, and probably more likely to break down than the simpler types of equipment in general use today.

5.1 TERRESTRIAL HEAT FLOW

The basic techniques of thermal logging for terrestrial heat flow work are presented by Beck (1965). In general, incremental temperature measurements are made at, say, 10 m intervals, using a Wheatstone bridge apparatus for the actual thermistor resistance readings. This is a slow and tedious process, and produces rather poor resolution (see figure 1.1). Next, laboratory thermal conductivity measurements are made on core material at intervals along the borehole. The product of thermal conductivity and temperature gradient at a given level in the borehole (in the absence of disturbing factors such as groundwater flow or surface temperature effects) is a measure of the heat flow across that level. A plot of heat flow values at various depths is the heat flow profile of the borehole.

The continuous logging system may be of use in several ways in terrestrial heat flow applications. First, it greatly reduces the tedium of the actual field work, allowing boreholes to be logged rapidly while yielding gradient profiles of excellent precision and reliability. Since the T-log is continuous, it allows the correlation of thermal conductivity results with the associated temperature gradient at the precise point along the borehole from which each core sample was taken. In addition, the continuous T-log may be used as an aid in the selection of core material upon which the conductivity measurements are to be made. Examination of the continuous gradient profile allows

selection of samples which are more likely to be representative of a given section of the borehole than samples which are chosen at random or at equal intervals along the hole. This could prove to be an important factor in improving the reliability of heat flow determinations.

The prototype continuous logging equipment is somewhat less portable than the incremental equipment commonly used in heat flow work, especially because the system at present requires a generator or other AC power source supplying on the order of 1000 W, primarily for the motor drive. If considerable back-packing of equipment is a routine necessity for a given research group, it should not be difficult to modify the equipment design and improve the portability of the system considerably.

5.2 STRATIGRAPHIC CORRELATION

Since the heat flow along a borehole rarely changes by more than 20% from a mean value in the absence of disturbing factors such as heat sources and sinks (Beck and Judge, 1969), and since the thermal gradients are approximately proportional to the thermal resistivities of the formations under these conditions, it follows that a temperature gradient log is generally a good approximation of a thermal resistivity log. Although successful use of temperature logs and temperature gradient logs for stratigraphic correlation has been reported by several authors (Roy, 1963; Kappelmeyer and Haenel, 1974; Beck, 1976a), the progress of research in this area has been greatly impeded by the lack

of sufficient precison and resolution in the logs. As with most types of well log, the T-log may be used in a purely empirical manner for correlation between several boreholes in a given region. Certain 'signatures' or characteristic wave forms along the logs may be associated clearly with a given geologic formation, and can be used readily as markers on each of the logs. Smaller features may then be correlated in this same manner.

Thermal gradient logs have several drawbacks for use as a correlation tool. The frictional heat released in the drilling process, and the cooling (or warming) effect of the circulated drilling fluid alter the temperature profile of the borehole. It is necessary to allow at least a few days after the drilling has stopped, and preferably a few drilling periods, for the borehole to approach thermal equilibrium before the log is made (Judge, 1972). Convection cells can sometimes interfere with the precision of the T-log, especially in large diameter wells.

Thermal logging also has several advantages as a correlation tool. Thermal logging probes require no contact with the borehole wall, and thus present no contact problems in soft formations where pieces of the wall may have crumbled away. Thermal logs are not as strongly influenced as electrical logs by near-hole phenomena, and may be run in cased boreholes with little loss of resolution (see Chapter 4 for examples).

Beck (1976a) investigated the application of T-logs to

stratigraphic correlation in comparison with electrical resistivity logs (E-logs) from several holes in Australia. He found a strong inverse correlation between the T-logs and the E-logs (the latter having been smoothed so that they might be compared with the less detailed incremental T-logs). Figure 5.1 shows the complete electrical and thermal gradient logs for two boreholes, clearly demonstrating in both cases the 'mirror image' relationship between the two logs. Although he did not attempt to explain the reasons for this phenomenon, Beck states that the peaks showing strong positive correlation (such as the one at approximately 490 m in the Euthalla hole) are apparently diagnostic of coal seams or coal bearing strata. Beck further demonstrates the utility of thermal logs in stratigraphic correlation by using the Pleasant Hills T-log to correct a horizon (the top of the Hutton sandstone) which was apparently mispicked on the basis of the E-log.

It is beyond the scope of the present study to examine the relationships between T-logs and E-logs in detail, and to develop a complete interpretation theory for the application of T-logs to stratigraphic correlation. Hutt and Berg (1968) considered in some detail the relationships between thermal and electrical conductivities of consolidated sandstone rocks and ocean sediments. Their results will be discussed briefly here.

The work of Hutt and Berg is based on the premise that, for a given rock type, both the electrical and thermal

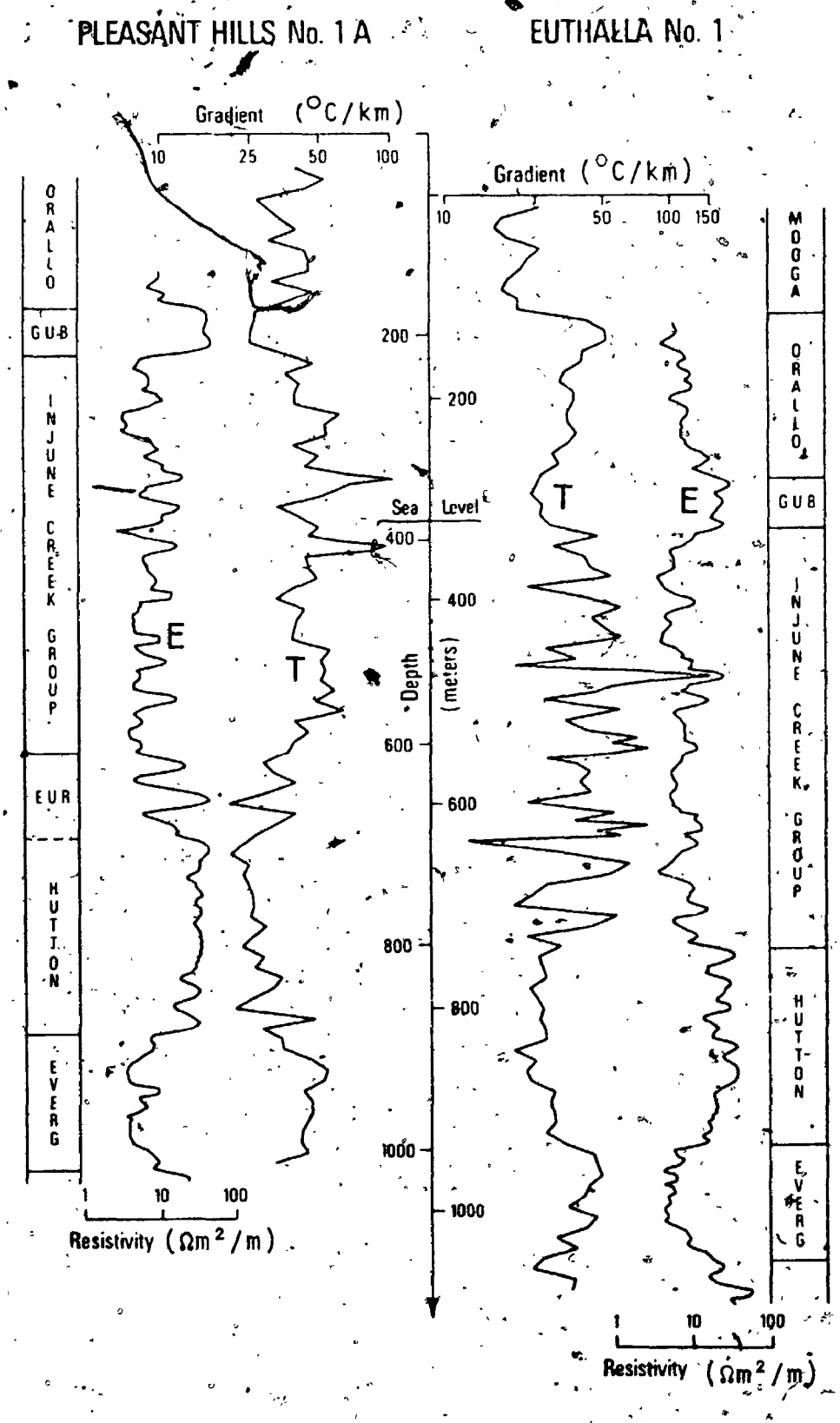

FIGURE 5.1: Comparison of smoothed electrical resistivity logs and incremental T-logs for two boreholes in Australia (after Beck, 1976)

conductivities are more sensitive to variations in porosity (and hence water content) than to variations in the solid constituents. In general the mineral grains present should have a considerably lower electrical conductivity than the (impure) water in the interstices. Thus an increase in porosity is accompanied by an increase in electrical conductivity. In the case of thermal conductivities, most minerals have a significantly higher conductivity than water. Thus, an increase in porosity is accompanied by a decrease in thermal conductivity. Hence, a general inverse relationship between electrical and thermal conductivity is predicted. Obviously this relationship breaks down as porosity approaches zero.

Hutt and Berg consider a number of theoretical models for the conductivity of rocks, and compare various combinations of these with experimental data. The data exhibit considerable scatter, especially the results for consolidated sandstones which, being less porous than the ocean sediments tested, do not agree as well with the theory. Nonetheless, the inverse correlation can be observed. Figure 5.2 shows this general increase in electrical conductivity relative to thermal conductivity for increased volume fraction of water content (porosity).

What about the behavior of rock types other than sandstone? Thermal conductivity in general still varies with porosity (Huang, 1971), and the inverse relationship between porosity and the ratio of electrical to thermal

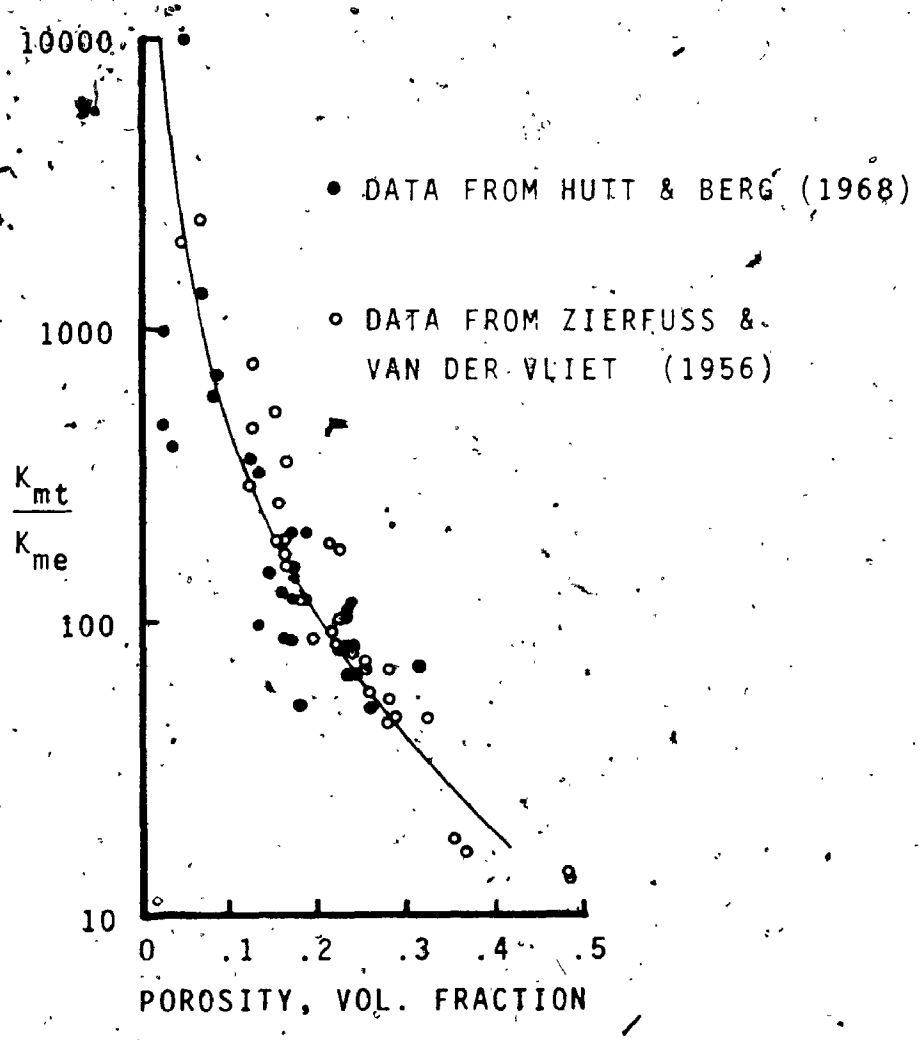

FIGURE 5.2: Relationship of thermal and electrical conductivities (K_{mt} and K_{me} respectively) to porosity in sandstones (after Hutt and Berg, 1968)

conductivity should still hold. This relationship becomes more complicated in rocks that are less porous than sandstones, and thus more sensitive to variations in the thermal conductivities of the solid constituents. A further complication is caused by the variations in electrical conductivity with concentration of free ions in the ground water, especially in carbonate rocks, which are more susceptible to solution than sandstones. Thermal conductivity is essentially unaffected by variations in ionic concentration. Sandstones tend to be texturally more homogeneous than other rock types, and thus present fewer problems in interpretation of well logs in general (Wyllie, 1960).

It is apparent that the potential application of continuous temperature logging to stratigraphic correlation is a subject deserving further investigation. A greater understanding must be developed of the factors affecting thermal conductivity of rocks in situ, as well as the relationships between T-logs and E-logs, at least in empirical terms. Unfortunately, we were unable to gain access in the course of this project to boreholes which had been logged electrically. Such studies should prove very interesting now that continuous T-logs of high precision and resolution can be obtained. It is quite possible that the extra expense involved in building a thermistor package into the front of an electrical logging tool will be offset by the additional information obtained from a single logging

run.

5.3 ENGINEERING APPLICATIONS

In general, the continuous logging system can be used in any application for which other thermal logging techniques are presently used. Continuous analog temperature logs are routinely run in the petroleum industry for various engineering applications. This logging technique is inherently as fast as the system developed in the present project. It suffers, however, from the built-in imprecision and lack of resolution common to analog techniques (as opposed to digital techniques), and contains no provision for deconvolution to compensate for probe response. The output is generally a chart recorder plot of temperature versus depth, which is far less sensitive to subtle thermal effects than the deconvolved gradient logs produced by the continuous digital system. Analog gradient logs are sometimes obtained, but these also are not deconvolved, and hence are fairly crude.

The temperature log is used for checking various aspects of the cementing of the well casing. The cement used between well casing and the surrounding rock releases heat as it sets. The height of the cement top, and local concentrations of cement in channels in the rock may be located by a temporary increase in the borehole temperature in such regions. If the cement has become contaminated with drilling mud while being injected, this temperature increase is generally reduced in magnitude but extended over a

greater time interval. Gas under high pressure escaping into a dry borehole from a producing formation experiences a significant pressure drop, accompanied by a consequent drop in temperature. It is often possible to locate such zones of gas entry by a local decrease in the borehole temperature. Similarly, temperature logs may be used for locating channels through which liquids enter the borehole, for locating zones of lost circulation in drilling, and for checking the effectiveness of such engineering techniques as artificial fracturing and acid treatment of the country rock (Kappelmeyer and Haenel, 1974). Once again it may be asserted that a logging technique offering better precision and resolution allows greater confidence and reliability in the interpretation of results, and may lead to developments which are at present unsuspected.

5.4 OTHER FIELDS OF RESEARCH

Finally, the continuous logging system could prove useful in many diverse fields of study. The in situ study of the thermal properties of rocks, monitoring the return to equilibrium of boreholes, permafrost studies in Arctic regions, physical oceanographic research, and studies of groundwater hydrology and pollution are examples of such potential applications. It is difficult to draw conclusions about such widely varying research areas, and each case must be considered individually, bearing in mind the advantages and disadvantages of continuous logging discussed above.

CHAPTER 6

DISCUSSION AND CONCLUSIONS

6.1 LIMITS ON ACCURACY

In order to evaluate what has been achieved in this project, and to indicate areas where the continuous logging equipment and technique can be improved and further developed, a discussion of the factors limiting the accuracy, precision and resolution of the method is in order at this point. Beginning with the temperature log, the main factors limiting the accuracy of the deconvolved temperature profile are:

(1) The accuracy of the thermistor calibration (resistance versus temperature)

(2) The accuracy of the resistance readings

(3) Self heating of the thermistors

(4) Errors in probe time constant determination, including deviations in form between the true and assumed probe step response

(5) The uncertainty involved in making any physical measurement

The accuracy of the thermistor calibration is a problem common to all temperature logging techniques which employ

thermistors, and hence need not be elaborated upon here. Appendix B outlines the calibration techniques which we use.

The main factor affecting the accuracy of the resistance reading (besides the quality of the multimeter, which should not be a problem with state of the art equipment) is the measuring technique used. In the four wire technique (separate pairs of wires for the test current and for sensing) the resistance is measured immediately at the load. Thus, the lead resistance is automatically removed and the digital meter registers only the thermistor resistance. In our case a two wire measuring technique was used since we were unable to obtain a four lead cable which was as noise free as our three lead cable. In this case lead resistance must be subtracted from the resistance readings before converting to temperature. Although in theory this should be simple, in practice this technique simply is not as accurate as the four wire technique due to the effect of many small sources of error (e.g. temperature coefficient of resistivity, slip-ring resistance variations), and due to the impossibility of monitoring all of the lead resistances during the experiment. Hence, the four wire technique, which is reccomended by most manufacturers of precision DMM's, should be used whenever possible.

Self heating of the thermistors is Joule heating due to the current passing through them. In general, the higher the current or the larger the thermistor dissipation

constant, the greater the problem. This problem can be minimized by using more thermistors in parallel and by calibrating the probe under conditions as near as possible to those encountered in the field.

Deconvolving the data with an erroneous time constant will introduce errors into the temperature curve. If the assumed time constant is too short the deconvolved curve will tend to lag the actual temperature profile (although not as badly as in the case where the time constant is ignored altogether). If the assumed time constant is too long, the deconvolved curve will overshoot the actual temperature curve at changes in gradient, and in general will 'lead' the actual profile. Accurate probe time constant determination is probably more important for temperature profiles than for gradient profiles. In general, the probe step response should be measured under conditions as nearly like those encountered in the borehole as possible. The modified deconvolution technique described in section 2.8 should be used for maximum accuracy.

In making temperature measurements one should not forget the uncertainty involved in making any physical measurement; not only does the probe approach the temperature of the borehole fluid, but the converse is also true. This uncertainty should be a smaller problem in continuous logging than in the incremental technique, since the probe is constantly moving and entering undisturbed water.

The accuracy of the depth scale for the temperature profile is limited by the following factors:

(1) The accuracy of the pulley calibration (meters per revolution of the well head pulley)

(2) The presence of uncompensated cable slip or stretch

(3) Probe drag

The effective circumference of the well head pulley in our case is about 0.25 m. The precise calibration of this pulley is discussed in Appendix C. Cable stretch is a complicated phenomenon which must be compensated for in the results if maximum depth accuracy is desired. This also is discussed in Appendix C. At very high logging speeds, especially in mud filled holes, probe drag could cause the recorded depths to be somewhat deeper than the actual depths. An order of magnitude calculation in our case indicates the effect of probe drag (in water) to be less than 0.5 kg at the maximum lowering rate which we used (18 m/min), and thus this factor can be neglected in the present case.

Several factors which are of little importance in the temperature measurements, but which have a limiting effect on the accuracy of the gradient log, are given below:

(1) Probe velocity

(2) Sample rate

(3) Instrument resolution

(4) Filter length

(5) Electrical noise

(6) Inaccuracies and variations in the logging speed

Lowering rate, sample interval, instrument resolution, filter length and probe time constant exert a more or less mutually interdependent effect on the accuracy and resolution of the gradient profile. If the measuring instrument had perfect resolution (i.e. no round off error), and if there were no noise, then three point deconvolution and gradient operators could be used in the data reduction. In this case the accuracy and resolution would be independent of time constant, and would be linearly dependent upon lowering speed and sample interval. By definition, the limit of resolution would be the Nyquist frequency which, in space coordinates would be:

$$2(V)(\Delta t) \tag{6.1}$$

where V is probe velocity (m/sec)

Δt is sample interval (sec)

Assuming a lowering rate of 18 m/min and a sample interval of 0.3 seconds gives a resolution of 0.09 meters. This is the theoretical limit under these conditions. Given a measuring instrument with limited precision, but no other noise, then the situation is far more complicated. For a given instrument resolution (and filter length), T-log resolution is determined by the probe time constant, lowering velocity and sample rate, but the relationship is no longer linear. Take an extreme case as an illustration.

Given an effective instrument resolution of 1°C, and a borehole which varies linearly from a temperature of 9°C at the top to 10°C at the bottom, it is clear that the temperature output is going to be a step function, suddenly jumping from 9°C to 10°C at some point along the borehole. The location of this point is nearly independent of the sample interval (the maximum error is approximately equal to the sample interval), but will depend somewhat on probe velocity and time constant, although not in a linear manner. The introduction of significant electrical noise into the system naturally complicates matters, by adding extraneous anomalies to the gradient profile, and generally necessitating a longer combined operator. It is due to the extremely complex and interrelated nature of the above factors that the figures cited for precision and resolution in this work have been obtained empirically from direct study and comparison of the gradient logs.

Accurate determination and monitoring of logging speed is important since the amplitude of the output gradient log is inversely proportional to the logging speed used in the computer program which calculates the gradients (Appendix A). Furthermore, It is not uncommon for the logging speed to increase by 5 to 10% during a run, due to the increasing weight of cable in the borehole (see figure 6.1). If this factor is not considered in the data reduction, a significant error in gradient will result. Monitoring the logging speed is not difficult, however. This is

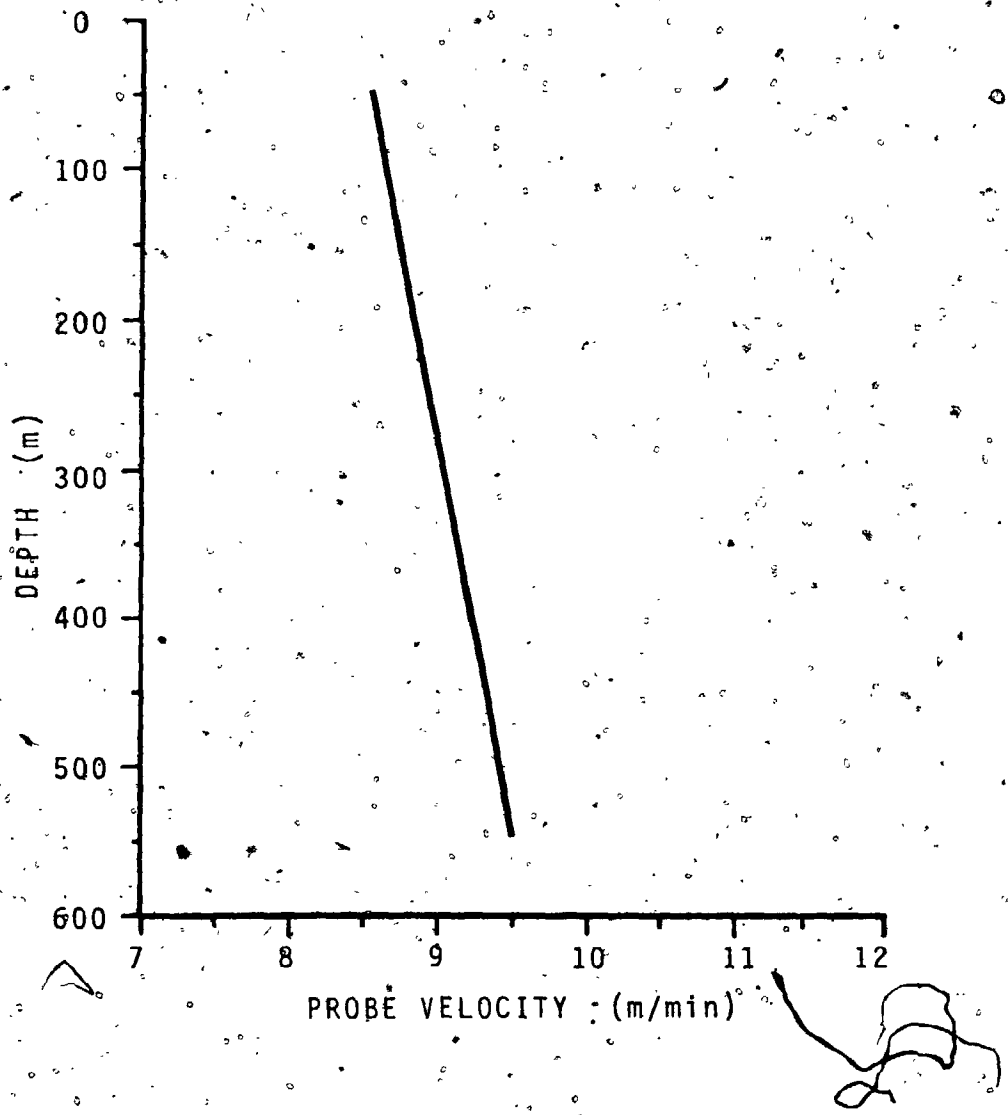

FIGURE 6.1: Variation in probe velocity with depth, due to increased weight of cable in the borehole

accomplished in the data reduction process over intervals of, say, 200 readings (about 1 minute) by the relation:

$$V = \frac{(N_P)(F_P)}{(N_R)(\Delta t)} \qquad (6.2)$$

where N_P = number of pulley revolutions

F_P = pulley calibration factor (m/rev)

N_R = number of resistance readings

Δt = sample interval (sec)

See Appendix A for details on the data reduction.

6.2 REFINING THE EQUIPMENT

If the continuous gradient logging technique is to be used routinely for heat flow investigations or other work, certain improvements and refinements are indicated. some of these are summarized below.

(1) Since the effectiveness of the method has been demonstrated, the purpose of the prototype equipment has been served. This can now be redesigned and rebuilt with performance, ruggedness, and portability given greater emphasis than cost. Because of the wide variance in the requirements of the potential applications of the continuous logging technique, such design changes must be made with a particular application in mind.

(2) The use of a four lead shielded or armored cable is highly recommended, providing one can be found with good noise characteristics. This would allow the four lead measuring technique to be used, as discussed in section

6.1.

(3) Substitution of a digital tape recorder (incremental or buffered synchronous) for the D-A converter and FM recorder should greatly simplify the data reduction process (see Chapter 2 and Appendix A for details). It is also important, however, to consider the ruggedness and portability of this type of unit, as reliability in the field is more important than convenience in the data reduction.

(4) One of the persistant problems in temperature logging stems from the great length of cable (usually 1 km or more) between the measuring instrument and the sensor. By building a specialized digital resistance meter into the probe, information can be brought up the cable in serialized BCD (binary coded decimal) form, a procedure which is relatively insensitive to electrical interference. Another possible method for accomplishing this is to frequency modulate the resistance reading in the probe, and decode this FM signal at the surface (see Judge, 1972). This, however, is essentially an analog technique, and hence may cause the resolution to suffer (see Chapter 1).

(5) Precision and resolution of the gradient logs can be enhanced in general by making any of the following improvements:

(a) Reduction of electrical noise by any available means

(b) Reduction of probe velocity.

(c) Reduction of probe time constant

(d) Improving instrument resolution (i.e. reading to, say, 0.1 ohm rather than 1.0 ohm).

(e) Use a thermistor probe with a greater nominal resistance (say, 50000 ohms instead of 5000 ohms). This has an effect similar to (d).

(f) Increase sample rate

Of course, electrical pickup may render several of these improvements impractical under certain conditions. For instance, increasing the resistance ten-fold was found to increase the noise by a similar amount in the field tests. These tests were performed in especially noisy environments however, and normally electrical interference should present no problem. Furthermore, even though low current digital multimeters are available with very fast sample rates (up to 1000 Hz in one model), such an instrument will probably not have as good a common-mode rejection as the slower meters. If noise is a great problem, this should be borne in mind. Reducing the probe time constant generally means using smaller thermistors which, all else being equal, means a greater self-heating problem. Using a slower probe velocity is similar to using a probe with a faster time constant and an increased sample rate. Since the temperature difference between sample points is reduced along with reduced probe velocity, it is clear that less and less benefit will

accrue from successive reductions in probe velocity, an example of the law of diminishing returns.

6.3 CONCLUSIONS

What has been accomplished to date in this project to design and develop a high precision tool for the continuous logging of borehole temperature gradients allows the following conclusions to be drawn:

(1) The combined operator developed in Chapter 2 yields precise and repeatible results at low computing costs, even in the presence of considerable electrical noise. If noise spikes greater than, say, $0.1^{\circ}C$ are encountered, these should be removed from the data before processing in order to maintain maximum precision. Such extreme noise conditions should not normally be encountered in routine field work. Calculation and application of this time-domain operator is a relatively straightforward process, and it should thus be useful to the worker who does not have an extensive background in time series analysis. The relative lengths of the individual terms in the combined operator are not critical. As a rule of thumb, the smoothing, deconvolution, and gradient terms should be roughly of the same length. The smoothing term should generally be of the form of a cosine bell or a stretched cosine bell.

(2) A continuous gradient logging technique has been developed which offers excellent precision (better than $\pm 0.5^{\circ}C/km$) and resolution (at least 2 m, and, under

certain conditions, better than 0.5 m) at rapid logging rates (say, 18 m/min). The reliability and utility of the T-log for fine-scale work is enhanced considerably if two or more logs are superimposed.

(3) In order to obtain this same detail and resolution using the incremental logging technique, hundreds of hours of logging time would be required (see figure 1.1).

(4) A log may be made both while lowering the probe and while raising it. Although the results of the up-hole technique exhibit considerably greater error, they can serve at least as a rough check on the down-hole log.

(5) The problem of the geologic interpretation of T-logs has been discussed at some length in Chapter 5. Much work remains to be done here. Tremendous effort has been expended over many years in developing other well logging techniques, such as electrical resistivity and SP, as stratigraphic correlation and structural mapping tools. As a result, these techniques can sometimes be used today for interpretations of amazing subtlety and detail (see Pirson, 1970, for some interesting examples). With some development, continuous gradient logging may become a valuable addition to the list of high resolution logging tools available today.

APPENDIX A

COMPUTER PROGRAMS

Some of the more important computer programs used in the reduction of the field data will be presented in this appendix. Sufficient comment statements are included to allow the programs to be understood by anyone interested enough to study them. In addition, a brief description of the purpose and use of each of the routines will be included below. A flow chart for the data reduction process is shown in figure A.1.

A.1 INTERPRETATION OF THE DIGITIZED TAPE

Program RICTST is a program supplied by the University Computer Centre (and modified slightly by the author) for the purpose of assembling the coded information from the digitized tape into a string of integer values varying from -1024 (representing -2.5V on the analog tape) to +1024 (representing +2.5V on the analog tape). The four parallel channels of information from the analog tape are recorded in serial form on the digitized tape.

Subroutines RICOPN, RICRED, and ADBX, are concerned primarily with the mechanics of bit manipulation to suit the specific format requirements of the PDP-11 A-D

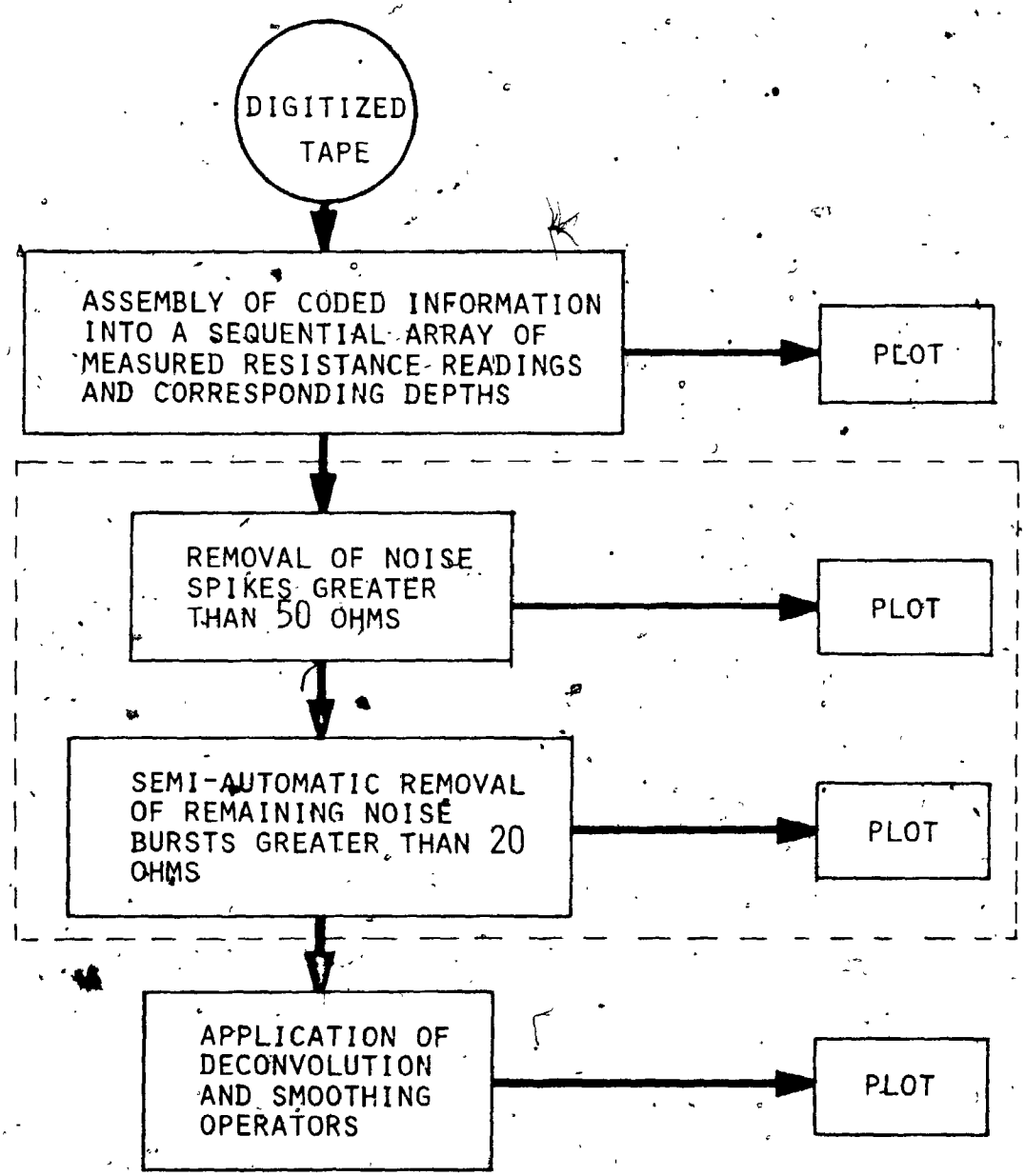

FIGURE A.1: Flow chart for the data reduction. The noise removal steps (inside dashed line) were necessary in the early field tests, when electrical interference was a problem.

converter, and the Control Data Cyber-73 computer on which the actual data processing was done. These subroutines are highly specialized, and of little interest here, and hence are not presented.

Subroutine MESS was written by the author for the purpose of sorting the string of integral coded digitized voltage values (assembled for each of the 4 channels by RICTST) into the actual series of resistance readings and associated depth values which would have been recorded directly had an incremental or buffered sychronous digital tape recorder been available for the field work. Subroutine MESS is primarily a controlling subroutine which in turn calls subroutines LIMITT, SETT, TRIGGER, READING and DEEP for the calculations and manipulations required. The routing through these various subroutines is variable and somewhat complicated, and is controlled by the integer parameter KEY. Essentially, the digitized information from channel 4 (see section 3.4) is searched by subroutine TRIGGER until a data display signal (i.e. indicating the output of a new resistance reading) is found and confirmed. The corresponding integer coded voltage values from the other 3 channels are then converted into a resistance reading by subroutine READING, and this value is written in binary on disk (or tape), along with the current depth value. Concurrently with the search for a data display signal, channel 4 is also monitored by subroutine DEEP for the occurrence of a depth signal from the well head pulley

microswitch. When one is found and confirmed, this information is stored until subroutine READING is called, at which time it is written on disk, as described above. Subroutine MESS requires that the initial values for depth (D, in pulley revolutions) and resistance (KONST, to the next lowest thousand ohms) be provided by the user before the program is run. Changes of resistance range (from, say, 5999 to 6000 ohms) are monitored by READING, and compensation is made for this in the value of KONST. This allows us to record only the ones, tens, and hundreds places in the resistance readings, since the more significant thousands and ten thousands places are supplied by READING.

```
      PROGRAM RICTST(TAPE1=514,OUTPUT,TAPE2=514)
C  NOTE -- TAPE1 must be the first file specified in the
C       program card.  the buffer is set to 100B to reduce
C       unused buffer space
      DIMENSION CHANEL(4,80)
      INTEGER CHANEL
      LOGICAL LFIRST
      DIMENSION ARRAY(640)
      INTEGER ARRAY
      LFIRST=.TRUE.
      IX=0
C  call RICOPN(unit,mode)
C  TAPE is defined in request card AS TAPE1
C  mode = 1
      CALL RICOPN(1,1)
C  skip the header block
      CALL RICRED(ARRAY,NWORD,IERR),RETURNS (99)
C  ARRAY = array to hold 640 8 bit bytes
C  NWORD = number of words return from RICRED
C       should be 640 always
C  IERR = error code returned
C  start processing data here
C  read in one record from TAPE
10    CALL RICRED(ARRAY,NWORD,IERR),RETURNS (99)
C  convert two bytes of data into an integer
C  and store them in CHANEL
      CALL ADBX(ARRAY,CHANEL,NWORD)
C  user can start processing the a-d data here
      IX=IX+1
      IF(IX.LE.0) GO TO 10
      CALL MESS(CHANEL,LFIRST,KBOTTOM)
      LFIRST=.FALSE.
      GO TO 10
C  tape error (including eof or eot)
C  refer to RICRED writeup for IERR codes
99    PRINT 100,IERR
      PRINT 110,KBOTTOM
100   FORMAT(*  IERR=*,I3)
110   FORMAT(1H1,I6,* VALUES WRITTEN ON DISK*)
      STOP
      END
```

```
      SUBROUTINE MESS(CHAN,LFIRST,KBOTTOM)
C     NOTE:  must put LFIRST loop in main program such that the
C     first time the subroutine is called, LFIRST=.TRUE.,
C     but never again.  (put LFIRST=.FALSE.
C     after call to MESS in main program)
      LOGICAL LFIRST
      INTEGER CHAN
      DIMENSION CHAN(4,80)
      IF(.NOT.LFIRST) GO TO 10
C     initialize values which are valid only for first call to
MESS
      KBOTTOM=0
C     D is initial reading on pulley counter
C     (D=0 indicates probe starts precisely at  top of hole)
      D=0
C     KONST is initial resistance reading rounded down to
C     next 1000 ohms
      KONST=10000
C     KEY controls progress through the various subroutines
      KEY=1
C     KOUNT is a controlling index for subroutine TRIGGER
      KOUNT=0
C     KOUNT2 is a controlling index for subroutine SETT
      KOUNT2=0
C     KOUNTD is a controlling index for subroutine DEEP
      KOUNTD=0
10    CONTINUE
C     make sure all values within range of validity of
C     calculations
      CALL LIMITT(CHAN)
C     initialize values for this call to MESS
      KK=1
      J=0
      GO TO(20,30,40),KEY
C     begin looking for non-trigger mode.
20    CALL SETT(CHAN,J,D,KEY,KOUNT2,KOUNTD)
      GO TO(50,30),KEY
C     test for trigger mode
30    CALL TRIGGER(CHAN,J,D,KEY,KOUNT,KOUNTD)
      GO TO(50,50,40),KEY
C     calculate total resistance value of last 3 digits on
C     on meter
C     calculations
C     and write resistance along with current value of D
40    CALL READING(CHAN,J,KK,D,KEY,LFIRST,KONST,KBOTTOM)
      GO TO 20
50    RETURN
      END
```

```
      SUBROUTINE LIMITT(CHANEL)
      INTEGER CHANEL
      DIMENSION CHANEL(4,80)
C  make sure all values within range of validity of
      DO 5 J=1,80
      DO 5 I=1,4
      IF(CHANEL(I,J).GT.636) CHANEL(I,J)=636
5     IF(CHANEL(I,J).LT.-636) CHANEL(I,J)=-636
      RETURN
      END



      SUBROUTINE SETT(CHAN,J,D,KEY,KOUNT2,KOUNTD)
      INTEGER CHAN
      DIMENSION CHAN(4,80)
      J=J+1
      IF(J.LE.80) GOTO 35
      GO TO 80
35    CONTINUE
      CALL DEEP(CHAN,J,D,KOUNTD)
40    CONTINUE
      IF(CHAN(4,J).GT.-200.AND.CHAN(4,J).LT.0) GO TO 50
      IF(CHAN(4,J).GT.380) GO TO 50
      J=J+1
      IF(J.LE.80) GOTO 45
      GO TO 80
45    CONTINUE
      CALL DEEP(CHAN,J,D,KOUNTD)
      KOUNT2=0
      GO TO 40
50    KOUNT2=KOUNT2+1
      IF(KOUNT2.EQ.3) GO TO 60
      J=J+1
      IF(J.LE.80) GOTO 55
      GO TO 80
55    CONTINUE
      CALL DEEP(CHAN,J,D,KOUNTD)
      GO TO 40
60    CONTINUE
      KEY=2
      KOUNT2=0
80    RETURN
      END
```

```
      SUBROUTINE TRIGGER(CHAN,J,D,KEY,KOUNT,KOUNTD)
      INTEGER CHAN
      DIMENSION CHAN(4,80)
      J=J+1
      IF(J.LE.80) GO TO 5
      GO TO 40
5     CONTINUE
      CALL DEEP(CHAN,J,D,KOUNTD)
10    CONTINUE
      IF(CHAN(4,J).LT.327.AND.CHAN(4,J).GT.0) GO TO 20
      IF(CHAN(4,J).LT.-200) GO TO 20
      J=J+1
      IF(J.LE.80) GO TO 15
      GO TO 40
15    CONTINUE
      CALL DEEP(CHAN,J,D,KOUNTD)
      KOUNT=0
      GO TO 10
20    KOUNT=KOUNT+1
      IF(KOUNT.EQ.5) GO TO 30
      J=J+1
      IF(J.LE.80) GO TO 25
      GO TO 40
25    CONTINUE
      CALL DEEP(CHAN,J,D,KOUNTD)
      GO TO 10
30    CONTINUE
      KEY=3
      KOUNT=0
40    RETURN
      END
```

```
      SUBROUTINE READING(CHAN,J,KK,D,KEY,LFIRST,KONST,
     1  KBOTTOM)
      LOGICAL LFIRST
      INTEGER CHAN
      DIMENSION CHAN(4,80)
C  calculate total resistance value of last 3 digits on
C  meter
      ONE=(CHAN(1,J)+636)/128
      TEN=((CHAN(2,J)+636)/128)*10
      HUN=((CHAN(3,J)+636)/128)*100
      OHMS=ONE+TEN+HUN
      IF(LFIRST.AND.KK.EQ.1)GO TO 10
C  compensate for change of range on meter
      IF(OHMS-OMEGA.GT.500) KONST=KONST-1000
      IF(OHMS-OMEGA.LT.-500) KONST=KONST+1000
C  calculate total resistance reading
10    RES=OHMS+KONST
      WRITE(2) D,RES
      OMEGA=OHMS
      KK=KK+1
      KBOTTOM=KBOTTOM+1
      KEY=1
      RETURN
      END



      SUBROUTINE DEEP(ICHAN,J,D,KOUNTD)
      DIMENSION ICHAN(4,80)
      IF(ICHAN(4,J).GT.0) GO TO 40
      IF(KOUNTD.GE.4) GO TO 50
      GO TO 60
40    KOUNTD=KOUNTD+1
      GO TO 70
50    D=D+1
60    KOUNTD=0
70    RETURN
      END
```

A.2 APPLICATION OF THE COMBINED OPERATOR

Program LONGFAL takes the series of resistance readings and associated pulley rotation values written by subroutine READING (see section A.1), and produces the smoothed, deconvolved temperature gradient series and associated smoothed depth series. The program writes N pairs of resistance and depth values at a time on to disk (or tape) where N can be any integer value greater than the combined operator length. By keeping N relatively small (in the sample program included here, N = 200), LONGFAL requires only moderate core memory, and can work on an indefinitely long time series.

Input parameters to LONGFAL include the thermistor calibration constants (see Appendix B), and the direction of travel of the logging tool (down or up). Program LONGFAL calls subroutine FILOP which computes the smoothing, deconvolution, and gradient terms, and combines them into a single operator using FOLD, a convolution subroutine which may be found in Robinson (1967a). The arguments in the call to FILOP include the number of points in the gradient operator (and hence the deconvolution operator) and the number of points in each of the sides and the flat top of the stretched cosine bell smoothing operator (see figure 2.8). Other input arguments are the thermistor probe time constant (seconds) and the initial descending rate (m/min). FILOP returns the combined operator and the number of points in that operator. The descending rate is recalculated from

the pulley depth signals and the known sample rate of the digital multimeter, and FILOP recalled after each N data values are written on disk. Thus, LONGFAL automatically compensates for variations in probe velocity (see Chapter 6).

Subroutine DEPTHOP provides LONGFAL with a linear least squares smoothing operator which, when convolved with the stepwise series of pulley rotation values, produces a corresponding smoothed series of depth values in meters. This operator is short (say, 11 points) and so has enough zeros added to each end to make it the same length as the combined operator, for convenience in writing LONGFAL.

The output from LONGFAL is a binary disk (or tape) file containing pairs of temperature gradient values and associated depth values, suitable for plotting in the form of the T-log.

```
      PROGRAM LONGFAL(INPUT,OUTPUT,TAPE1,TAPE2,TAPE6=OUTPUT)
C  TAPE1 is generally output disc
C  TAPE2 is generally input disc
C  A is output time series
C  TS is input time series
C  B is output depth series
C  DS is input depth series
      DIMENSION A(400),TS(400),DECOP(200)
      DIMENSION B(400),DS(400),DEEPOP(200)
      LOGICAL DOWN
C  AA,BB,CC are thermistor parameters
      AA=-6.9514774
      BB=5143.8333
      CC=-156609.91
C  stretch correction parameters S=AAA*Z**BBB
      AAA=.00044
      BBB=4./3.
C  N is number processed at a go
C  this program writes N values each trip through
C  N must be greater than nfpts
      N=200
      KOUNT=N
C  LIMIT is no of pts to be processed total
C  (i.e. (no. pts in profile - bad pts at ends) rounded down
C  to next lowest even N
      LIMIT=4000
C  if lowering probe (DOWN=.T.), if raising probe (DOWN=.F.)
      DOWN=.TRUE.
C  DR is initial descending rate (m/min)
      DR=8.5
      WRITE(6,100)
C  PULFAC is pulley factor (revolutions/meter)
      PULFAC=3.955
C  NFPTS is no of pts in filter operators
C  DECOP and DEEPOP are filter operators
      CALL FILOP(17,9,17,DR,12.,NFPTS,DECOP)
      CALL DEPTHOP(11,PULFAC,NFPTS,DEEPOP)
C  next loop is to skip unwanted data at the beginning
      NSKIP=100
      DO 1 I=1,NSKIP
1     READ(2) X,XX
      N1=KOUNT+NFPTS-1
      NA=NFPTS-1
C  read in first data string
      DO 2 I=1,N1
      READ(2) DS(I),TS(I)
C  calculate temperature
      ARG=(BB*BB+4.*CC*ALOG(TS(I))-4.*AA*CC)
      ROOT=ARG**.5
      DENOM=2.*(ALOG(TS(I))-AA)
      TS(I)=((BB+ROOT)/DENOM)-273.15
2     CONTINUE
5     CONTINUE
C  perform convolution
      DO 10 J=1,N
```

```
      A(J)=0.
      B(J)=0.
      J1=J-1
      DO 10 K=1,NFPTS
      KK=K+J1
      KKKK=NFPTS+1-K
      A(J)=A(J)+DECOP(KKKK)*TS(KK)
10    B(J)=B(J)+DEEPOP(KKKK)*DS(KK)
      DO 15 I=1,N
C  correct sign of gradient if raising probe
      IF(.NOT.DOWN) A(I)=-1.*A(I)
C  correct for cable stretch
      S=AAA*(B(I)**BBB)
      B(I)=B(I)+S
15    WRITE(1) B(I),A(I)
      WRITE(6,200) DR
      DO 20 I=1,NA
      DS(I)=DS(I+N)
20    TS(I)=TS(I+N)
      IF(KOUNT.EQ.LIMIT) GO TO 30
C  read in a new data string
      DO 25 I=NFPTS,N1
      READ(2) DS(I),TS(I)
C  calculate temperature
      ARG=(BB*BB+4.*CC*ALOG(TS(I))-4.*AA*CC)
      ROOT=ARG**.5
      DENOM=2.*(ALOG(TS(I))-AA)
      TS(I)=((BB+ROOT)/DENOM)-273.15
25    CONTINUE
      RATE=(DS(N1)-DS(NFPTS))/FLOAT(N1-NFPTS)
      DR=47.25*RATE
      CALL FILOP(17,9,17,DR,12.,NFPTS,DECOP)
      KOUNT=KOUNT+N
      GO TO 5
30    CONTINUE
100   FORMAT(* PROBE VELOCITIES USED IN
     1  CALCULATIONS (M/MIN)*/)
200   FORMAT(F10.2)
      STOP
      END
```

```
      SUBROUTINE FILOP(LDERIV,LSIDE,LFLAT,DR,TC,
     1  LSUPER,FSUPER)
      DIMENSION FDERIV(200),FDECON(200),FSUPER(700),F2(400),
      DIMENSION FAVG(500)
C  LDERIV is length of derivative operator (odd)
C  LSIDE is length of side of cos bell (multiple of 9)
C  LFLAT is length of flat of cos bell (odd)
C  DR is descent rate in m/min
C  TC is time const of probe in sec
C  DIGINT is digitization interval in km
      DIGINT=DR*(.3/60000.)
C  SPACON is space equivalent of time constant in km
      SPACON=TC*DR/60000.
C  calculate derivative operator
      NA=(LDERIV-1)/2
      TERMA=0.
      DO 10 I=1,NA
      AI=FLOAT(I)
10    TERMA=TERMA+2.*AI*AI
      TERMA=TERMA*DIGINT
      FDERIV(1)=FLOAT(NA)/TERMA
      DO 20 I=2,LDERIV
20    FDERIV(I)=FDERIV(I-1)-(1./TERMA)
C  calculate deconvolution operator
      DO 30 I=1,LDERIV
30    FDECON(I)=FDERIV(I)*SPACON
      FDECON(NA+1)=1.
C  calculate smoothing operator (stretched cosine bell)
      AXE=0.
      KON1=LSIDE+1
      KON2=LSIDE+LFLAT-1
      KON3=LSIDE+LFLAT
      KON4=2*LSIDE+LFLAT-2
      KON4A=KON4+1
      DO 40 I=1,LSIDE
      AI=FLOAT((I*180/LSIDE)-90)
      FAVG(I)=1.+SIN(AI*3.14159/180.)
40    AXE=AXE+FAVG(I)
      DO 50 I=KON1,KON2
      FAVG(I)=FAVG(I-1)
50    AXE=AXE+FAVG(I)
      DO 60 I=KON3,KON4
      FAVG(I)=FAVG(KON4A-I)
60    AXE=AXE+FAVG(I)
      DO 70 I=1,KON4
70    FAVG(I)=FAVG(I)/AXE
      KON5=KON4+LDERIV-1
      CALL FOLD(KON4,FAVG,LDERIV,FDERIV,KON5,F2)
      KON6=KON5+LDERIV-1
      LSUPER=KON6
      CALL FOLD(LDERIV,FDECON,KON5,F2,KON6,FSUPER)
      RETURN
      END
```

```
      SUBROUTINE DEPTHOP(LSMOO,PULFAC,LTOTAL,DEPO)
      DIMENSION DEPO(LTOTAL)
      N1=(LTOTAL+1)/2
      N2=LSMOO/2
      N3=N1-N2
      N4=N1+N2
      DO 10 I=1,LTOTAL
10    DEPO(I)=0.
      DO 20 I=N3,N4
20    DEPO(I)=1./(PULFAC*LSMOO)
      RETURN
      END
```

APPENDIX B

THERMISTOR CALIBRATION AND TIME CONSTANT DETERMINATION

Two thermistor probe assemblies were used in the field testing of the continuous logging method. The first, C-10, was used for the first three successful runs in the UWO borehole. This assembly consists of 10 Fenwal glass bead thermistors (nominal resistance 100kΩ each) wired in parallel and embedded in epoxy resin inside a slightly flattened brass tube (see figure 3.1). The second probe, C-20, which was used in the remaining field tests, contains 20 thermistors of the above type wired in parallel and embedded in epoxy resin inside a round brass tube. The techniques used for calibrating these probes and determining their respective time constants are described in this appendix.

B.1 THERMISTOR CALIBRATION

The two probes were calibrated against a Tinsley model #5187 SA platinum resistance thermometer, immersed (along with the probes) in an aluminum block submerged in water inside a Hotpack model #334 refrigerated bath-circulator. The resistance readings of the platinum resistance thermometer were made using a Honeywell-Rubicon Muellet

bridge. The resistance readings of the thermistor probes were made with the digital multimeter used in the field tests, so that self-heating effects should be essentially the same under field and laboratory conditions.

A curve of the form

$$R = \exp\left(A + \frac{B}{\Theta} + \frac{C}{\Theta^2}\right) \tag{B.1}$$

where R is probe resistance (ohms)

Θ is temperature (K)

A, B, C are experimentally determined constants

is fitted to the calibration data for each probe. The parameters A, B, and C are then used in solving for in the computer data reduction using the following expression:

$$\Theta = \frac{B + (B^2 + 4C\ln R - 4AC)^{\frac{1}{2}}}{2\ln R - A} - 273.15 \tag{B.2}$$

where Θ is now in ^{o}C.

Figure B.1 shows the calibration curve of probe C-10 as an example.

B.2 TIME CONSTANT DETERMINATION

The thermistor probe time constant is required for the deconvolution of the measured temperature data. This time constant is the time required for the probe to reach 1-1/e of the final temperature when exposed to a step temperature change. This step change is accomplished in practice by allowing the probe to come to equilibrium temperature in

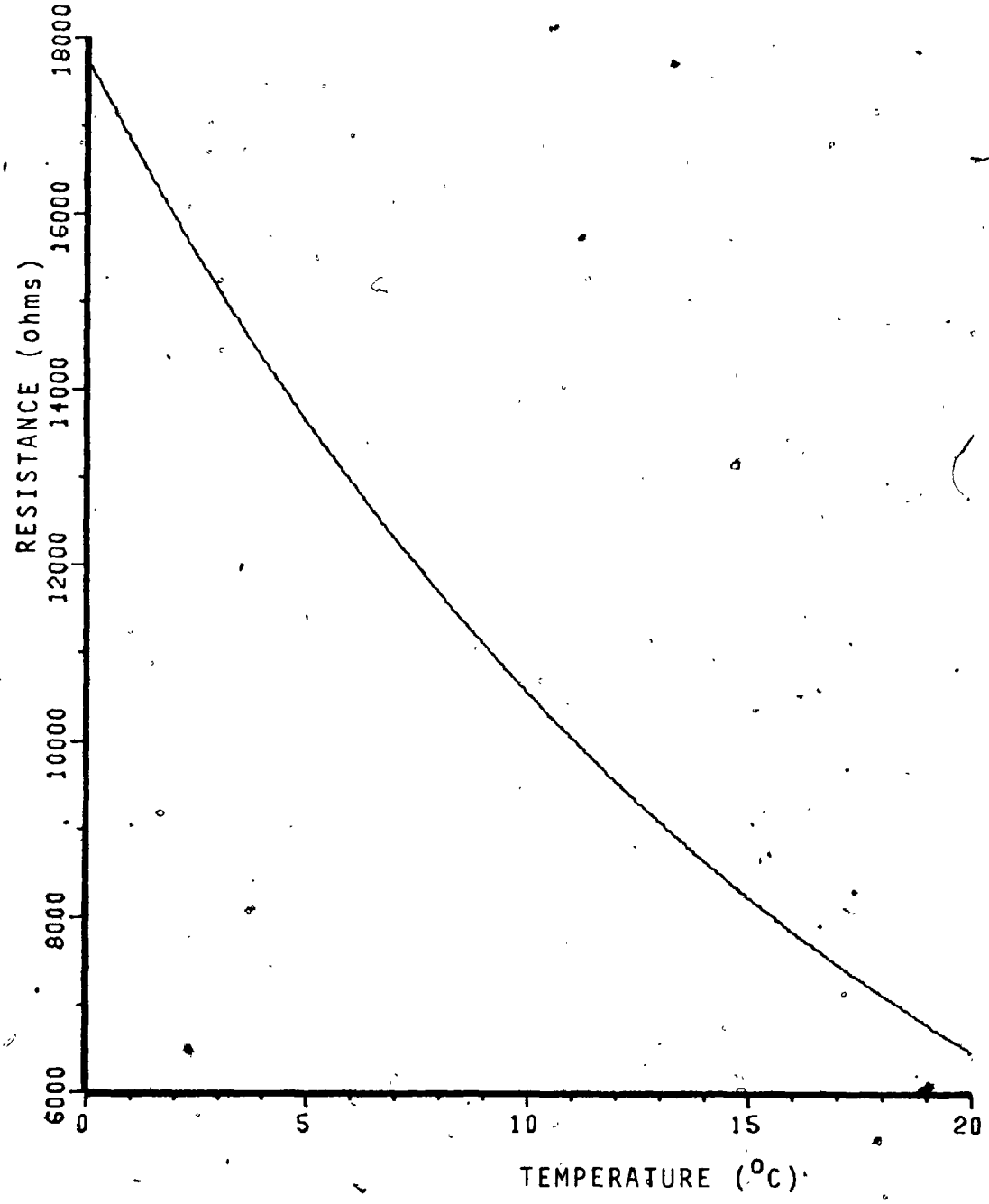

FIGURE B.1: Example of a thermistor calibration curve, for probe C-10.

air, and then plunging it into the Hotpack constant temperature bath, which is maintained a degree or so higher or lower than room temperature. The BCD output of the Data Precision multimeter is recorded as for the field tests (see Chapter 3), and the results are plotted as normalized temperature against time. Figures B.2 and B.3 show smoothed step response plots for the two thermistor probes used in the field tests. Also shown in each case is the theoretical unit step response of the form

$$\theta(t) = 1 - \exp(-t/T) \tag{B.3}$$

having the same 1-1/e time constant as the experimental data. The apparent time constant for probe C-1Ø is seen to be about 2.7 seconds, while the apparent time constant for probe C-2Ø is about 1Ø seconds. For maximum precision in deconvolution, the procedure outlined in section 2.8 should be followed. In this case the actual time constant to be used in deconvolution (T_{ac}) is equal to the apparent time constant (T_{ap}) less the initial lag, D. In the case of probe C-1Ø, as an example, this works out to:

$$\begin{aligned} T_{ac} &= T_{ap} - D \\ &= 2.7 - Ø.7 \\ &= 2 \text{ sec} \end{aligned}$$

The data are deconvolved using the actual time constant (2 seconds), and are plotted shifted in space by and amount

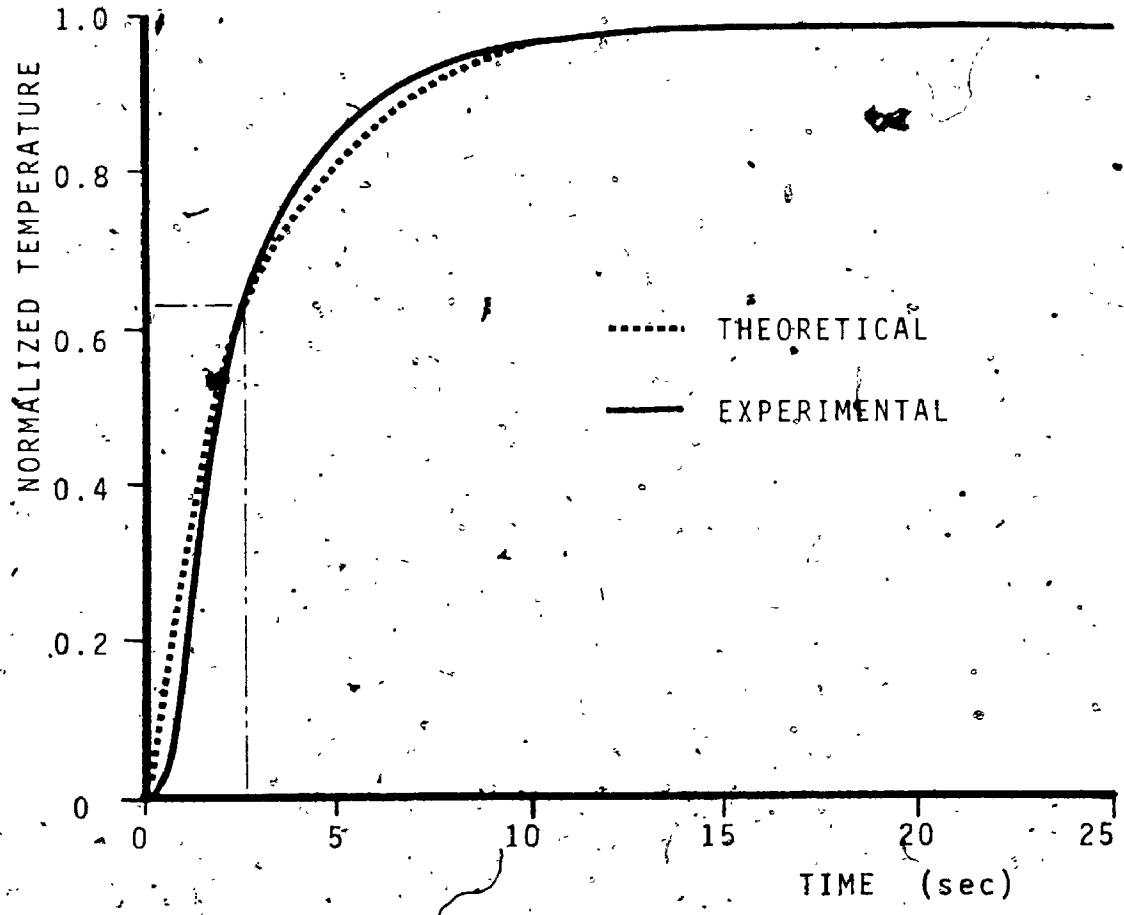

FIGURE B.2: Theoretical and smoothed experimental step responses for thermistor probe C-10.

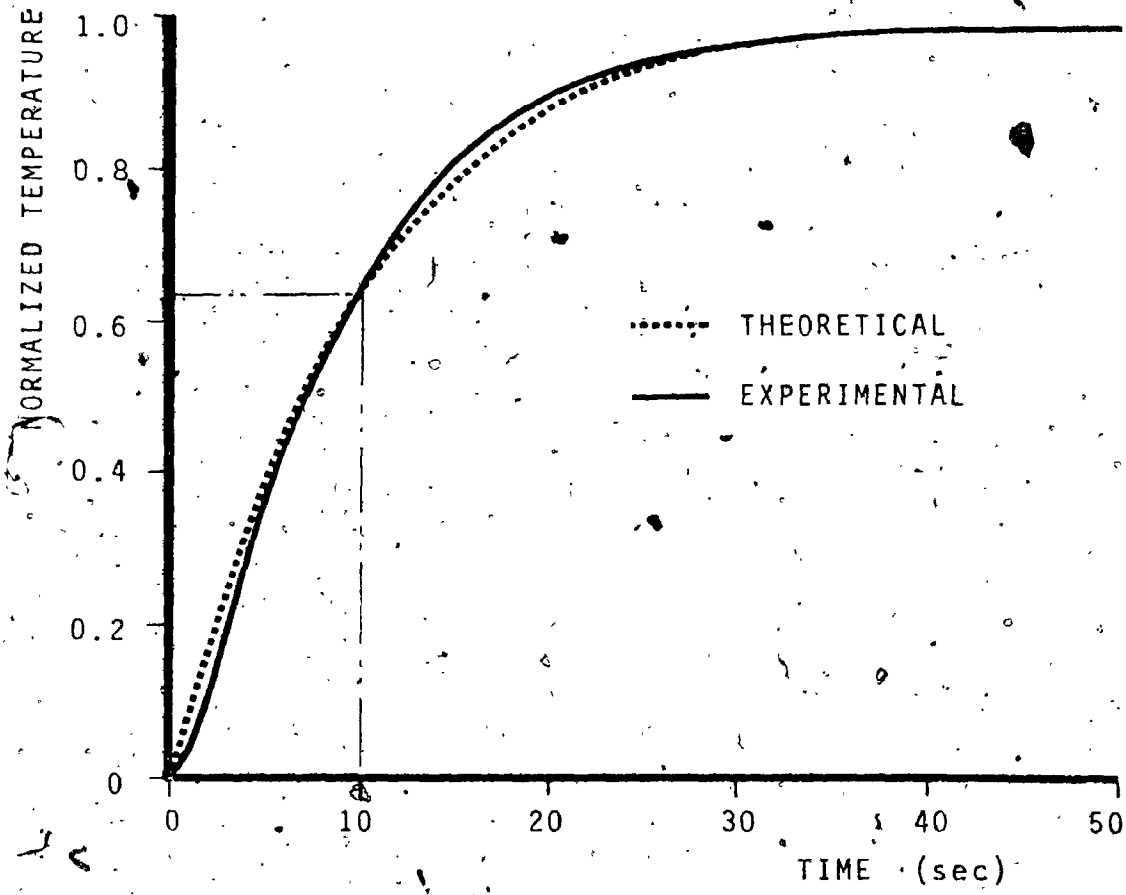

FIGURE B.3: Theoretical and smoothed experimental step responses for thermistor probe C-20.

ΔZ. Assuming the probe was lowered at V = 18 m/min (0.3 m/sec), then:

$$\Delta Z = (D)(V)$$
$$= (0.7\text{sec})(0.3\text{m/sec})$$
$$= 0.21 \text{ m}$$

The results must be shifted closer to the top of the borehole by an amount ΔZ = 0.21 meters for maximum precision.

APPENDIX C

DEPTH CORRECTIONS

For most applications of the continuous gradient logging system it is desirable to achieve maximum precision in the depth scale of the output plot. For this to be accomplished it is necessary that the wellhead pulley be accurately calibrated in terms of revolutions per meter of cable passing over it. This is done simply by marking the cable at known intervals (say, 50 m), and by dividing the number of pulley revolutions by the length of cable known to have passed over it. For the prototype equipment used in these tests, the pulley factor was established by this method to be approximately 3.96 rev/m.

Another factor which must be considered is cable stretch, a general term which can be divided into recoverable (elastic) and permanent (plastic) components. In theory the elastic stretch for a given short length of cable occurs immediately after leaving the reel and before it passes over the depth monitor pulley. Thus, this component of stretch is automatically included in the depth indicated by the pulley counter, and may be ignored. Plastic stretch (including untwisting of the cable) is a

function of time and hence, compensation is not automatic as in the case of elastic stretch. The depth counter reading is noted as each of the cable marks passes over the pulley into the hole, and again as the cable is wound out of the hole. The difference between depth readings at corresponding marks on the cable is an indication of cable stretch. This assumes that the cable has not slipped on the pulley, a problem which may occur if the pulley bearings are stiff.

Cable stretch is plotted against depth, and a curve of the form

$$S = A\ Z^B$$

where S is cable stretch (m)

Z is depth (m)

A and B are experimentally determined parameters may be fitted to the data to allow a continuous stretch correction to be applied in the computer data reduction (Appendix A). Figure C.1 shows such a plot for one of the early field tests of the continuous logging system.

Both the stretch correction and the depth pulley calibration contain unavoidable sources of error. As an example, the cable is marked at known intervals while laid out on the ground, in an unstressed condition. The plastic stretch correction, however, makes use of the marks while the cable is in a stressed condition, and hence, after

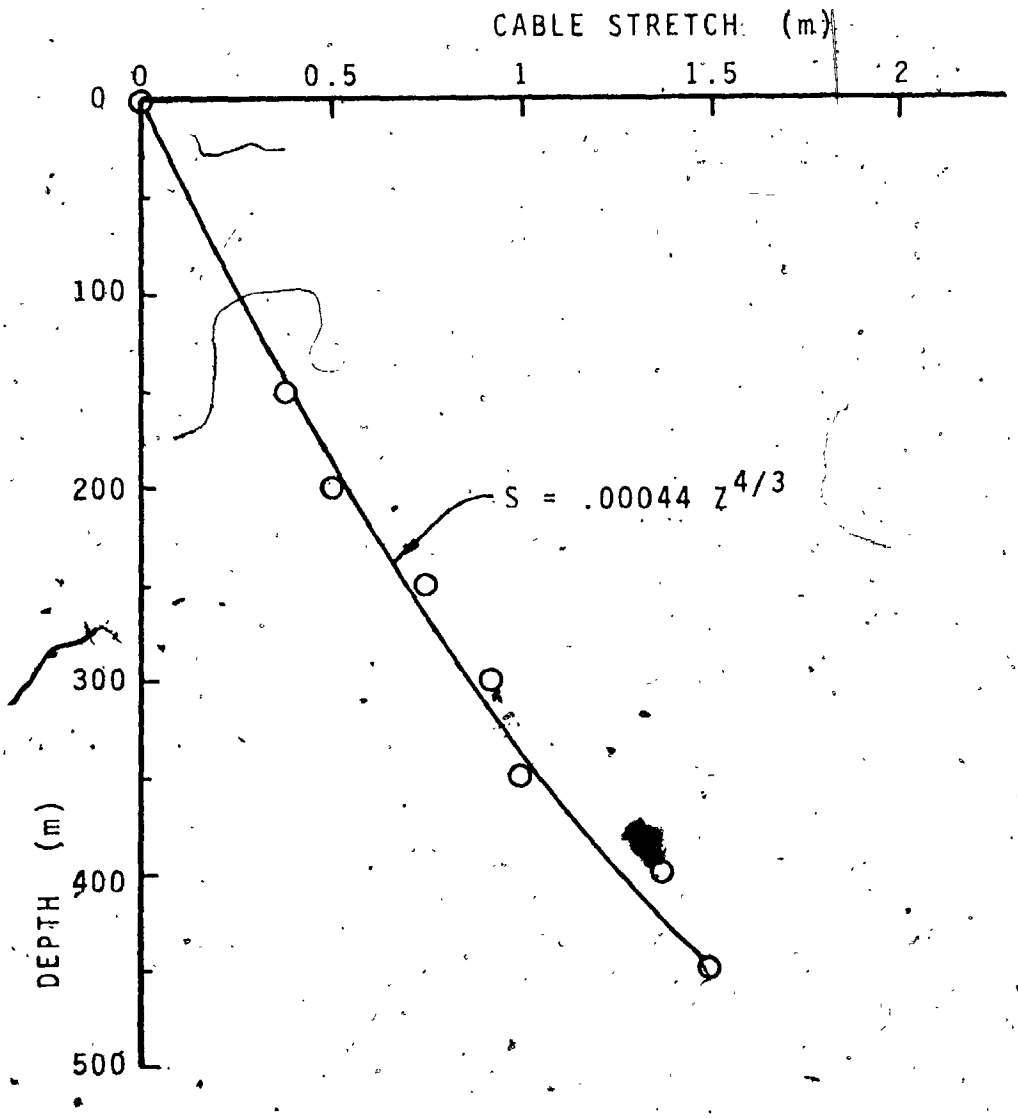

FIGURE C.1: Plot of cable stretch with depth for one of the early field tests.

elastic stretch has occurred. These are second order effects and consequently should not be of great importance. In any event, for the present it must be said that no better method for accomplishing the depth correction or calibration is available. A direct measurement is of course impossible, and a theoretical treatment is prohibitively complex, due to the lack of sufficiently precise data on the mechanical characteristics of the cable under all conditions.

REFERENCES

Beck, A.E., Techniques of measuring heat flow on land, in Terrestrial Heat Flow, ed. W.H.K. Lee; Am. Geophys. Un, Monograph No. 8, Washington, pp 24-57, 1965.

Beck, A.E., The use of thermal resistivity logs in stratigraphic correlation, Geophysics, 41, (in press), 1976a.

Beck, A.E., Climatically perturbed temperature gradients and their effect on regional and continental heat flow means, Tectonophysics, (in press), 1976b.

Beck, A.E., and A.S. Judge, Analysis of heat flow data - I. Detailed observations in a single borehole; Geophys. J., 18, 145-158, 1969.

Brigham, E.O., The Fast Fourier Transform, Prentice-Hall, 1964.

Bryant, H.L., Production well logging techniques, Geophysics, 25, 905-927, 1960.

Carslaw, H.S., and J.C. Jaeger, Conduction of Heat in Solids, Oxford University press, 1959.

Conaway, J.G., and A.E. Beck, Continuous logging of temperature gradients, Tectonophysics, (in press), 1976.

Costain, J.K., Probe response and continuous temperature measurements, J. Geophys. Res., 75, 3968-3975, 1970.

Hsu, H.P., Fourier Analysis, Simon and Schuster, 1970.

Huang, J.H., Effective thermal conductivity of porous rocks, J. Geophys. Res., 76, 6420-6427, 1971.

Hutt, J.R., and J.W. Berg, Jr., Thermal and electrical conuctivities of sandstone rocks and ocean sediments, Geophysics, 33, 489-500, 1968.

Jessop, A.M., personal communication, 1975.

Jessop, A.M., and A.S. Judge, Five measurements of heat flow in southern Canada, Can. J. Earth Sci., 8, 6, 711-716, 1971.

Johnson, R.E., and F.L. Kiokemeister, Calculus with Analytic Geometry (third edition), 105-107, Allyn and Bacon, 1964.

Judge, A.S., Geothermal Measurements in a Sedimentary Basin, Ph.D. thesis, University of Western Ontario, 1972.

Kanasewich, E.R., Time Sequence Analysis in Geophysics, University of Aberta Press, 1973.

Kappelmeyer, O., and R. Haenel, Geothermics, Gebruder Borntraeger, 1974.

Miller, I., and J.E. Freund, Probability and Statistics for Engineers, Prentice-Hall, 1965.

Pirson, S.J., Geologic Well Log Analysis, Gulf Publishing Co., 1970.

Rice, R.B., Inverse convolution filters, Geophysics, 27, 4-18, 1962.

Robinson, E.A., Multichannel Time Series Analysis with Digital Computer Programs, Holden-Day, 1967a.

Robinson, E.A., Predictive decomposition of time series with application to seismic exploration, Geophysics, 32, 418-484, 1967b.

Robinson, E.A., and S. Treitel, Principles of digital Wiener filtering, Geophys. Prospecting, 15, 311-333, 1967.

Sanford, B.V., and W.E. Koepke, unpublished geologic log of the UWO borehole, 1963.

Simmons, Gene, Continuous temperature logging equipment, J. Geophys. Res., 70, 1349-1352, 1965.

Streeter, V.L., Fluid Mechanics, (Fourth Edition), McGraw-Hill, pp 233-249, 1966.

Treitel, S., and E.A. Robinson, The stability of digital filters, IEEE Transactions on Geoscience Electronics, Vol. GE-2, 6-18, Nov. 1964.

Upitis, U., unpublished B.Sc. thesis, University of Western Ontario, 1963.

Wyllie, M.R.J., Log interpretation in sandstone reservoirs, Geophysics, 25, 748-778, 1960.

Zierfuss, H., and G. Van Der Vliet, Laboratory measurements of heat conductivity of sedimentary rocks, Bull. Amer. Assoc. Petr. Geol., 40, 1956.